Characterization of Chondrocyte Fate and Nutrition Property during Cartilage Culture Process

Masrina binti Mohd Nadzir

September 2012

Characterization of Chondrocyte Fate and Nutrition Property during Cartilage Culture Process

A dissertation submitted to

THE GRADUATE SCHOOL OF ENGINEERING SCIENCE

OSAKA UNIVERSITY

In fulfillment of the requirements for the degree of

DOCTOR OF PHILOSOPHY IN ENGINEERING

By

Masrina binti Mohd Nadzir

September 2012

Preface

This work was conducted under the supervision of Professor Masahito Taya at Division of Chemical Engineering, Graduate School of Engineering Science, Osaka University, from 2007 to 2012.

The main objective of this thesis is to characterize the chondrocyte fate and nutrition property during cartilage culture towards generating clinically applicable cultured construct. The changes in cell fate with age, the availability and transport of nutrients, as well as the application of strategy to regulate the architecture of cultured cartilage are discussed. The author hopes that the findings obtained in this work would offer the engineering fundamentals for future developments of cultured tissues.

Masrina binti Mohd Nadzir

Division of Chemical Engineering
Graduate School of Engineering Science
Osaka University
Toyonaka, Osaka 560-8531, JAPAN

Contents

Abstract

Characterization of the chondrocyte fate and nutrition property during cartilage culture is important towards generating cultured construct with a desired quality for clinical uses. In Chapter 1, the relationship between the morphology of young chondrocytes (population doubling, $PD = 0$) and the structure of high density collagen type I coated substrate (CL substrate) was clarified. It was found that the decay of collagen fibril formation due to preservation caused the spreading of cells, indicating that the non-preserved CL substrate is most suitable for evaluation purpose. Chapter 2 emphasizes comprehension of the influence of *PD* levels on chondrocyte fate with age in the cultured cartilage. At the middle age of cell population ($PD = 5.1$ and 6.6), the high frequency of cells with ALP activity and single hypertrophic cells with collagen type II formation was recognized on the CL substrate and in CL gel, respectively, supporting the consideration that the elevated gene expression of collagen type II was attributed to terminal differentiation rather than redifferentiation. In Chapter 3, a direct measurement system was constructed to estimate the dissolved oxygen (DO) concentration in the CL gel culture with seeding density of 2.0×10^6 cells/cm^3. In the static culture of CL gel, chondrocytes grew predominantly at the peripheral of the gel and formed barrier to the diffusion of oxygen, subsequently causing the gradient of DO concentration. The insufficient supply of nutrient caused low proliferation in the deeper region of the construct, which leads to the heterogeneity of cell distribution. The improvement of oxygen supply to the culture by shaking condition and with a gas-permeable bottom did not significantly enhance the cell growth at the bottom region, suggesting the limitation of alternative nutrient such as protein. Chapter 4 deals with the diffusion of oxygen and protein at the periphery of cultured cartilage. Using a system mimicking the periphery of CL gel, it was revealed that the transport of large-molecular-weight nutrient was highly influenced by the formation of the extracellular matrix (ECM) in cell aggregates, probably arising from the changes in cell-cell distances and matrix structure. In the last chapter, Chapter 5, a low seeding density culture of 2.0×10^5 cells/cm^3 was used to limit the cell growth and ECM production at the periphery of the cultured cartilage. The addition of insulin-like growth factor-1 (IGF-1) to this low seeding density culture enabled the regulation of cell behavior and the formation of desired chondrocyte aggregates.

The results of this research can be applicable for controlling the quality of cultured cartilage as well as generating cultured tissues with specific functions.

General Introduction

Articular cartilage

Articular cartilage is the whitish layer found on the diarthrodial joints of bones. The articular cartilage primarily comprises extracellular matrix (ECM) and lacks blood vessels, lymphatic vessels, and nerves. The ECM is produced and maintained by the chondrocyte, the only cell type present in the articular cartilage. In turn, the ECM provides the chondrocytes with a protective environment in the face of high mechanical stress, thus helping to maintain their phenotype. Furthermore, the ECM offers storage of cytokines and growth factors required by the chondrocyte and acts as a barrier to nutrients that have reached the cells (Buckwalter and Makin, 1997a, 1997b).

The ECM of the articular cartilage predominantly comprises water, collagen, and proteoglycans. Water is the most abundant component of the ECM, accounting for approximately 60% to 80% of the wet weight. It provides nutrition and a medium for lubrication, creating a low-friction gliding surface (Bhosale and Richardson, 2008). Collagen is the second largest component of the articular cartilage. Collagen type II forms the principal component of the framework and provides tensile strength to the articular cartilage. The other collagen types provide functions such as helping chondrocytes to attach to the matrix, forming nucleate fibrils, and aiding in cartilage mineralization (Bhosale and Richardson, 2008). The third largest components are the proteoglycans. These protein polysaccharide molecules provide compressive strength to the articular cartilage and maintain the fluid and electrolyte balance in the articular cartilage (Buckwalter and Makin, 1997a). Deformation of the ECM produces signals that may affect the proper functioning of chondrocytes.

Treatment of articular cartilage defects by autologous chondrocyte transplantation

In general, there are three main types of cartilage injury: matrix disruption, partial-thickness defects, and full-thickness defects. Matrix disruption occurs from blunt trauma in which, the damage to ECM is not extreme. If this occurs, the remaining viable chondrocytes will increase their synthetic activity to repair the damage. Partial-thickness defects demonstrate disruption of the cartilage surface that does not extend to the subchondral bone, whereas full-thickness defects arise from damage that transverses the entire cartilage thickness and penetrates the subchondral bone (Temenoff and Mikos, 2000). Unlike skin, in which both the vasculature and adjacent tissues provide cells to mediate the wound healing process, the avascularity of the articular cartilage and the dense ECM surrounding the chondrocytes give the articular cartilage limited self-repairing ability (Kinner *et al.*, 2005; McPherson and Tubo, 2000). Thus, treatment of the defected area is necessary.

Based on the promising results of autologous chondrocyte transplantation (ACT) in animal models of articular cartilage injury (Grande *et al.*, 1989), chondrocyte transplantation in human patients was initiated by Brittberg *et al.* (1994). In this technique, viable chondrocytes were obtained from the un-involved area of the injured cartilage and propagated by monolayer culture. The propagated cells released from the culture vessel were then injected into the area of the defect, and the defect was covered with a sutured periosteal flap. In spite of the satisfactory clinical outcomes, concerns have been raised regarding the reexpression of the chondrocyte phenotype after the dedifferentiation of cells in a prolonged monolayer culture, the possibility of leakage of chondrocytes from the graft site, and the uneven distribution of the injected chondrocytes inside the defect (Ochi *et al.*, 2001). One attempt to resolve these concerns involves employing tissue engineering technology to create cartilage-like tissues in a three-dimensional (3-D) culture system.

Development of cultured cartilage

The ACT technique has evolved over the years with improvement in the efficiency of tissue regeneration and surgical outcome. Its fundamental design comprises the three elements of tissue engineering, namely the cells, the scaffolds that bear these cells, and a suitable cultivation environment. In general, autologous chondrogenic cells are inserted into a biodegradable scaffold that supports their growth and chondrogenesis. The cell-laden scaffold is then cultivated with environmental factors appropriate for enhancing cell performance.

Although various natural and synthetic materials are available for the scaffold, few of these materials have been proven safe for human use. Ochi *et al.* (2001) applied Atelocollagen gel as a scaffold because the antigenic determinants have been removed from the peptide chain of this collagen material. Thus, a tissue transplanted with Atelocollagen gel has a low inflammatory reaction (Kusaka *et al.*, 1987) and satisfactory clinical results (Ochi *et al.*, 2002). A schematic representation of the employment of collagen as a scaffold for the ACT technique in cartilage repair is shown in **Fig. 1.**

Necessity of studying chondrocyte fate and nutrition property during cartilage culture process

An ideal cultured cartilage for ACT should contain the appropriate amount of ECM components with a uniform spatial distribution within the construct, and resemble the native cartilage in terms of structural and functional properties (Blunk *et al.*, 2002). In general, two of the main factors influencing the properties of the cultured cartilage with a collagen gel scaffold are the state of chondrocytes when embedded in the scaffold and the availability of nutrients to cells during culture. Therefore, knowledge regarding the fate of

chondrocytes before being embedded in the scaffold and the property of nutrition in the cultured cartilage are important for the design and generation of high quality cultured cartilage for clinical use. **Table 1** lists examples of studies reporting cell fates caused by several elements and the properties of nutrients in cultured cartilage.

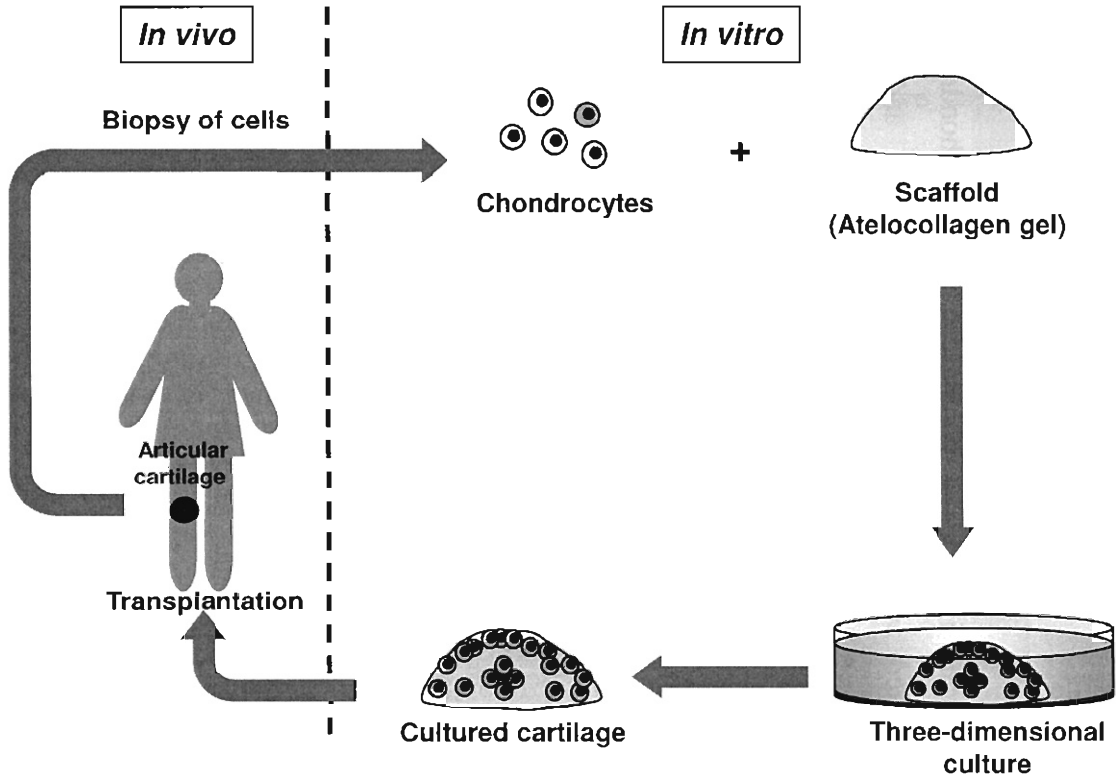

Fig. 1 Autologous chondrocyte transplantation with cultured cartilage using a collagen scaffold

Chondrocyte fate with age

Chondrocyte fate can be roughly classified into two categories: fate associated with behavior (such as cell migration and division) and fate with age. Chondrocyte fate with age is typically affected by the process of serial monolayer culturing for chondrocyte expansion. Benya and Shaffer (1982) reported that once articular chondrocytes were cultured on tissue

Table 1 Selected studies on the fate of chondrocytes and the property of nutrition in the cultured cartilage

Elements in chondrocyte fate and nutrition property	Findings	References
Chondrocyte fate		
Passage number	The increase in passage number in the serial monolayer culture for chondrocyte expansion was accompanied with the decline in cell growth and cell dedifferentiation.	Munirah *et al.*, 2008; Darling and Athanasiou, 2005
Seeding density	Chondrocytes seeded at 1.0×10^5 cells/cm^3 formed loose aggregate accompanied with the poor production of collagen type II. On the other hand, cells seeded at 1.6×10^6 cells/cm^3 formed dense aggregates rich in collagen type II.	Khoshfetrat *et al.*, 2009
Addition of growth factors		
Bone morphogenic protein-7 (BMP-7)	Cells in treated cultured construct showed a spheroidal morphology with no sign of dedifferentiation.	Gavénis *et al.*, 2007
Transforming growth factor-beta 1 (TGF-β1)	TGF-β1 promoted chondrocyte migration with deteriorated proliferation in the early culture phase of cultured cartilage.	Khoshfetrat *et al.*, 2008
Nutrition property		
Oxygen concentration	Different oxygen tensions (4, 10.5, and 21%) showed no effect on chondrocyte proliferation and nutrient (oxygen and glucose) consumption in a bioreactor microcarrier culture.	Malda *et al.*, 2004b
Glucose concentration	For thick scaffold under static culture, cell growth was found to be sensitive to the change in glucose concentration compared to other nutrient (oxygen).	Lin *et al.*, 2011

culture plastic, they exhibited a more fibroblastic morphology and a switch in production from collagen type II to collagen type I. These cells reportedly underwent a redifferentiation process with the production of collagen type II when released from the culture vessel and placed in suspension culture. However, studies showed that after several passages, the chondrocytes started to lose their ability to redifferentiate (Darling and Athanasiou, 2005; Kino-oka *et al.*, 2009). In addition, cell growth declined with increasing passage number (Munirah *et al.*, 2008). This decline in proliferative capacity could be interpreted as an expression of aging at the cellular level. The intrinsic measure of the "age" of a cell in culture is the population doubling (*PD*) level, which is the total number of times the cells in the population have doubled since the primary isolation. Changes in chondrocytes secondary to an increasing *PD* level (ageing) could lead to tissue heterogeneity and spontaneous development of cultured cartilage with poor practical value.

Nutrition properties in the cultured cartilage

In a conventional static culture of tissue-engineered cartilage with high cell seeding density ($\geq 1.6 \times 10^6$ cells/cm^3), the maintenance of cartilage homeostasis depends mainly on passive diffusion of essential nutrients. Cells typically grow predominantly at the scaffold/medium boundary, reducing tissue porosity and forming a physical barrier owing to the accumulation of ECM (Kino-oka *et al.*, 2005a). This physical barrier combined with nutrient consumption by chondrocytes at the scaffold periphery severely limit the diffusion of nutrients, causing nutrient gradients that subsequently result in a lack of cell growth at the inner part of the construct (Kino-oka *et al.*, 2005a, 2008; Malda *et al.*, 2004a). In addition, the different environmental conditions at the construct's periphery and inner region result in different levels of phenotype debilitation and cell maturation (Park *et al.*, 2007), further complicating tissue heterogeneity.

Outline of the present study

Characterization of chondrocyte fate and identification of the nutrition property during cartilage culture process are two important steps (**Fig. 2**) in improvement of the quality of tissue-engineered cartilage. **Figure 3** shows the scope of this study, which comprises two parts and five chapters. The first part addresses the importance of the *PD* level to the fate of chondrocytes in collagen gels (Chapters 1 and 2), and the second part focuses on the availability of nutrients in collagen gels during culture (Chapters 3, 4, and 5). A general overview of the present study is briefly described in the following paragraphs.

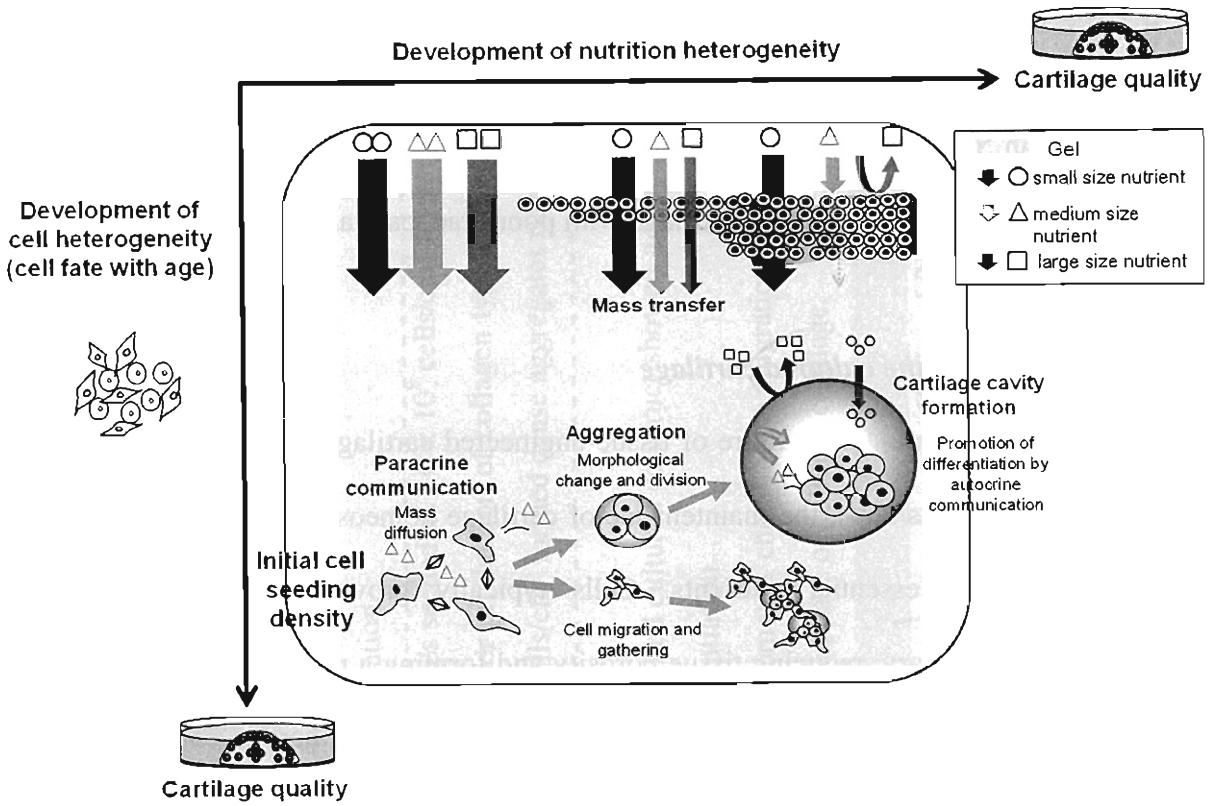

Fig.2 Schematic representation of factors influencing the quality of cultured cartilage

In Chapter 1, to clarify the relationship between the morphology of young chondrocytes and the structure of high density collagen type I coated substrate (CL substrate), morphological evaluation of cells was conducted after 1 day of incubation on preserved CL substrates. Scanning electron microscope (SEM) was used to observe changes in collagen coating, focusing on the structure of collagen fibrils.

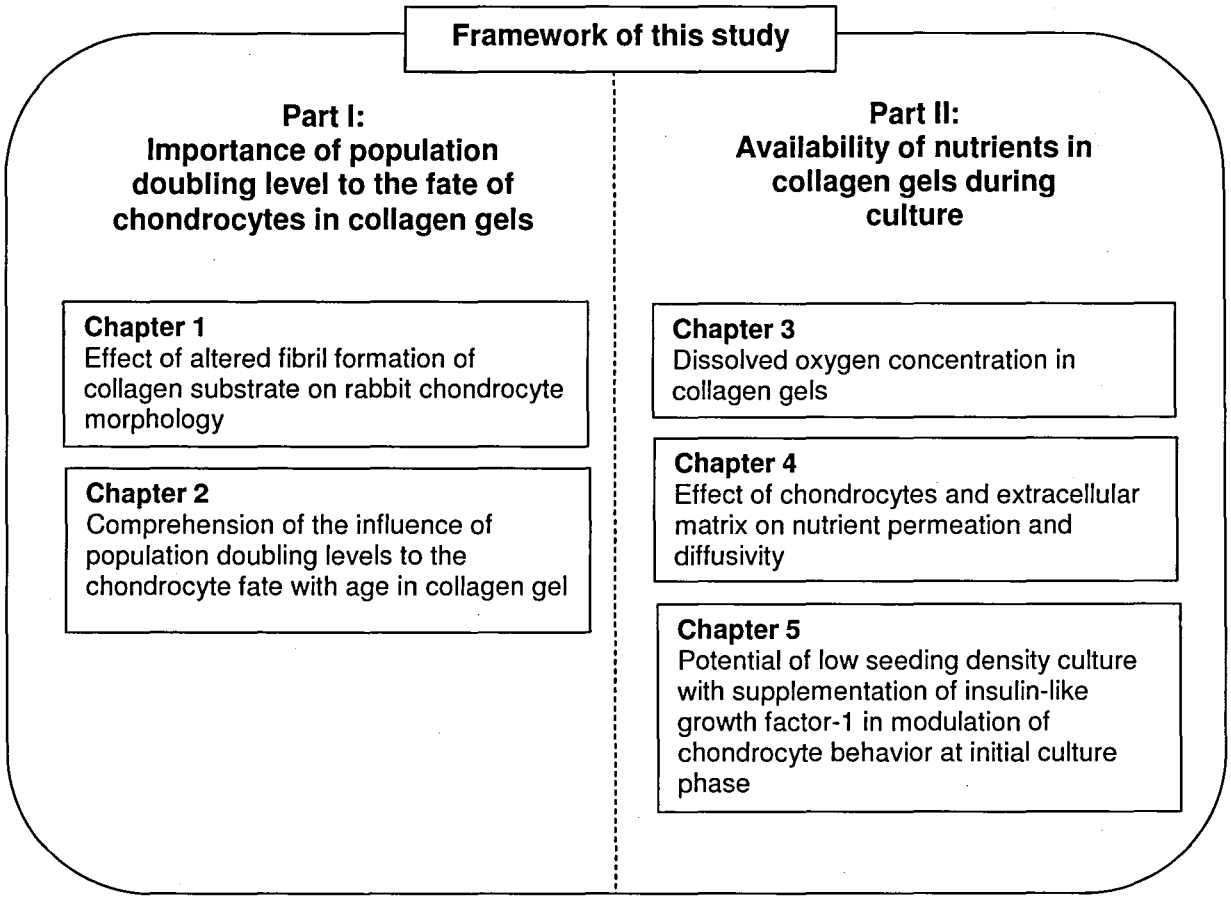

Fig.3 Outline of this study in terms of characterization of chondrocyte fate and nutrition property during cartilage culture process

Chapter 2 emphasizes comprehension of the influence of *PD* levels on chondrocyte fate with age in the cultured cartilage. Because of technical restrictions in evaluation of cell fate in the collagen gel (CL gel), the CL substrate was used for cell evaluation. The cell

phenotype on the CL substrate was distinguished by morphological assessment and alkaline phosphatase staining and correlated with the cell population in the CL gel.

In Chapter 3, a direct measurement system was constructed to estimate the dissolved oxygen (DO) level in cultured cartilage of a conventional static culture. The DO level was also estimated in cultures under shaking conditions and with a gas-permeable bottom. The spatial distribution of cells in the cultured cartilage is discussed in terms of nutrient availability.

Chapter 4 deals with the diffusion of oxygen and protein at the periphery of cultured cartilage. A system mimicking the periphery of CL gel was used to clarify the influence of ECM and cell cytoplasm on nutrient diffusion.

In the last chapter, Chapter 5, a low seeding density culture was used to limit cell growth and ECM production at the periphery of the cultured cartilage. In addition, the effect of insulin-like growth factor-1 (IGF-1) on the formation of cell aggregates in the culture in the initial culture phase was examined.

Part 1

Importance of population doubling level to the fate of chondrocytes in collagen gels

One of the important factors which govern the quality of cultured cartilage is the state of chondrocytes prior to embedding in a scaffold. In the development of the cultured cartilage, the state of chondrocytes typically depends on the age of the donors and the "age" of cells. Indeed, chondrocytes from articular cartilage exhibit a number of age-related changes in their phenotype. Among these changes are decreased responses to growth factors, increased apoptosis and decreased extracellular matrix production (Guerne *et al.*, 1995; Adam and Horton, 1998). In the serial passage culture employed for cell expansion, chondrocytes age increased with the number of passages. This is evident from the declined cell growth (Munirah *et al.*, 2008) which could be interpreted as the ageing of cells. The population doubling (*PD*) accurately assessed cell growth (Greenwood *et al.*, 2004) and is an intrinsic measure of the age of cells *in vitro*. It was reported that dedifferentiated chondrocytes lose its ability to redifferentiate with increasing *PD* (Kino-oka *et al.*, 2009). Furthermore, Mukaida *et al.* (2005) reported that the dedifferentiated chondrocytes from passaged culture resulted in hypertrophic differentiation in a 3-D culture. Therefore the information of chondrocyte fate with age at various *PD* levels could be applied for controlling the quality of cultured cartilage.

From the viewpoint mentioned above, the evaluation of chondrocytes was conducted on the high density collagen type I coated substrate (CL substrate). Initially, the relationship between the structure of the substrate and the morphology of young chondrocyte ($PD = 0$) was clarified in Chapter 1, and subsequent evaluations was conducted for cells of higher *PD* in Chapter 2 for understanding the chondrocyte fate with age.

Chapter 1

Effect of altered fibril formation of collagen substrate on rabbit chondrocyte morphology

1.1 Introduction

Collagen is a popular ECM used as the substrate on culture surface as well as in scaffold of sponge or gel. The self-assembling nature in collagen polymerization leads to the specific structure of collagen fibrils. The collagen fibrils, which consist of abundant binding sites to integrins on cytoplasmic membrane, play an important role in the control of cell behaviors such as attachment, spreading and migration, thereby in close relation to cellular fate of proliferation and differentiation.

The typical process of collagen coating consists of pouring acidic collagen solution onto culture surface, followed by soaking and drying for adsorption of collagen on the surface, and neutralizing for polymerization with fibril formation. Some researchers have reported the influences of collagen treatment conditions (Yunoki *et al.*, 2004; Rada *et al.*, 1993), and duration of soaking and drying (Jacquemart *et al.*, 2004; Dupont-Gillain *et al.*, 2004) on the structure of collagen fibrils. In the previous study, the procedure of CL substrate was established by vacuum drying after loading acidic collagen, which led to fully developed fibril formation on a culture surface (Kino-oka *et al.*, 2005b). In the culture of chondrocytes, it has been revealed that the round-shaped cells maintained in a differentiated state with producing collagen type II (Kino-oka *et al.*, 2009; Shakibaei *et al.*, 1997). The CL substrate was reported to sustain the round shape of differentiated chondrocytes, although dedifferentiated cells exhibit the spindle shape, suggesting that the CL substrate was a useful tool for understanding the cellular state of chondrocytes (Kino-oka *et al.*, 2009).

In the present study, the preparation of CL substrate was conducted under various preservation conditions that were set as operational variables to alter the degree of collagen fibril formation. The structural alterations of the preserved collagen substrates were observed and examined in relation to the morphological behaviors of rabbit chondrocytes.

1.2 Materials and Methods

1.2.1 Preparation of CL substrates

For preparing the substrate, 5.25 ml of acidic solution of bovine collagen type I (0.5% collagen I-AC; Koken Co., Ltd., Tokyo) was poured into a 25 cm^2 T-flask (Corning Inc., Corning, NY, USA) aseptically, giving 1.05 mg of collagen per cm^2 of flask bottom surface. The water in the flask was then evaporated in a vacuum chamber for 3 days at room temperature to coat the bottom with acidic collagen. The preservation process of the surface coated with collagen was conducted at room temperature. The preservation conditions were varied by atmosphere and period as follows; under nitrogen gas for 4 days (Condition I) and 7 days (Condition II), and under air for 4 days (Condition III) and 7 days (Condition IV). After the preservation, the surface was rinsed with sterile phosphate buffered saline (PBS; Sigma, St. Louis, MO, USA) for the neutralization of collagen and the CL substrates experiencing the preservation process were subjected to analyses.

Here, the CL substrate without the preservation process was prepared as a reference substrate by the neutralization just after the evaporation in the vacuum chamber.

1.2.2 Scanning electron microscopic observation

For observing the fine structure of coated collagen, the specimens were prepared for scanning electron microscopy as described previously (Kino-oka *et al.*, 2005b). In brief, the

substrates were fixed with 2.5% glutaraldehyde for 2 h, followed by dehydration with serial gradients of aqueous ethanol solution. After freeze-drying with *t*-butyl alcohol and sputter coating with platinum (approximately 3 nm thick), the specimens were examined under SEM (S-5000L; Hitachi, Tokyo).

1.2.3 Chondrocyte preparation and incubation on substrates

Chondrocytes were prepared by excising articular cartilage slices from humeri, femora and tibiae of Japanese white rabbits (approximately one month old) as described elsewhere (Yamamoto *et al.*, 2002). The isolated chondrocytes were subcultured using a 75 cm^2 T-flask (Corning Inc.) at an inoculums size of 1.0 x 10^4 cells/cm^2 as described previously (Kino-oka *et al.*, 2005b). The chondrocytes were harvested 3 days after seeding in the primary culture, during which the living cells could attach on the flask without multiplying and were defined as a cell population with $PD = 0$. The cells were then incubated on the prepared substrates for 1 day in a similar manner as the subculture.

1.2.4 Evaluation of chondrocyte morphology, adhesion and cytoskeletal formation

Quantitative morphological analysis of adherent cells on the substrates was conducted by capturing the surface image of each flask bottom through a charge-coupled device camera attached to an optical microscope as described previously (Kino-oka *et al.*, 2005b). More than 80 cells were randomly selected for determining cell roundness R_C, calculated by employing image processing software (Image-Pro Plus version 6.2, Media Cybernetics, Sliver Spring, MD, USA) using the following equation:

$$R_c = \frac{2(\pi A_c)^{1/2}}{l_c} \tag{1.1}$$

where A_C and l_C denote the area and peripheral length of a single cell, respectively. The

frequency of round-shaped cells f_R was then estimated from the distribution of R_C using the following equation:

$$f_R = \frac{\text{number of cells giving } R_C > 0.9}{\text{total number of cells examined}} \quad (1.2)$$

In the present study, the cell with $0.9 < R_C \leq 1$ was defined to be a round morphology.

The adhesion and cytoskeletal formation of cells on the substrates were analyzed by SEM, and confocal laser scanning microscopy for F-actin and vinculin, respectively. Staining of intracellular F-actin and vinculin was conducted as described elsewhere (Kino-oka *et al.*, 2007).

1.3 Results

Figure 1.1 shows the fine structures of the CL substrates prepared under various conditions in the preservation process. The CL substrate under atmosphere of nitrogen gas for 4 days (Condition I) exhibited three dimensional single fibrils with a well-developed network (**Fig. 1.1B**), which suggests to possess a well-defined D-periodic banding pattern on the fibril (Kino-oka *et al.*, 2005b), similarly to the reference CL substrate without the preservation process (**Fig. 1.1A**). However, further prolongation of preservation period (Condition II) led to the flat network with immature-fibril foundation (**Fig. 1.1C and D**). In addition, the exposure to air in the preservation process (Condition III) caused the inhibition of the fibril formation and the granule structure of collagen appeared (**Fig. 1.1E and F**). The prolongation of exposure to air (Condition IV) diminished the fibril formation (**Fig. 1.1G and H**).

For evaluating the prepared substrates in a physiological aspect of cellular response, the morphology of rabbit chondrocytes was examined on these substrates. As shown in **Fig. 1.2**, the f_R value on the CL substrate of Condition I was 0.62, the value of which was

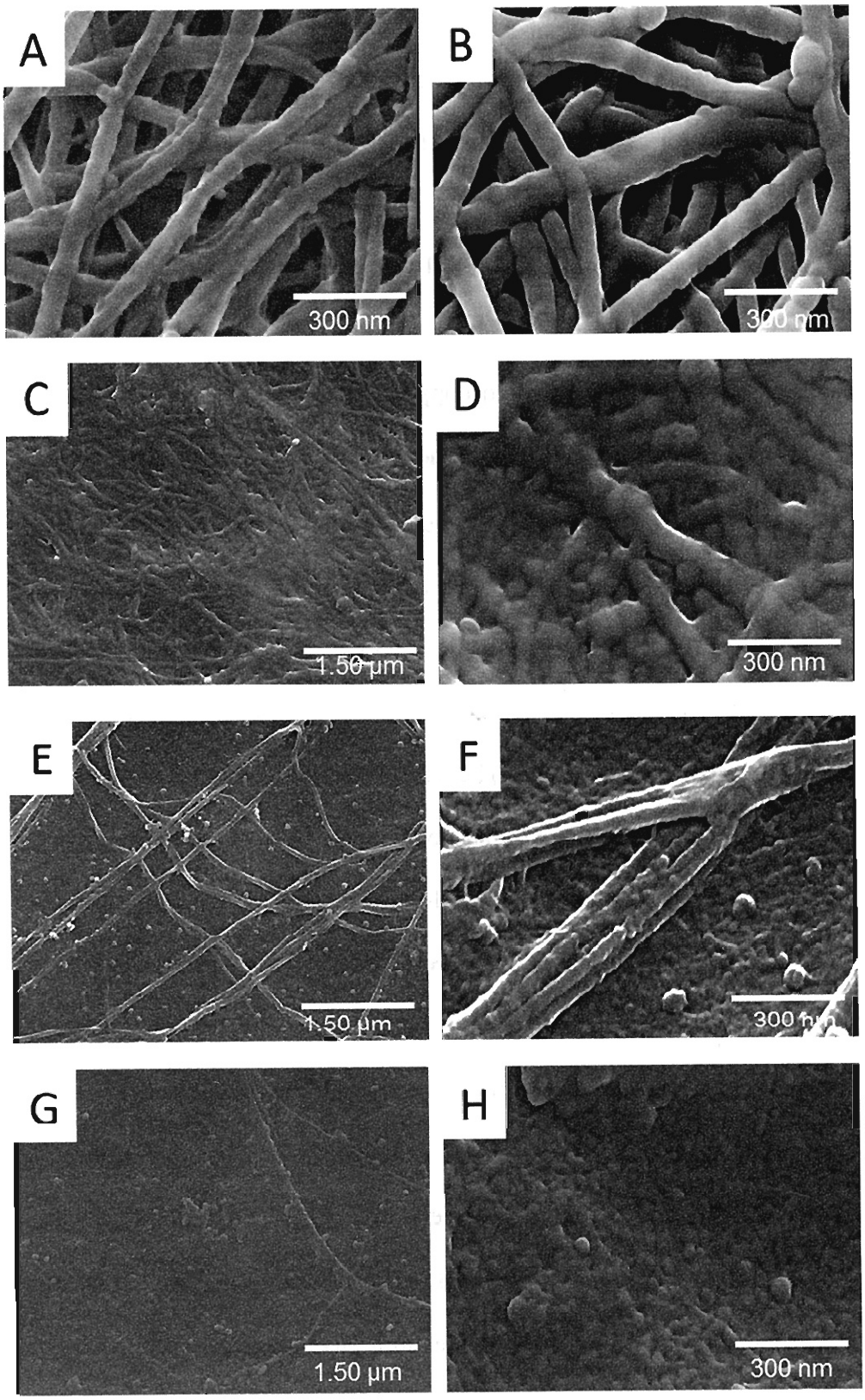

Fig. 1.1 SEM images showing surface structures of CL substrate without preservation (A), and CL substrates with preservation under Conditions I (B), II (C, D), III (E, F) and IV (G, H).

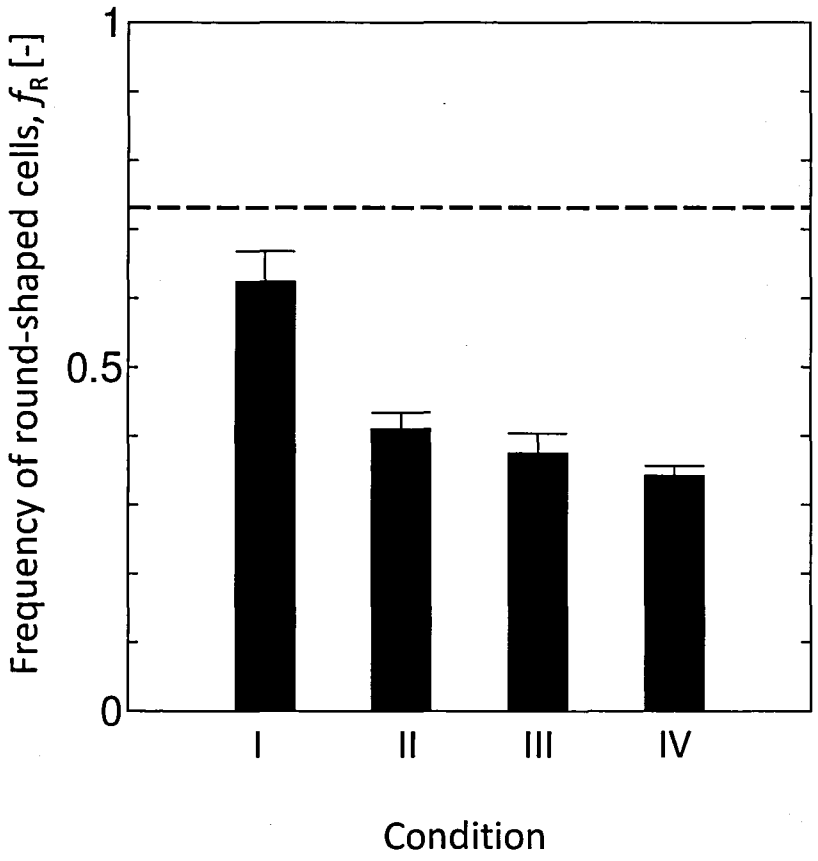

Fig. 1.2 Frequency of round shape cells, f_R, of chondrocytes attached to CL substrates prepared under various conditions. The broken line shows the data using the CL substrate without preservation. The data were obtained from more than 80 cells examined in three independent experiments. The bars show the standard deviations (SDs) (n = 3).

slightly lower than that on the reference CL substrate. However, f_R of cells on the substrates of the other conditions exhibited the lower levels than f_R = 0.4 with no significant dependency on the conditions. These results indicated that the prolongation and air exposure in the preservation process caused the spreading of chondrocytes in accordance with the decay of fibril formation.

Figure 1.3 shows the representative SEM images of chondrocytes on the CL substrates. The cell on the CL substrate without preservation exhibited a mound-round shape with the development of many fine fibrils binding the cell to the substrate with less fillopodia (**Fig. 1.3A and 1.4**).

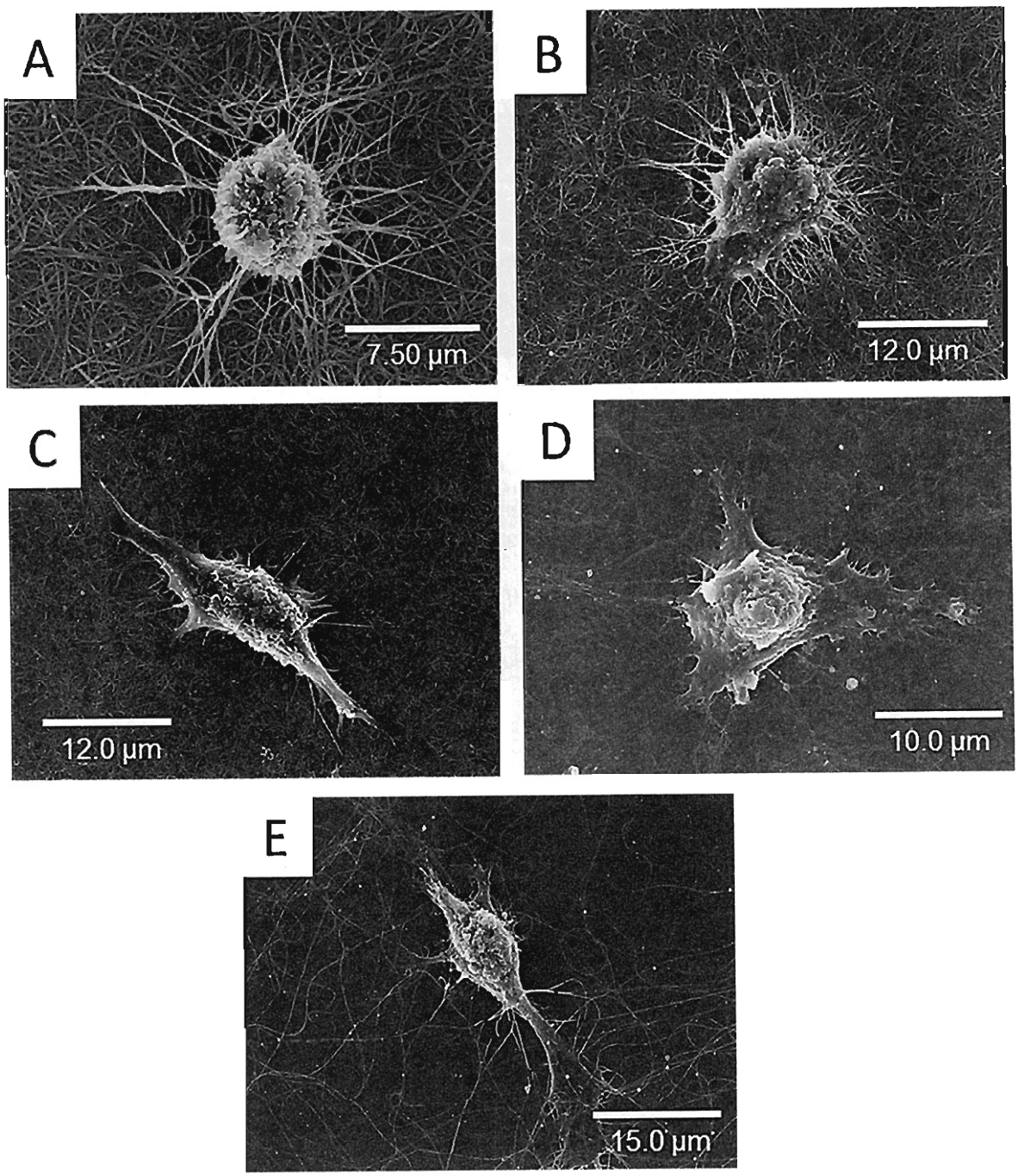

Fig. 1.3 SEM images showing chondrocytes on CL substrate without preservation (A), and CL substrates with preservation under Conditions I (B), II (C), III (D) and IV (E).

The cell on the CL substrate of Condition I developed small filopodia while still keeping a mound shape (**Fig. 1.3B and 1.5A**). The cells on the other substrates (Conditions II to IV) developed broader filopodia, making flat-stretched shapes (**Fig. 1.3C to E and 1.5B to D**).

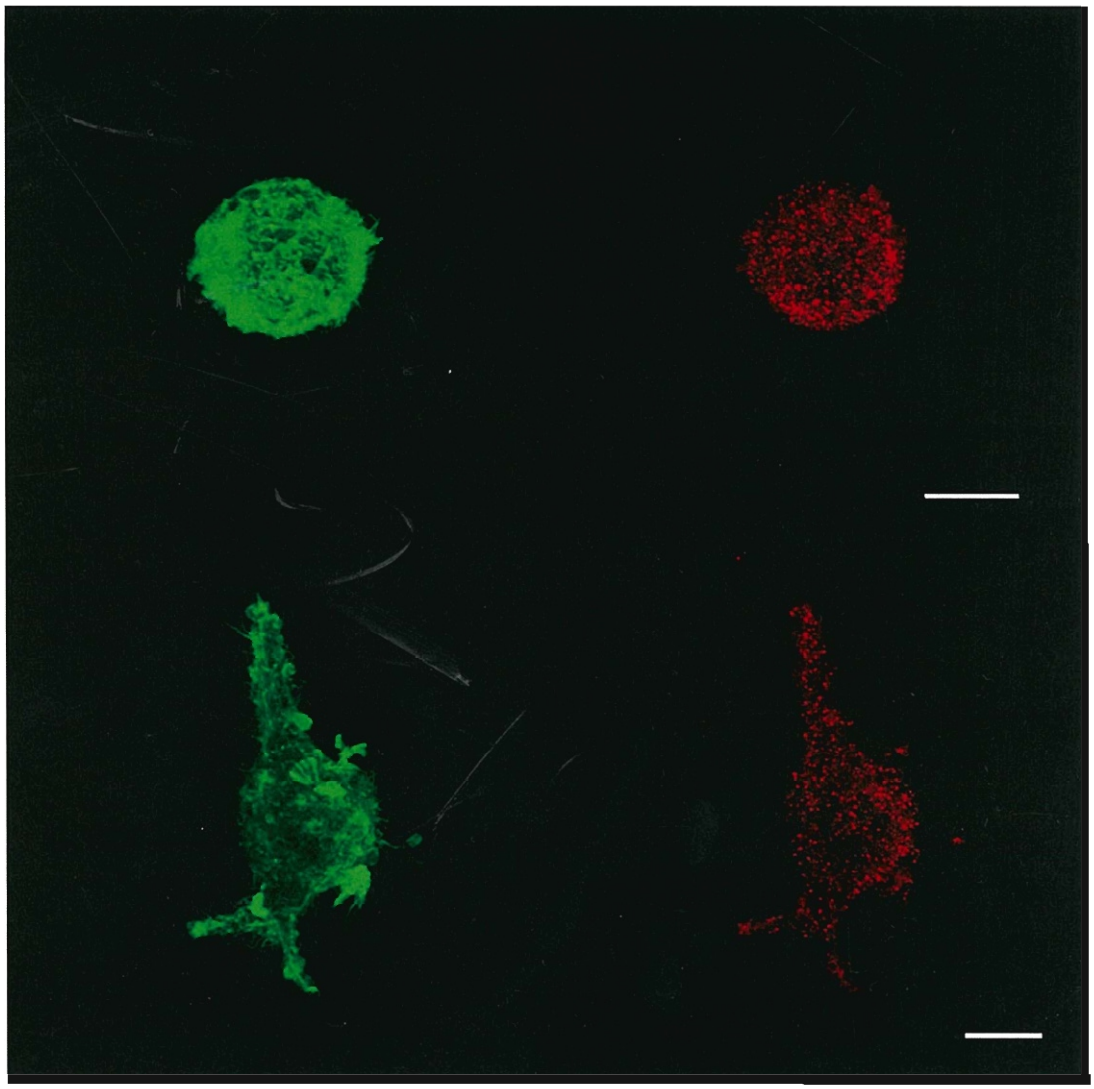

Fig. 1.4 Immunostaining of actin cytoskeleton (green) and vinculin (red) of chondrocytes cultured for 1 day on CL substrates without preservation. The scale bars show 10 μm.

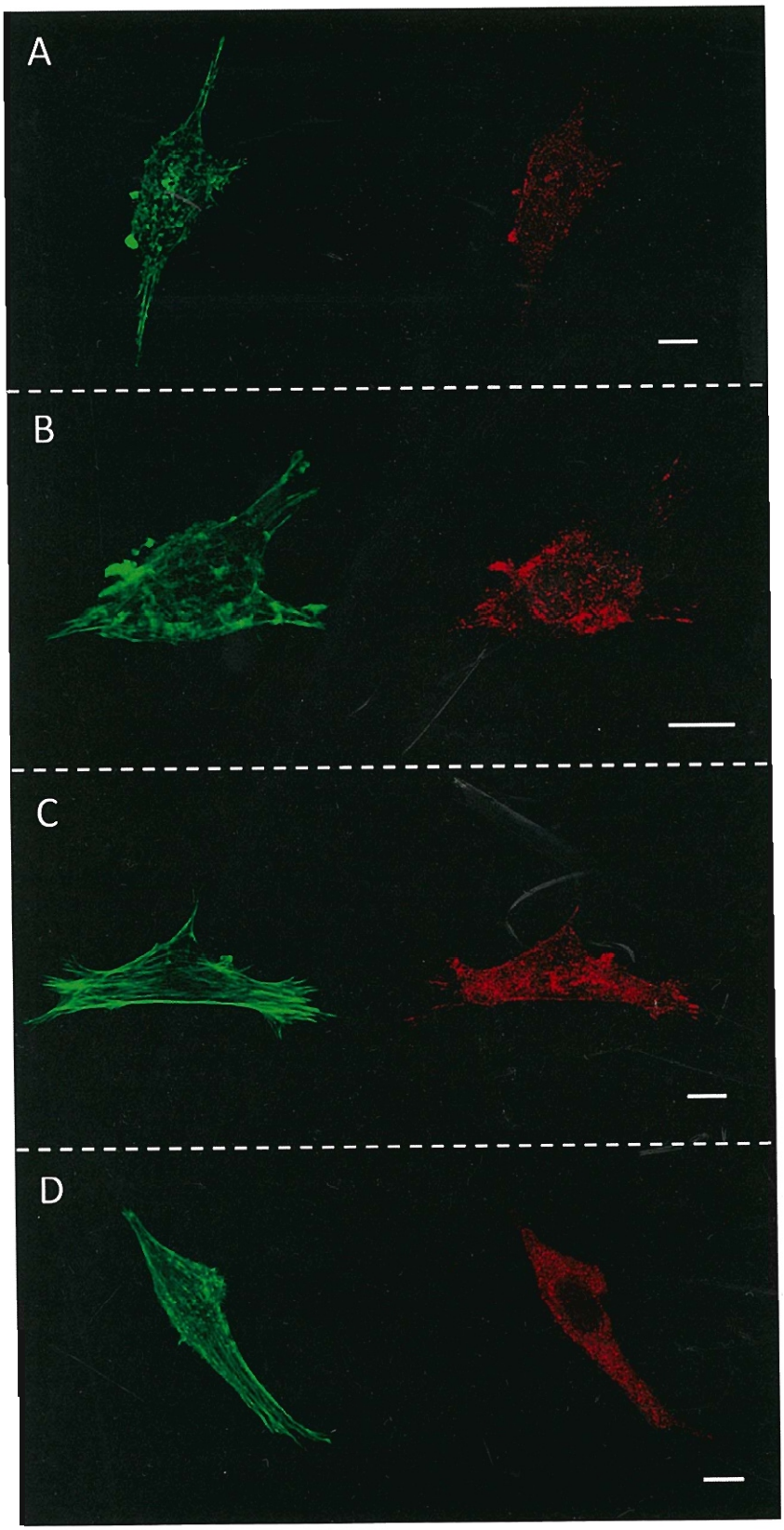

Fig. 1.5 Immunostaining of actin cytoskeleton (green) and vinculin (red) of chondrocytes cultured for 1 day on CL substrates preserved under Conditions I (A), II (B), III (C) and IV (D). The scale bars show 10 μm.

1.4 Discussion

The assembly of collagen molecules into fibrils has been shown to be an entropy-driven process, likewise in the cases of other protein self-assembly systems (Kadler *et al.*, 1987). These processes are promoted by the loss of solvent molecules from the surface of protein molecules resulting in assemblies with circular cross section, as reviewed in a literature (Kadler *et al.*, 1996). The fibril formation can be governed by some factors influencing the crosslinking of collagen. Yunoki and Matsuda (2008) reported crosslinking of collagen gel using 1-ethyl-3-(3-dimethylaminopropyl)-carbodiimide (EDC) during collagen fibril formation and they found a poor formation of collagen fibrils with non-distinguishable D-periodic pattern at a high concentration of EDC. Furthermore, they mentioned that the spaces between the collagen fibrils were occupied with non-fibrous collagen. While the formation of collagen fibrils was suggested to occur through the aggregation of soluble collagen particles followed by the fibril growth (Wood, 1960), the simultaneous crosslinking process during the collagen fibril formation could cause the lost or reduced potential to form fibril due to random and non-fibrous aggregation of the collagen particles (Yunoki and Matsuda, 2008). In the current work, the CL substrate without preservation consisted of well-developed collagen fibrils. However, this type of fibrils was not observed on the CL substrates with preservation process accompanied by exposure to air. The oxidation by air was reported to facilitate the intramolecular crosslinking (Krishna and Kiick, 2009). Therefore, the exposure to air in the current study was considered to cause the lack of well-developed fibrils in the substrates due to crosslinking of collagen by oxidation during the fibril formation. In addition, the degree of collagen crosslinking is expected to be suppressed by the replacement of oxygen with nitrogen gas in atmosphere during the preservation process.

Adhesion between cells and ECM is known to modulate numerous critical cellular events through interactions of cell's adhesion receptors with ECM binding sites. The similar distribution and amount of vinculin spots in the cells attached to the reference substrate (**Fig. 1.4**) and substrates of Conditions I, II, III and IV (**Fig. 1.5A to D**) suggested that the spreading of cells on the substrates with preservation were not attributed to the changes in the binding sites on the substrates but to other factors, such as the changes in substrate stiffness. It is documented that ligand density and matrix compliance are highly coupled variables that determine the cell responses such as cell spreading, cell shape and molecular organization (Engler *et al.*, 2004). For example, smooth muscle cells cultured on soft polyacrylamide gel and rigid glass with collagen type I coating were found to respond strongly to increasing collagen density on the glass but to be less responsive to the collagen density on the soft gel (Engler *et al.*, 2004). Cells are considered to sense their physical environment and apply traction strength to the adhesion site. This leads to the deformation of the cell morphology which depends on the substrate stiffness. Thus, on a softer substrate where the deformation is significant, the actin stress fiber/focal adhesion would be more relaxed than on the stiffer substrates (Kobayashi and Sokabe, 2010). The cell on the substrate of Condition I exhibited a cortical F-actin network (**Fig. 1.5A**), similarly to that on the substrate without preservation (**Fig. 1.4**) which is normally observed on a soft substrate (Solon *et al.*, 2007). On the other hand, the cytoskeletal formation of Conditions III and IV exhibited more organized and well-developed stress fibers indicating that these conditions produce stiffer substrates, compared to Condition II. These results suggested that the exposure to air caused the oxidization which facilitated the crosslinking of collagen, leading to poor fibril formation of collagen, and the substrate stiffness was enhanced, being responsible for the stretched shape of cells with well-developed stress fibers.

In conclusion, this chapter clarified the maintenance of the round morphology of chondrocytes on the substrates with single collagen fibrils and well-developed networks. The formation of the collagen fibrils could be inhibited by exposing the collagen coated substrate to air. The poor development of collagen fibrils caused the spreading of cells on the substrates, possibly due to an increase in stiffness of the substrates.

1.5 Summary

The degree of collagen fibril formation was altered by varying the preservation conditions. The collagen substrate under atmosphere of nitrogen gas for 4 days exhibited well-developed collagen fibril network accompanied with the frequency of round-shaped chondrocyte cells (f_R) of 0.62, the value of which was slightly lower than that on the reference substrate. The exposure to air and prolongation of preservation led to further degradation of collagen fibril networks accompanied with f_R of less than 0.4. This indicated that the decay of collagen fibril formation was responsible for the spreading of cells.

Chapter 2

Comprehension of the influence of population doubling levels to the chondrocyte fate with age in collagen gel

2.1 Introduction

In reconstructive surgery for repairing articular cartilage defects, serial monolayer cultures of isolated chondrocytes are performed for expanding cells so as to be sufficient for subsequent tissue cultures. One of the drawbacks in this approach is the partial or complete loss of proliferative ability with increasing passage number of subculture (Dominice *et al.*, 1986), which leads to hindering spatial growth in a scaffold typically employed for tissue reconstruction.

The decrease in proliferating vitality of chondrocytes *in vitro* has been associated with cellular senescence due to aging toward terminal differentiation. The progression of chondrocytes toward terminal differentiation is characterized by prolonged state of cell cycle arrest with significant increase in apparent cellular volume as well as with enhancement of collagen type X synthesis and alkaline phosphatase activity (Buttitta and Edgar, 2007; Hunziker *et al.*, 1987; Kronenberg, 2003). However, the transition toward terminal differentiation in serial monolayer cultures for cell expansion of chondrocytes is still unclear and the effort to study its progression in 3-D cultures has been hampered by lack of a suitable *in vitro* model.

An alternative is to use a two-dimensional (2-D) culture system for the evaluation of cell behavior. However, it is well-known that chondrocytes dedifferentiate when grown *in vitro* on a traditional tissue culture polystyrene (PS) surface in a way of monolayer manner, acquiring a fibroblastic-like morphology, and that instead of the cartilage-specific collagen

(collagen type II), they synthesize the collagen type I (von der Mark *et al.*, 1977; Chacko *et al.*, 1969). Despite the fact that chondrocytes in suspension and pellet cultures have potential to undergo terminal differentiation (Stephens *et al.*, 1992; Ballock and Reddi, 1994; Kato *et al.*, 1988), the limitation for single cell analysis in these systems prevent thorough understanding of the cell phenotypes and the heterogeneity in the cell population.

The previous findings have resolved this dilemma by modifying a conventional PS surface by coating with high-density collagen type I (CL substrate). The CL substrate provides a 3-D mimicking environment to chondrocytes, and enabled to evaluate the cell states for dedifferentiation in a quantitative manner (Kino-oka *et al.*, 2005b). Recent studies have demonstrated that the cell morphology indicates the states of rabbit chondrocytes, and on the CL substrate the morphological change from round to stretch shape was observed during serial subcultures with higher mRNA expression of collagen type I, suggesting that the cell morphology can offer an indicator for chondrogenic potency during dedifferentiation process (Kino-oka *et al.*, 2009).

The time-lapse observation of each single cell yields a wealth of quantifiable data on cellular properties such as changes in cell morphology, adhesion, migration and cell division pattern. Another feature for time-lapse experiment allows the movie to be rewound, thus one can survey the morphological and behavioral properties of the cells which were targeted at the end of culture, in a backward manner. As mentioned in Chapter 1, chondrocytes maintained its round morphology on the substrates with single collagen fibrils and well-developed networks. Thus, in the current study, the CL substrate without preservation process was employed for the evaluation of chondrocyte phenotypes by morphological analysis of time-lapse images of individual cells. Furthermore, the cells passaged at various population doubling levels were used to understand the progression of chondrocytes towards terminal

differentiation as well as dedifferentiation in the heterogeneous population on the CL substrate and in the CL gel.

2.2 Materials and Methods

2.2.1 Preparation of cells with varied population doubling levels

The chondrocyte isolation and the primary culture were conducted as described in Section 1.2.3. When about 80% confluence of cells was achieved on the flask bottom, the cells were detached for subsequent passage by using 2.0 ml of 0.25% trypsin solution.

The number of viable cells (n_c) in the flask was determined by the trypan blue exclusion test through direct counting of the detached cells on a hemocytometer under an optical microscope. The differential value of population doubling (ΔPD) was calculated as follows:

$$\Delta PD = \log_2 \left(\frac{n_c + \Delta n_c}{n_c} \right) \tag{2.1}$$

where Δn_c is the differential in the number of viable cells in each passage. As mentioned in Section 1.2.3, $PD = 0$ was defined as the freshly isolated chondrocytes at 3 days after seeding in the primary culture, during which the living cells could attached on the PS surface without multiplying. The subsequent value of PD was obtained by summation of ΔPD with respect to each passage conducted. In this work, three groups of the cell populations, namely $PD = 0$, $PD = 5.1$, 6.6, 7.2 and 8.5, and $PD = 12.5$ and 14.5, were prepared as young, middle and old age states, respectively.

2.2.2 Analysis of cell behaviors on collagen type I coated substrate and on tissue culture polystyrene surface

CL substrate without preservation process was prepared as described in Section 1.2.1, giving a collagen coating with approximately 70 μm thickness. Cell population at a given *PD* value was incubated on the CL substrate and PS surface for 12, 24, 48, 72, and 96 h. The cells were subjected to the detection of alkaline phosphatase (ALP) activity using Fast Red Substrate System® (Dako, Carpinteria, CA, USA) at the end of each culture and the frequency of ALP-positive cells were estimated as a ratio of them to the total cells.

To investigate the cell behaviors, the time-lapse observation of cells incubated on the CL substrate and PS surface was carried out for 72 h, as described previously (Kino-oka *et al.*, 2004), and images were captured every 10 min at 6 random positions or more. The cells on the CL substrate and PS surface were subjected at 72 h of culture time (t) to the detection of ALP activity and the backtracking of more than 100 cells was then conducted to evaluate cell behaviors. The time course of morphology was obtained to estimate the R_C by Equation 1.1 in Section 1.2.4.

2.2.3 Incubation of cells embedded in collagen gel and observation of cell behaviors

The chondrocytes at a prescribed *PD* value were suspended in the culture medium and then mixed with a 4-fold volume of 3% Atelocollagen solution (Koken Co., Ltd.) as described elsewhere (Kino-oka *et al.*, 2005a, 2005b). The mixture (0.1 cm^3) was transferred to a 6-well plate (Nunc; Nalge Nunc International, Rochester, NY, USA) and subjected to gelation at 37°C for 1.5 h, yielding a dome-shaped gel of approximately 0.8 cm diameter and 0.2 cm top height. To examine the cell growth and ECM formation, the triplicate CL gels incubated for 14 days were subjected to the staining of cytoplasm and

collagen type II respectively, according to procedures described in the previous study (Khoshfetrat *et al.*, 2009), and the specimen of CL gel was mounted on a glass-bottomed dish (Asahi Glass Co., Ltd., Tokyo) for 3-D observation of cell morphology and ECM parameter using a confocal laser scanning microscope (CLSM; model FV-300, Olympus, Tokyo). Here, more than 60 cells were provided for the semi-quantitative analysis.

2.2.4 Total RNA extraction and real-time RT-PCR analysis

Total RNA was extracted from the cells using an RNeasy mini kit (Qiagen, Hilden, Germany), and RNA sample was subjected to DNase-I (Qiagen) treatment according to the manufacturer's protocol. Reverse transcription from RNA was carried out as indicated previously (Khoshfetrat *et al.*, 2009). Gene expressions were examined by means of quantitative real time PCR with a Chromo4™ detector and furnished program (Bio-Rad Laboratories, Hercules, CA, USA) according to procedures indicated in the previous report (Khoshfetrat *et al.*, 2009). Specific primers for the glyceraldehyde 3-phosphate dehydrogenase (GAPDH) as a reference gene and the target genes (collagen types I, II and X) were designed as indicated in **Table 2.1**. PCR was performed using 0.2 μM of selected primers and SYBR Premix ExTaq™ (Takara Bio Inc., Shiga) under the conditions of 10 s at 95°C, followed by 40 cycles of 5 s at 95°C and 30 s at 60°C. The cycle threshold value (*C*t) for each gene was determined as cycle time when fluorescence of given sample became distinct from a base signal. The *C*t value of GAPDH was subtracted from that of target gene to obtain the Δ*C*t value, and the expression level was calculated in terms of $2^{-\Delta Ct}$.

Table 2.1 Sequences of primers used for real-time PCR analysis

Gene	Forward primer (5'→3')	Reverse primer (5'→3')
GAPDH	GGTGAAGGTCGGAGTGAACG	TGGCGACAACATCCACTTTG
Collagen type I	TCTGGAGAGGCTGGTACTGC	GGAGACCACGTTCACCTCTG
Collagen type II	CCACGCTCAAGTCCCTCAA	TCCAGTAGTCACCGCTCTTC
Collagen type X	CCAGGAAAACCAGGCTATGG	TTCGGTCCACTTGGTCCTCT

2.3 Results

2.3.1 Morphological and proliferative characteristics of cells

To investigate the influence of culture surfaces on terminal differentiation of the chondrocytes, the time profiles of cells density, frequency of ALP-positive cells and gene expression of collagen type X were estimated in the cultures of passaged cells (middle age state at PD = 8.5) on the CL substrate and PS surface. Appreciable growth of the cells was not observed on the CL substrate, suggesting that the cells are in a prolonged cell cycle arrest (**Fig. 2.1A**). In addition, the frequency of ALP-positive cells and the gene expression of collagen type X increased only in the culture on the CL substrate, in contrast with the negligible expressions of ALP activity and collagen type X gene on the PS surface (**Fig. 2.1B and C**). These cellular behaviors on the CL substrate indicated the chondrocyte terminal differentiation, which supports an idea that the assessment of ALP activity of the cells on the CL substrate digs out a possible population in a terminal differentiation state.

To classify chondrocyte population in the culture on the CL substrate, the time-lapse images of cells with or without ALP activity detected at t = 72 h were traced backward from t = 72 to 0 h and the time of cell division was recorded in cell population at PD = 6.6.

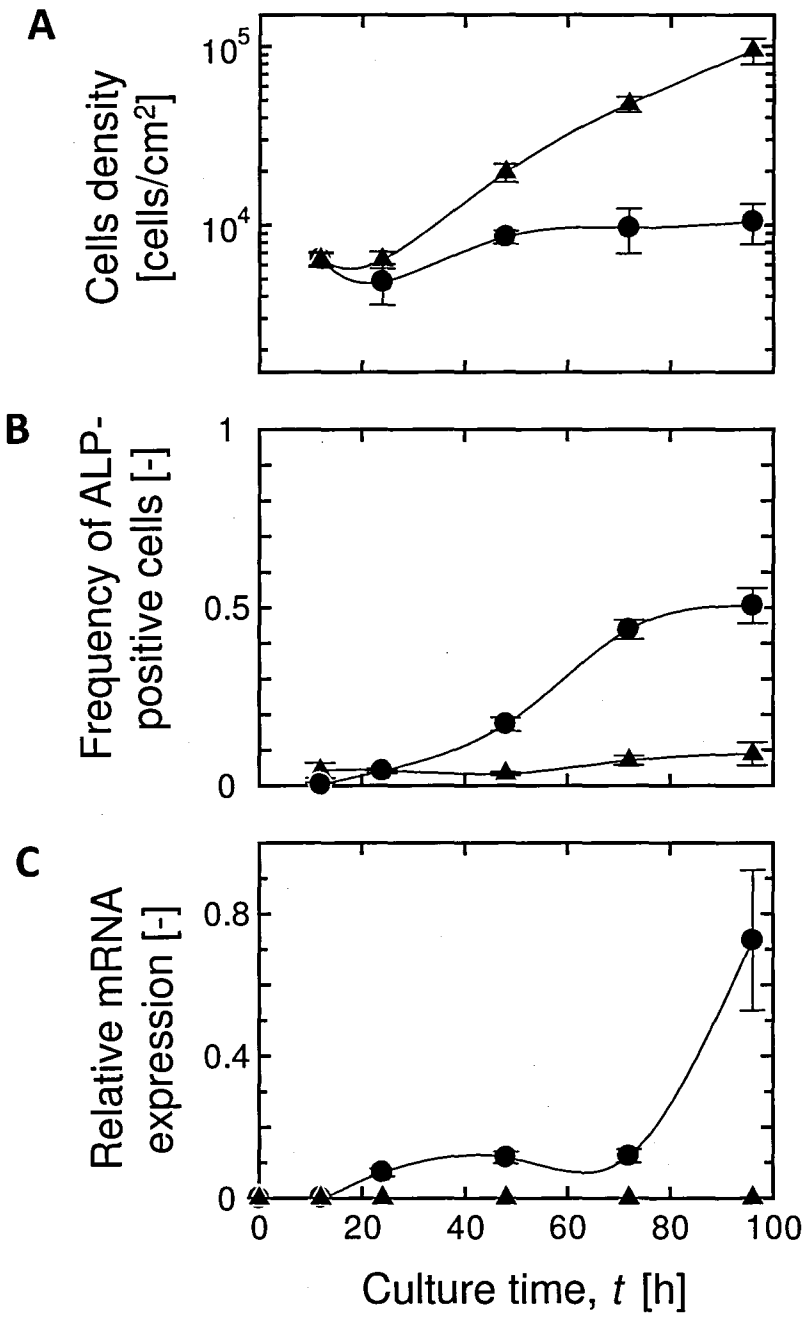

Fig. 2.1 Time profiles of cells density (A), frequency of ALP-positive cells (B) and gene expression of collagen type X (C) in cultures of chondrocytes at *PD* = 8.5 on PS surface and CL substrate. The data represent the average values with SDs determined from triplicate independent experiments. Symbol: Triangle; PS surface, and circle; CL substrate.

As typically shown in **Fig. 2.2**, ALP-negative chondrocyte population comprised of dividing and non-dividing cells for 72 h. The dividing cell for 72 h either had a round shape with $R_C > 0.9$ while maintaining this R_C level until $t = 25$ h (**Fig. 2.2A**) or had a spindle shape with periodical fluctuation below $R_C = 0.9$ (**Fig. 2.2B**). Each dividing cell maintain the cell area of about $A_C = 1000$ μm^2 throughout the culture. In addition, non-dividing cell showed a spindle shape accompanied with gradual increase in A_C to reach more than 2000 μm^2 after $t = 19$ h (**Fig. 2.2C**). On the other hand, as typically seen in **Fig. 2.3**, the population of cells exhibiting ALP activity consisted of dividing and non-dividing cells which exhibited $R_C < 0.9$ around $t = 24$ h. The A_C of dividing cell was maintained in the vicinity of $A_C = 1000$ μm^2 (**Fig. 2.3A**) until $t = 25$ h whereas the A_C of non-dividing cell increased and was in the range of 2000 to 3000 μm^2 from $t = 4$ h, giving a polygonal shape (**Fig. 2.3B**).

2.3.2 Variation in cell population on CL substrate with increasing population doubling

To investigate the change in phenotypes of chondrocytes, the cell populations at various *PD* values, corresponding to young, middle and old ages (*PD* = 0, 6.6 and 14.5, respectively), were estimated based on the variations in cell morphologies (R_C and A_C) at $t = 24$ h and ALP activity at $t = 72$ h. The cells in population at *PD* = 0 were predominantly negative in ALP activity with a round and non-stretched shape, namely $R_C > 0.9$ and $A_C < 1000$ μm^2 respectively (**Fig. 2.4A**). The frequency of cells exhibiting ALP activity increased by 1.3 times at *PD* = 6.6 (**Fig. 2.4B**) with a majority having $R_C < 0.9$ and 1000 μm^2 < A_C, being in a spindle or polygonal shape. A further increase to *PD* = 14.5 (**Fig. 2.4C**) caused the decrease in the frequency of cells exhibiting ALP activity and the increase in the frequency of round-shaped cells.

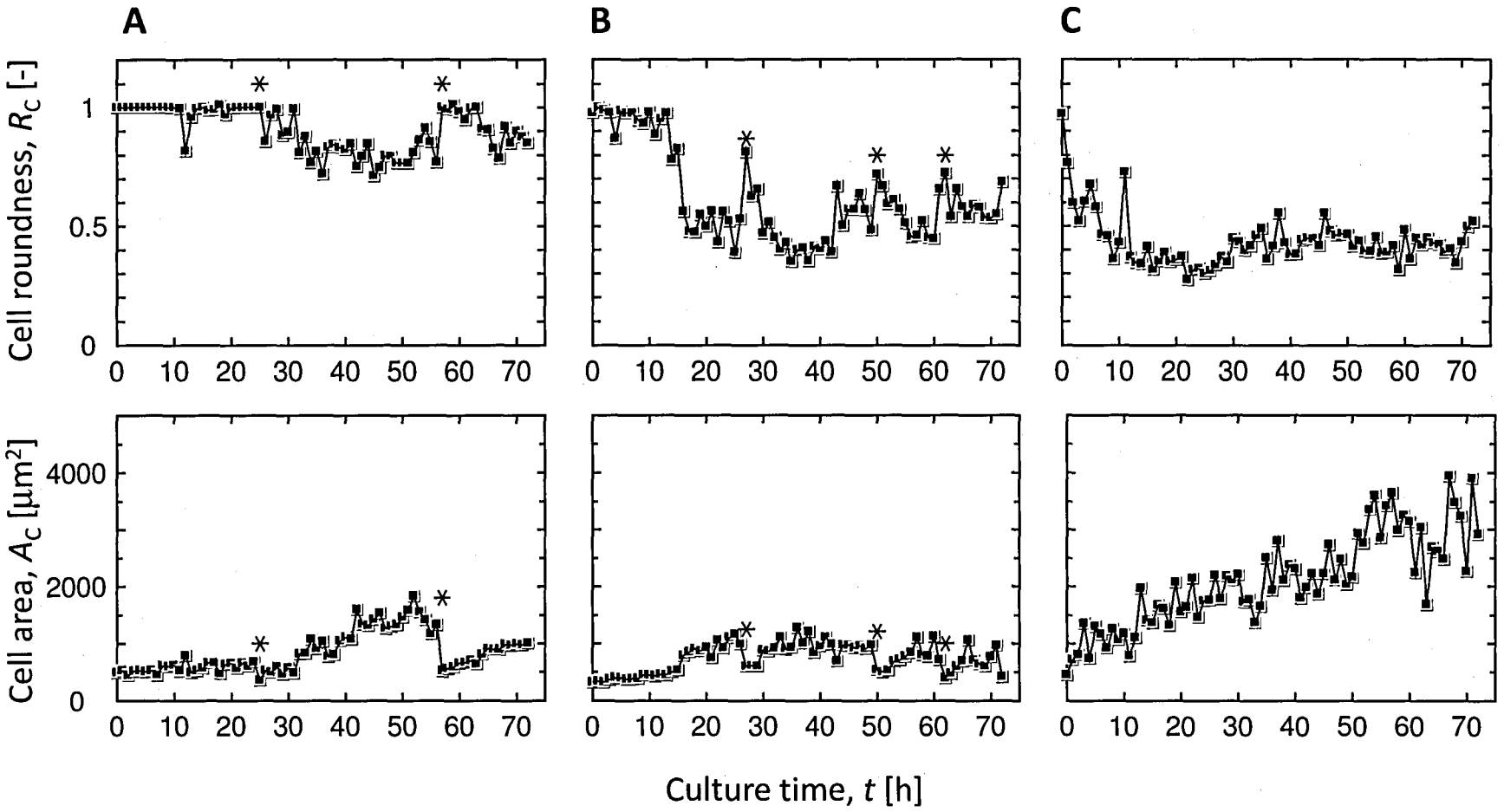

Fig. 2.2 Representative time-lapse variations of R_C and A_C of ALP-negative chondrocytes at PD = 6.6. The morphological evaluation was conducted for the dividing round-shaped cell (A), dividing spindle-shaped cell (B), and non-dividing spindle-shaped cell (C). The time of cell division is indicated by the asterisk.

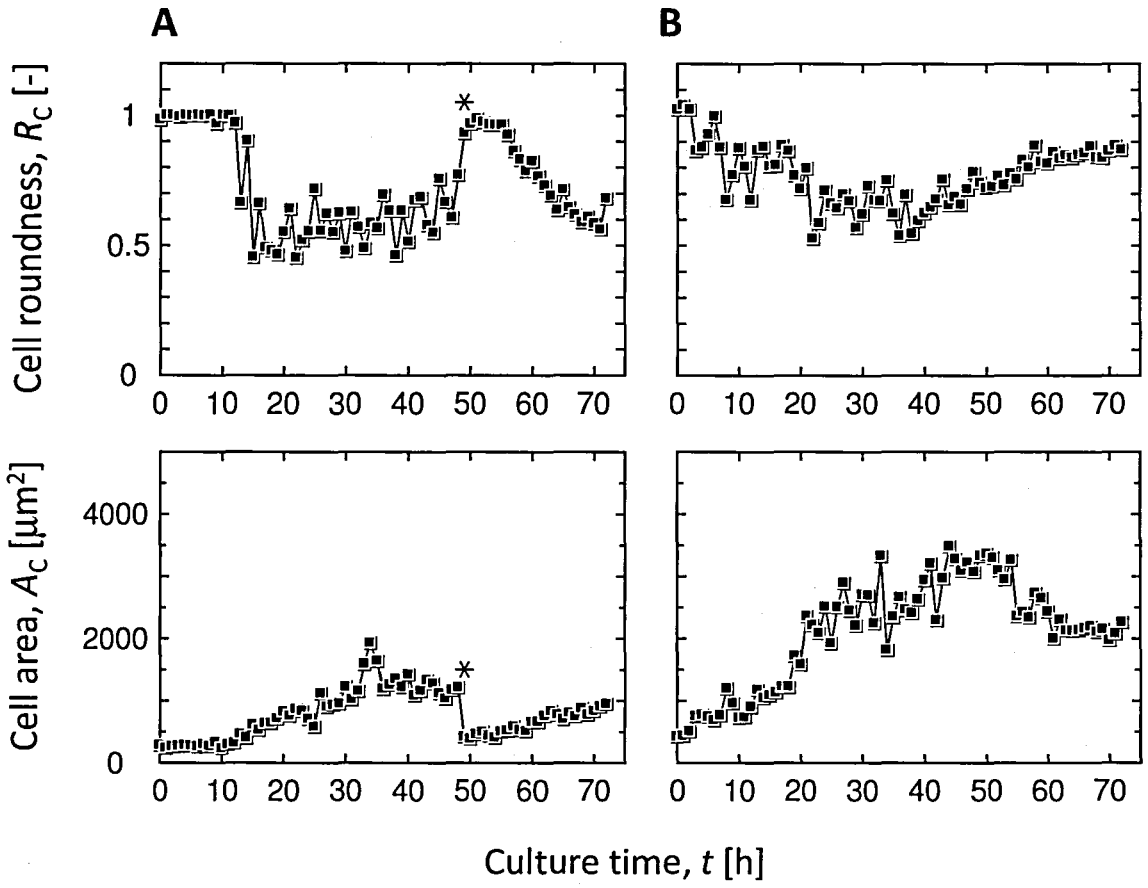

Fig. 2.3 Representative time-lapse variations of R_C and A_C of ALP-positive chondrocytes at PD = 6.6. The morphological evaluation was conducted for the dividing polygonal shaped cell (A), and non-dividing polygonal shaped cell (B). The time of cell division is indicated by the asterisk.

From the evaluation concerning occurrence of cell division during 72 h, it was revealed that the frequency of dividing cells without ALP activity was predominant at PD = 0 (**Fig. 2.5**). With an increase in PD, the frequencies of dividing cells with and without ALP activity gradually decreased, followed by an increase in the frequency of non-dividing cells without ALP activity. On the other hand, the frequency of non-dividing cells which possessed ALP activity was the highest at PD = 6.6.

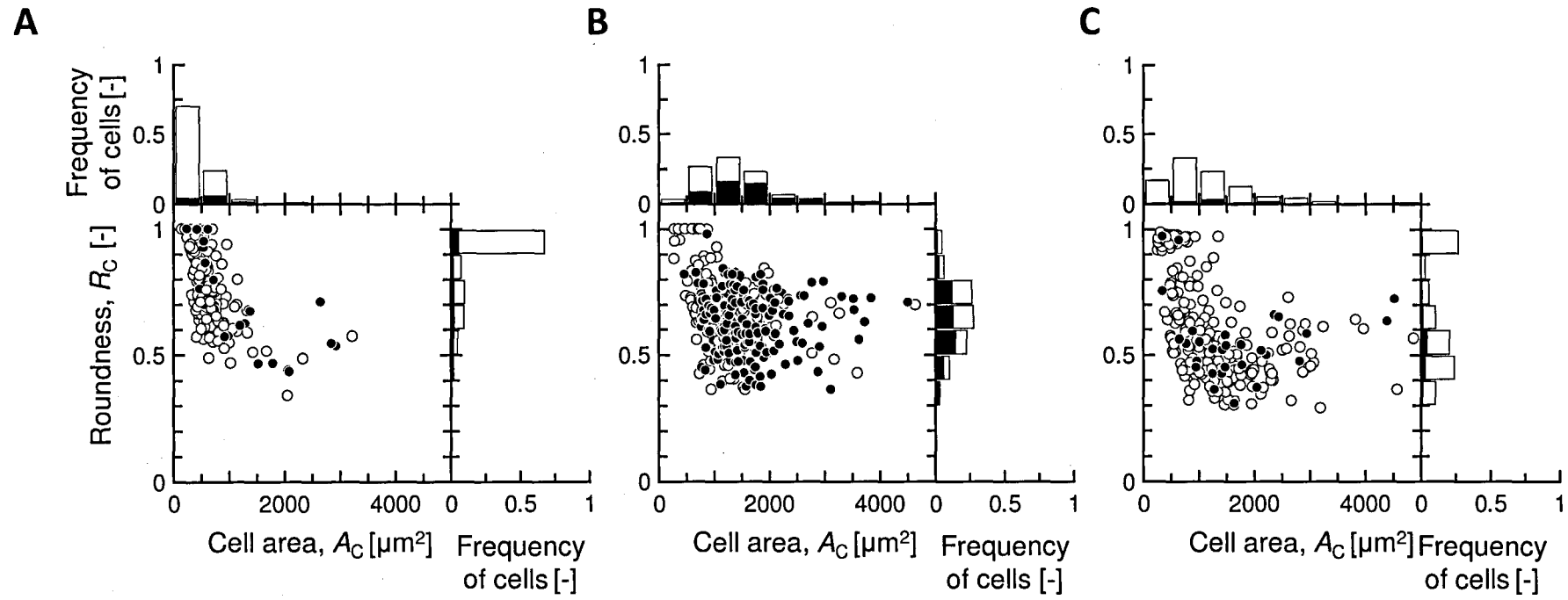

Fig. 2.4 Correlation between R_C and A_C values of chondrocytes at PD = 0 (A), PD = 6.6 (B), and PD = 14.5 (C). The data represent the analytical results obtained from more than 100 cells. Symbols: Closed bar and circle; ALP-positive cells, and open bar and circle; ALP-negative cells.

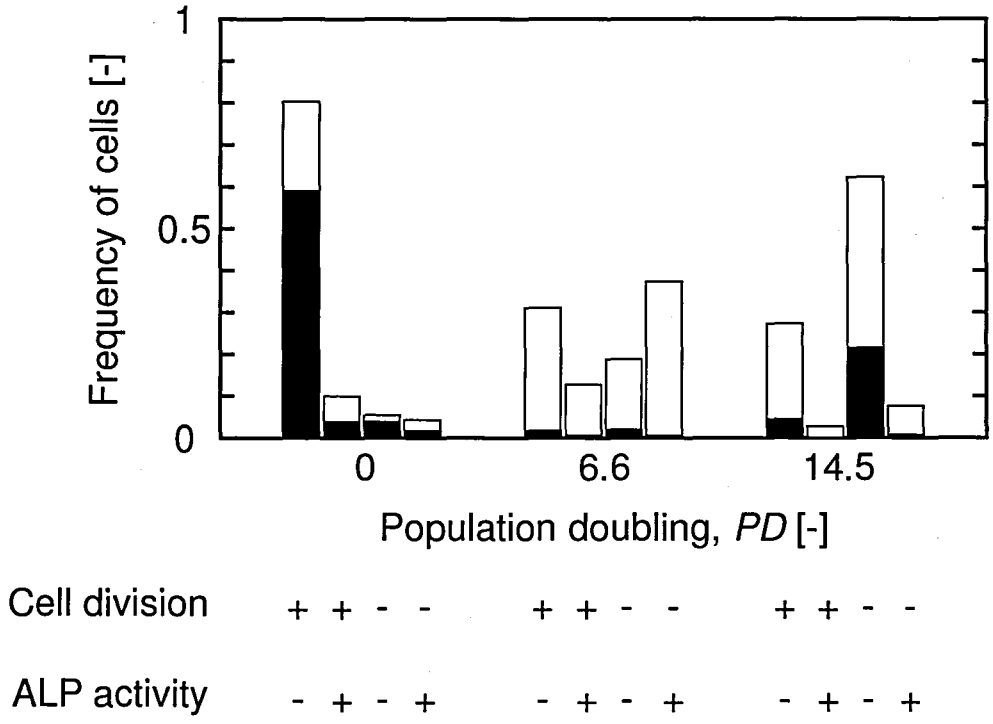

Fig. 2.5 Change in cell population types with increasing population doubling. The data represent the analytical results obtained from more than 100 cells. Symbols: Closed bar; cells with $R_C > 0.9$, and open bar; cells with $R_C < 0.9$.

To understand the phenotypes in cell population, the analyses of differentiation, dedifferentiation and terminal differentiation for passaged chondrocytes were conducted by gene expressions of collagen types I, II and X, respectively, at t = 24 h. As shown in **Fig. 2.6**, with increasing in *PD*, the collagen type I expression increased. On the other hand, both expressions of collagen types II and X were enhanced at *PD* = 5.1. The gene expression analyses were in fair agreement with the observation of cell morphology as well as cell-dividing and ALP activity patterns, indicating the progression of differentiated cells toward dedifferentiated and terminal differentiated states along with senescence.

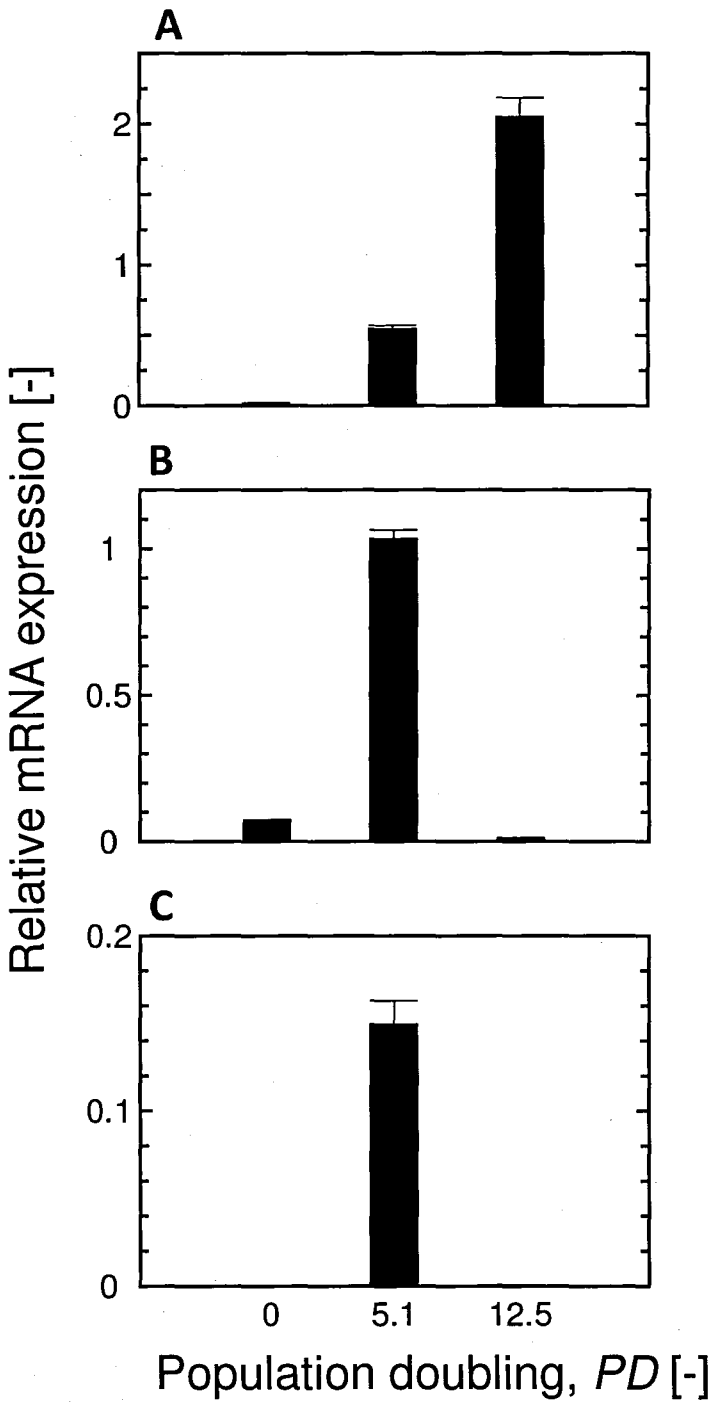

Fig. 2.6 Gene expressions of collagen types I (A), II (B), and X (C) in chondrocytes at various *PD* levels on CL substrate. The data represent the average values with the SDs determined from triplicate independent experiments.

2.3.3 Variation in cell population of chondrocytes embedded in collagen gel

The populations of chondrocytes passaged at various *PD* levels were embedded in the collagen gels. At 14 days, cell morphology in the populations which corresponded young, middle and old ages (*PD* = 0, 7.2 and 12.5, respectively) was estimated in a semi-quantitative manner by confocal laser scanning microscopy. As seen in **Fig. 2.7**, it was found that almost

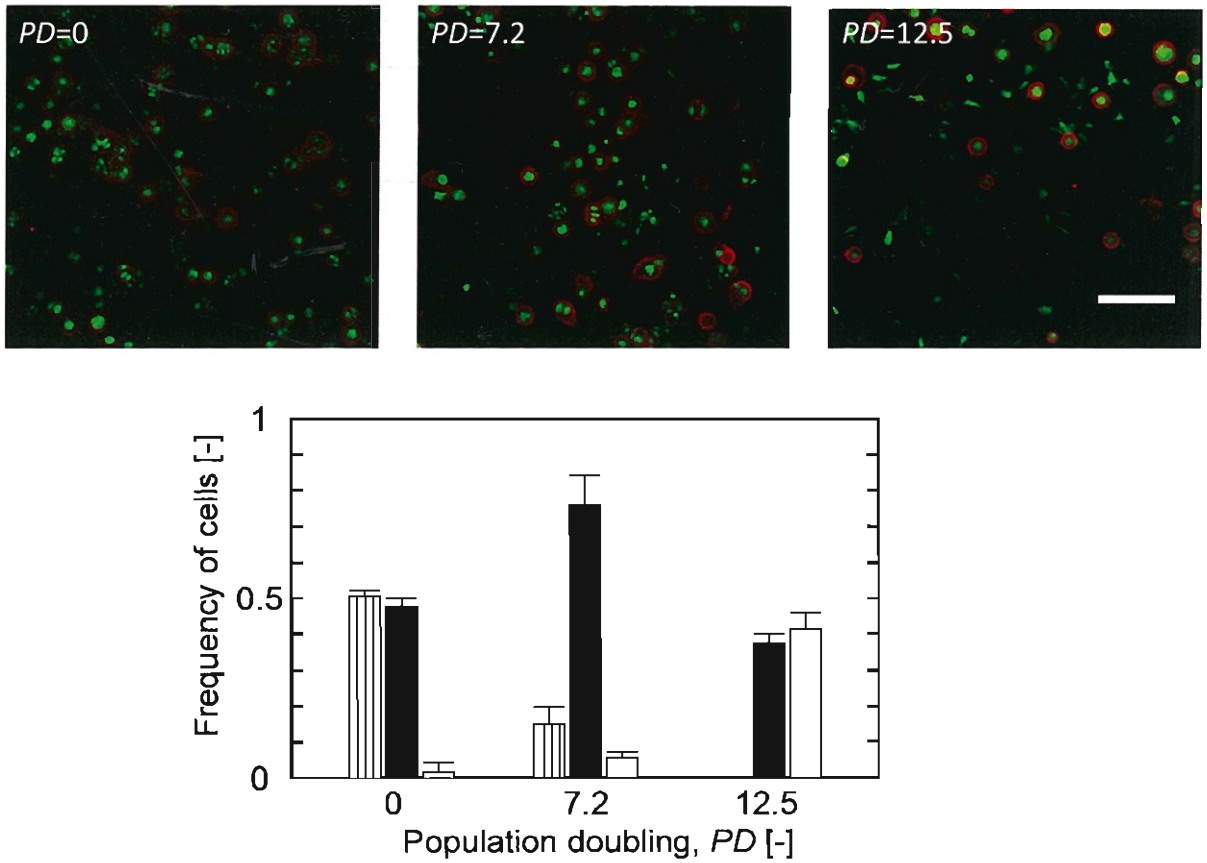

Fig. 2.7 Fluorescent images showing cytoplasm (green) and collagen type II (red) production of chondrocytes, and semi-quantitative estimation of cell population types of chondrocytes embedded in CL gels at various *PD* levels. The data represent the analytical results obtained from more than 60 cells examined in triplicate independent experiments. Symbols: Vertically striped bar; aggregated cells with collagen type II formation, open bar; spindle-shaped cells without collagen type II formation, and closed bar; single hypertrophic cells with collagen type II formation. The scale bar shows 200 μm.

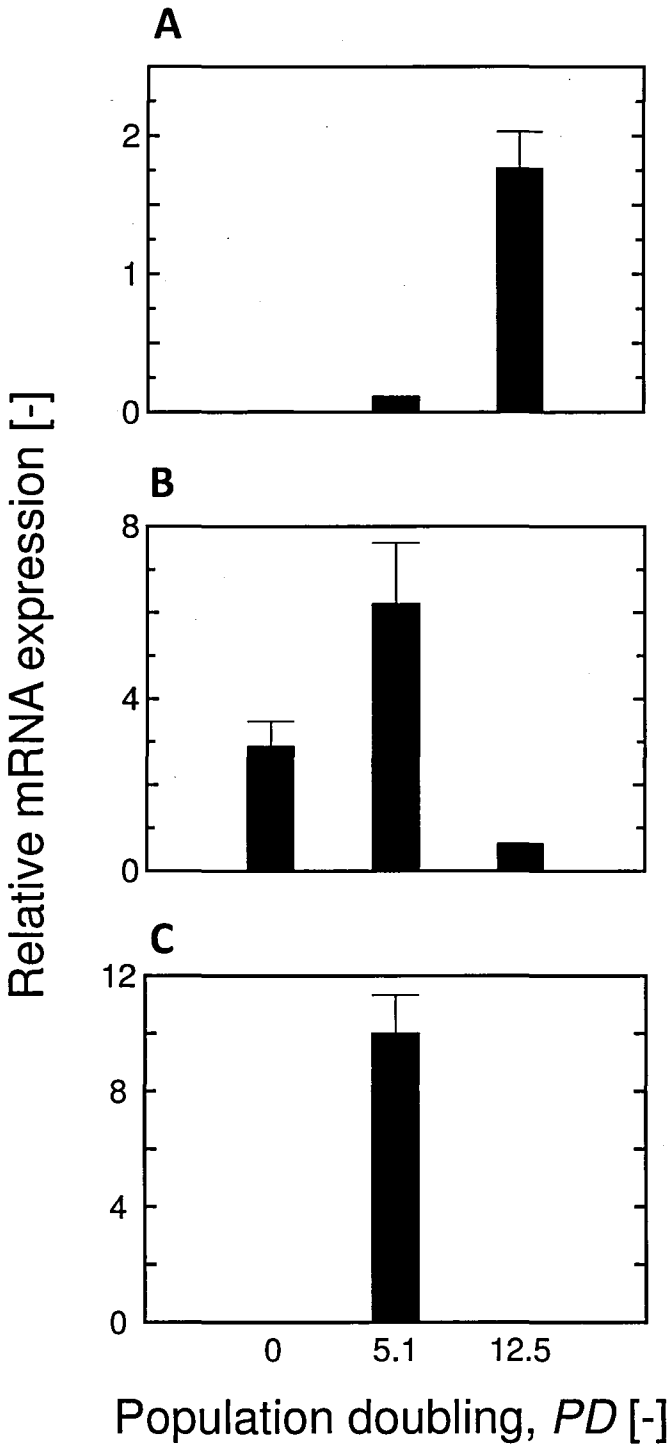

Fig. 2.8 Gene expressions of collagen types I (A), II (B), and X (C) in chondrocytes embedded in CL gels at various *PD* levels. The data represent the average values with the SDs determined from triplicate independent experiments.

all cells at *PD* = 0 were either aggregated or single hypertrophic cells producing collagen type II. On the other hand, the cells at *PD* = 7.2 were predominantly single hypertrophic cells with collagen type II production. An increase in *PD* led to the increased frequency of spindle-shaped cells without the expression of collagen type II whereas the frequencies of aggregated and single hypertrophic cells decreased.

Figure 2.8 shows the gene expressions of cells in the CL gels at various *PD* levels. With an increase in *PD*, the gene expression of collagen type I increased. On the other hand, the expressions of collagen types II and X were maximized at *PD* = 5.1, similarly to those trends on the CL substrate. These results mentioned above support the thought that the cell population composed of three phenotypes, namely differentiated, terminal differentiated and dedifferentiated cells.

2.4 Discussion

The current study was conducted to understand in detail the relation between cellular behaviors and cell phenotypes, which seems to be difficult to obtain by conventional techniques. It is well-known that cell phenotypes are regulated by interactions between cells and their surroundings, which are mediated by cell surface receptors such as integrins that bind to various molecules of the ECMs (Hirsch *et al.*, 1997). Cell morphologies on a collagen substrate, as described by the "receptor saturation model" (Gaudet *et al.*, 2003), are the effects of the interactions between cells and substrate through the quantitative balance of cell's integrin receptors and ligand-binding sites. In the case of substrate with high ligand density, strong inhibition of cell spreading takes place because the integrin receptors become saturated by the ligands and the bound receptors become clustered into a smaller area on the substrate. It has been reported that the blocking of integrin ß1 inhibited cell stretching in

culture of dermal fibroblast cells in collagen gels (Fujimura *et al.*, 2007), suggesting that the cell morphology in collagen gel relies on the exhibited balance between cell's integrin receptors and binding sites on collagen fibers in the gel, likewise in the case of cell morphology on the CL substrate.

In the previous study (Kino-oka *et al.*, 2009), the frequencies of round-shaped cells on the CL substrate and spherical-shaped cells in the CL gel were estimated and a convex relationship between these two parameters was observed. Furthermore, it was demonstrated that the analyses of collagen types I and II genes, which are typically expressed in differentiated and dedifferentiated chondrocytes, respectively, helped to understand the cell phenotypes in the CL gel by using the CL substrate. In the current study, the CL substrate was found to draw out the potential of chondrocyte's terminal differentiation, which was unattainable by using the PS surface (**Fig. 2.1**). Thus, the CL substrate was utilized as an evaluation tool to grasp the cell heterogeneity, being focused on terminal differentiated cells.

It is generally recognized that during passages *in vitro* a main fraction of the cell population consists of cells with lower replicative properties (Cristofalo and Sharf, 1973). In the previous study (Kino-oka *et al.*, 2005b), the time profiles of chondrocyte propagation in serial subcultures on the PS surface were valuated in terms of *PD* value. A linear increase in *PD* with elapsed culture time was observed up to $PD = 6$, keeping almost a constant of specific growth rate. However, a further increment of *PD* close to $PD = 7$ led to lowering in specific growth rate, which was considered to result from terminal differentiation of the cells. This relation between *PD* value and cell propagation is supported by the report that cell aggregates raised by division were observed evidently in the CL gel seeded with chondrocytes at $PD = 0$, but in the case of seeding at $PD = 7.2$, the singly existing cells emerged without division (Kino-oka *et al.*, 2009).

A distinctive feature of chondrocytes on 2-D culture is that they display a rounded or polygonal morphology and this morphology has been correlated with the synthesis of cartilage protein (Enomoto *et al.*, 2004; Horton and Hassel, 1986). Thus, the frequency of round-shaped cells on the CL substrate was considered to be an appropriate parameter to estimate the extent of differentiation in cell population during monolayer growth (Kino-oka *et al.*, 2009). In the present study, a decrease in the frequency of round-shaped cells at *PD* = 6.6 (**Fig. 2.4B**) was accompanied with an increase in gene expressions of collagen types I, II and X (**Fig. 2.6**). Since the expression of collagen type X is paralleled with that of collagen type II (Habuchi *et al.*, 1985; Solurch *et al.*, 1986; Adams and Shapiro, 2002), a majority of the collagen type II expression was considered to be attributed from terminal differentiated chondrocytes. These suggest that with increasing *PD*, chondrocytes undergo either terminal differentiation or dedifferentiation. **Figure 2.9** illustrates the possible change of chondrocytes toward terminal differentiated and dedifferentiated cells. Although terminal differentiation is associated with hypertrophy, in the current study, ALP-positive cells were found to be in polygonal shape on the CL substrate. In addition, an increase in cell area occurred at the initial stage of chondrocyte progression to terminal differentiation. A further increase was observed in the frequency of non-dividing chondrocytes with ALP activity, which implies the maturing of terminal differentiation. Another finding showed the progression of chondrocytes toward dedifferentiation. The spindle-shaped cells without ALP activity could proliferate, being a typical feature of dedifferentiated chondrocytes (Dominice *et al.*, 1986). In addition, the repetition of cell division led to cellular senescence, which can be explained from the enlargement of cell size (**Fig. 2.2C**), being a typical pattern of cell senescence (Cristofalo and Kritchevsky, 1969), and from the increased frequency of non-dividing cells without ALP activity (**Fig. 2.5**), together with the gene expression of collagen type I (**Fig. 2.6A**) with increasing *PD*. The increased frequency of cells with

$R_C > 0.9$ found at $PD = 14.5$ (**Fig. 2.4 C**) can be attributed to the temporal stretching of senescence cells.

The dedifferentiated chondrocytes are known to redifferentiate and up-regulate the synthesis of cartilage matrix proteins when placed in 3-D cultures. Mukaida *et al.* (2005) reported that the dedifferentiated chondrocytes, which was passaged on the PS surface, resulted in hypertrophic differentiation in a 3-D culture. In the present study using various populations of passaged chondrocytes, the fluorescence images of cells cultured at 14 days (**Fig. 2.7**) revealed three phenotypes, i.e., aggregated cells or singly occurring large cells with collagen type II formation, or spindle-shaped cells without collagen type II formation. Moreover, **Fig. 2.6 and 2.8** coincidently indicate that the gene expression of collagen type X was enhanced in the cell population at the middle age of *PD* not only on the CL substrate but also in the CL gel ($PD = 5.1$), compared with those at young and old ages of *PD* levels ($PD = 0$ and 12.5, respectively), and that this enhancement of collagen type X expression was particularly evident in the CL gel. This fact was in accordance with the observation that hypertrophic differentiated cells appeared in the population at middle age of *PD* level (**Fig. 2.7**). These findings suggest that the apparent redifferentiation in the CL gel is possibly caused by the hypertrophic differentiation.

In conclusion, this chapter revealed the cell potential of terminal differentiation accompanied by ALP activity at various *PD* levels, resulting in the characterization of terminal differentiated cells which exhibited the polygonal and relatively large shape ($R_C < 0.9$ and $1000\ \mu m^2 < A_C < 2000\ \mu m^2$, respectively). In the cell population at middle age, the frequency of the terminal differentiated cells increased compared with those in cell populations of young and old ages. The gene analysis suggested that the up-regulation of collagen type II expression in cell population at middle age was attributed not to

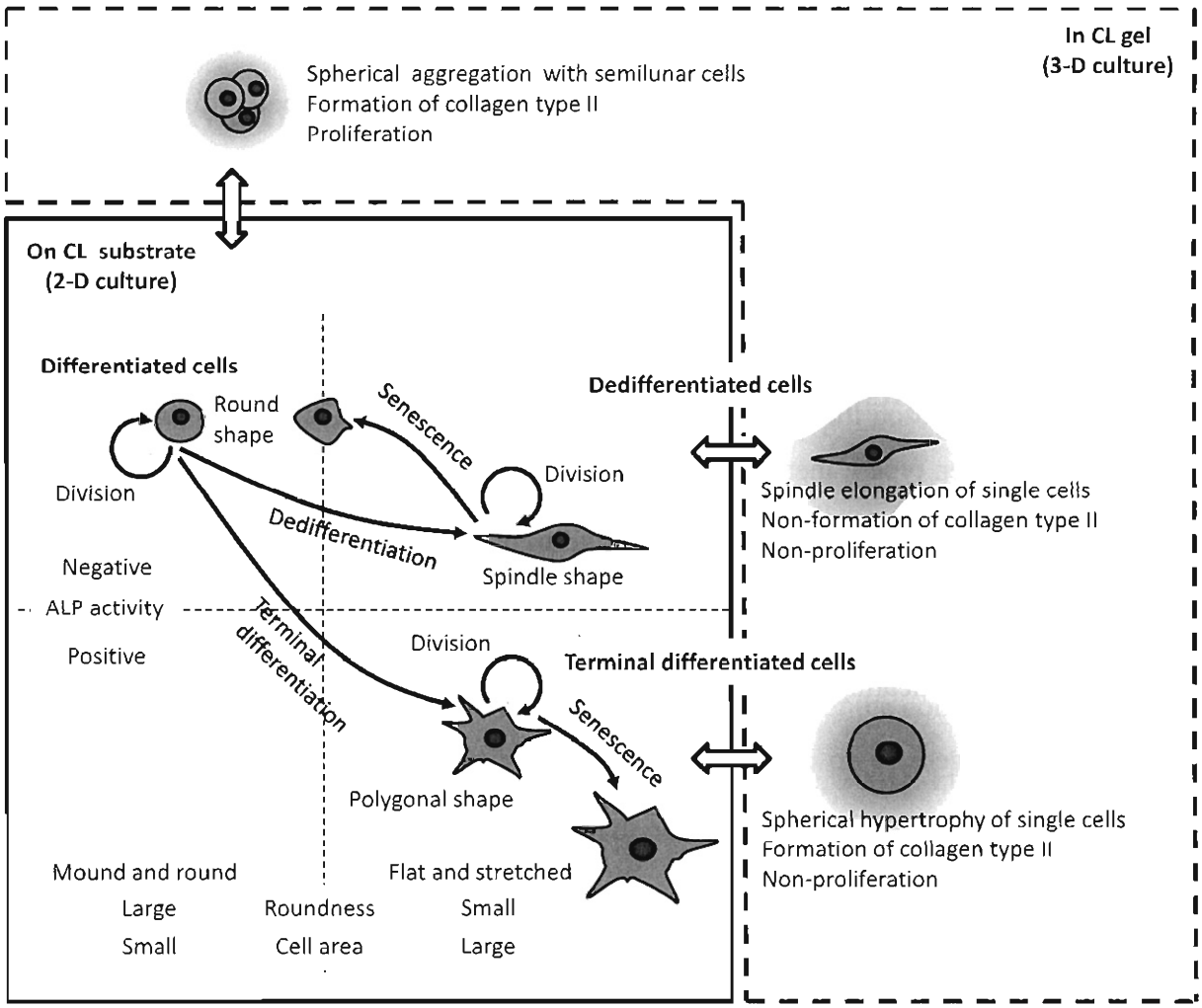

Fig. 2.9 Comprehensive illustration showing development of heterogeneous chondrocyte population on CL substrate (2-D culture) in relation to cell behavior in CL gel (3-D culture).

redifferentiation but to terminal differentiation. In addition, the dedifferentiated cells which made cell division and exhibited spindle shape without ALP activity increased with increasing *PD*. Further increment in *PD* caused the higher frequency of non-dividing and relatively small cells without ALP activity, suggesting the senescence of dedifferentiated cells.

2.5 Summary

The CL substrate was used to draw out the potential of terminal differentiation in chondrocytes in passaged cultures, which is unattainable by a PS surface, and was used as a tool to evaluate cell quality in three-dimensional culture with the collagen gel. With increasing age of cell population (*PD* = 0 to 14.5), the frequency of non-dividing spindle-shaped cells without ALP activity increased, accompanied with an increase in gene expression of collagen type I, meaning the senescence of dedifferentiated cells. At the middle age of cell population (*PD* = 5.1 and 6.6), the high frequency of polygonal shaped cells with ALP activity existed on the CL substrate together with up-regulated expressions of collagen types II and X, indicating the terminal differentiation of chondrocytes. When the chondrocytes passaged up to the middle age were embedded in collagen gel, the high frequency of single hypertrophic cells with collagen type II formation was recognized, which supports the consideration that the high gene expression of collagen type II was attributed to terminal differentiation rather than redifferentiation.

Part 2

Availability of nutrients in collagen gels during culture

The implantation of tissue-engineered construct is a potential treatment for articular cartilage defects. However, the creation of clinically relevant construct with spatially uniform cell distribution and sufficient quantities of ECM components still poses a challenge. One of the extremely important issues in the development of tissue-engineered cartilage is the nutrient transport. It is typical for viable tissue to form in the peripheral region of scaffold whereas the interior unable to support the growth of tissue due to lack of adequate diffusion (Ishaug-Riley, 1997). It has been reported that in a static culture, the concentrations of gases (O_2 and CO_2) were depleted in the culture media (Gooch *et al.*, 2001). In addition, the static culture condition caused the decreased growth rates of chondrocytes and low ECM (glycosaminoglycans (GAG) and collagen) production (Freed *et al.*, 1994; Pazzano *et al.*, 2000). Since transport within the scaffold in a static culture is mainly a function of passive diffusion, thorough understanding of the diffusion characteristics is critical for improving the quality of cultured construct.

From the viewpoint mentioned above, a direct measurement system was constructed to estimate the dissolved oxygen (DO) level in a cultured cartilage of a static culture in Chapter 3. In addition, enhancement of oxygen supply to the culture was conducted by introducing a shaking operation and a gas-permeable bottom. In Chapter 4, a system mimicking the peripheral of the CL gel was utilized to clarify the influence of ECM and cell cytoplasm on nutrient diffusion. In the last chapter, Chapter 5, a strategy was proposed to improve the inner region of scaffold for the formation of high quality chondrocyte aggregates.

Chapter 3

Dissolved oxygen concentration in collagen gels

3.1 Introduction

Brittberg *et al.* (1994) have established the autologous transplantation procedure using chondrocyte suspension through *in vitro* expansion, and made notable contribution to repairing defective parts. In this procedure, however, the chondrocyte expansion was conducted by a 2-D culture, causing low productivity of ECM. Ochi *et al.* (2004) proposed the use of tissue-engineered construct prepared by culturing chondrocytes in collagen gel. The construct through the 3-D culture led to higher production of ECM (Uchio *et al.*, 2000). However, the 3-D environment is expected to be under the insufficient supply of nutrients to cells inside the construct, which results in the deterioration of cell growth (Heywood *et al.*, 2004).

DO is a key nutrient to govern the growth activity. Kellner *et al.* (2002) indicated the distribution of DO in a cylinderal cultured cartilage, concluding that insufficient DO supply inside the cultured cartilage yielded an acellular region where the cell growth was severely suppressed. In the previous work (Kino-oka *et al.*, 2008), a static culture of rabbit chondrocytes embedded in collagen gel was performed according to the procedure reported by Ochi *et al.* (2004), and the confocal laser scanning microscopy revealed the heterogeneous cell distribution with growth deterioration in a deeper region from top surface of gel, suggesting the lack of nutrients in this deeper region. In the present study, a direct measurement system to estimate DO level in the tissue-engineered construct was constructed using an optical fiber sensor, and the spatial distributions of cells and DO were analyzed. In addition, the culture condition was modified by use of a shaking vessel with a gas-permeable

bottom to examine the effect of improved oxygen supply on the distribution profile of the cells in the gel.

3.2 Materials and Methods

3.2.1 Cell embedding in collagen gels

For static culture of rabbit chondrocytes, freshly isolated cells were suspended in culture medium and then mixed with a 4-fold volume of 3% Atelocollagen solution (Koken Co., Ltd.) at seeding cell density of 2.0 x 10^6 cells/cm^3. The gel placed on a 60 mm culture dish (Corning, Inc.) was incubated statically at 37°C under 5% CO_2 in air using medium as described elsewhere (Kino-oka *et al.*, 2008). Medium changes were conducted every two days. For shaking culture, the dish was put on a solid-geometrical rotary shaker (Mini shaker SHM-2001; LMS Co., Tokyo) at 20 rpm with an incline of 7°. A modified dish soled with gas-permeable film (Lumox™ dish; Greiner Bio-One, Frickenhausen, Germany) was employed for improving oxygen supply to the cells in the gel.

3.2.2 Determination of spatial cell distribution

For analyzing overall cell density in each gel (X), the triplicate samples were harvested, and the cells were suspended by the enzymatic digestion of gel, followed by direct cell counting on a hemocytometer (Kino-oka *et al.*, 2008). The local cell density in the gel ($\hat{X}$) was estimated using an FV300 CLSM (Olympus) with a spatial cell distribution analyzer (SCDA) as shown previously (Kino-oka *et al.*, 2008). In brief, a gel specimen was applied to the double-staining for living cell cytoplasm by CellTracker™ Green CMFDA (Invitrogen, Carlsbad, CA, USA) and for nucleus by TO-PRO3 (Invitrogen). The stained specimen was

subjected to the analysis of spatial cell distribution, and the custom-made software performed the quantitative determination of spatial cell positions in the specimen. The probability (P_C) of cell existence in a local region at given depth (Z) from top surface of the specimen was defined as follows.

$$P_C = \frac{\text{Regional number of cells existing at given depth, } Z}{\text{Total number of cells on examined stereoscopic image}} \quad (3.1)$$

The local cell density at a given region in each gel was obtained from $\widehat{X} = P_C X V_g / \hat{V}_g$, where V_g is the total volume and $\hat{V}_g$ is the volume at the local region. Here, the gel geometry is assumed to be a cylinder shape, so that the volume fraction is rearranged on a depth basis.

3.2.3 Measurement of DO concentration

Figure 3.1 shows the experimental set-up to measure a DO profile in a gel piece, employing an oxygen microsensor (PreSens Co., Regensburg, Germany) furnituring a needle of optical fiber with 3 mm naked sensing tip (50 μm in diameter) connected to an oxygen meter (Microx TX3; PreSens Co.).

The needle was inserted into cultured gel set on a dish with medium. The dish was placed on an electrically-driven stage (MMU-60; Chuo Precision Industrial Co., Tokyo) to control the position in vertical and horizontal directions. The DO measurement was performed under 5% CO_2 atmosphere at 37°C. If necessary, the medium was stirred by a magnetic bar for mimicking a shaking culture condition. Prior to the measurement, the top of gel was positioned manually at the sensor tip. Precise approach was confirmed using a camera (Artcam-300MI; Artray Co., Tokyo) equipped with a macro lens to define a boundary position, $Z = 0$. Then, the stage was elevated to introduce the sensor tip to $Z = 2.0$ mm in gel. After achieving a steady state of DO concentration, the sensor was pulled out through gel

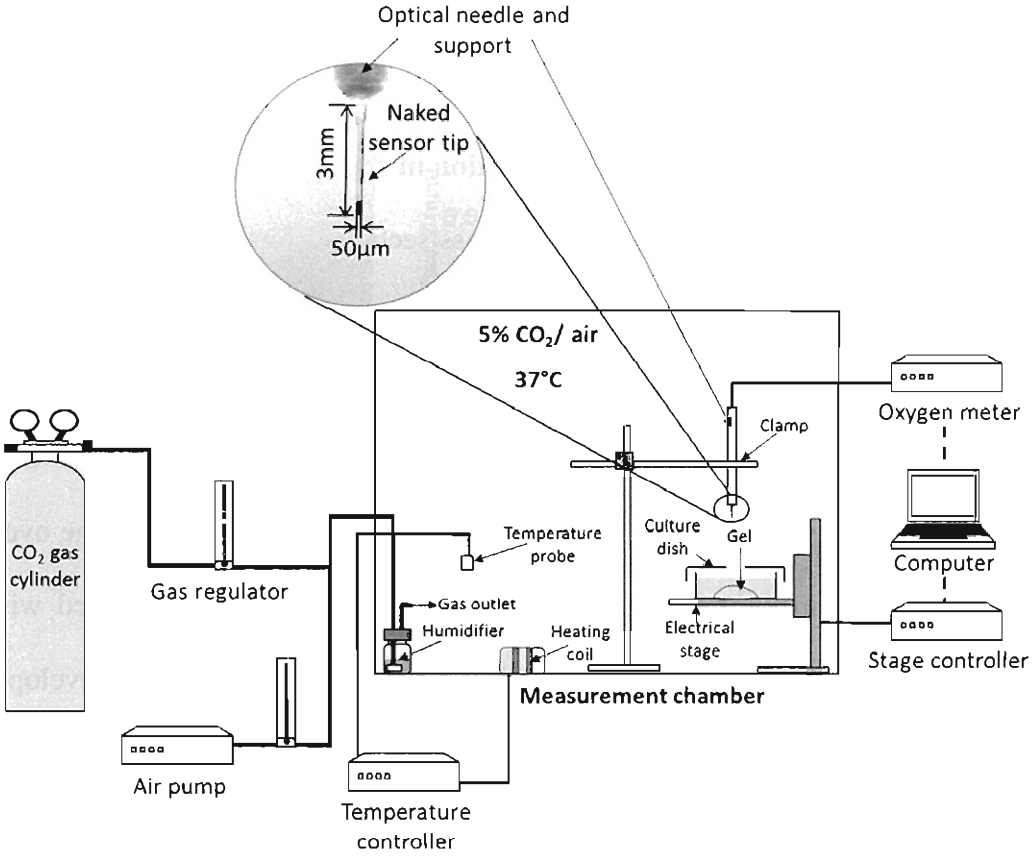

Fig. 3.1 Experimental set-up for measuring of DO concentration in gel. The dashed lines indicate signal flows to regulate the 3-D position of measurement.

gradually at a 20 μm step. The DO concentration at a given depth ($\widehat{C}_O$), was determined by averaging five measurements. The measurement interval was set to be 5 min. These procedures were executed automatically by using a custom-made program on LabVIEW software (National Instruments, Austin, TX, USA). Data were recorded as an average of triplicate samples, with the statistical-analysis using unpaired *t*-test.

3.3 Results

3.3.1 Profiles of cell density and DO concentration in static culture

Figure 3.2A shows the representative cross-sectioned images of cell distribution in the gels sampled at culture time, t = 7, 14 and 21 days in the static cultures (Condition 1). At t = 7 days, homogenous distribution of cells in the gel appeared with small cell aggregates. With elapsed time, the cell division occurred to form cell aggregates and the active proliferation was observed at the rim close to the gel surface. At t = 21 days, the overall cell density was achieved to be X = 1.0 x 10^7 cells/cm^3, and the gel was covered with cells, although the smaller aggregates existed in the deeper part of gel, developing the heterogeneity of spatial cell distribution. As seen in **Fig. 3.2B**, the local cell density ($\widehat{X}$) was found to be constant along gel depth at t = 7 days. With elapsed time, $\widehat{X}$ at the top surface ($0 < Z \leq 0.13$ mm) increased, achieving $\widehat{X}$ = 1.7 x 10^7 cells/cm^3 at t = 14 days, which was 9.5 times higher than that at the bottom in the gel (1.88 mm $< Z \leq$ 2.0 mm). The active growth until t = 21 days formed the dense cell layer with $\widehat{X}$ = 5.7 x 10^7 cells/cm^3 at the top surface in the gel, although the growth at the bottom was found to be low, being $\widehat{X}$ = 5.0 x 10^6 cells/cm^3. These suggested that the limitation of nutrient supply caused the low activity of cell growth at the deeper part of the gel. Concerning DO profile in the gel, as shown in **Fig. 3.2C**, $\widehat{C}_O$ was kept almost constant at t = 7 days, giving $\widehat{C}_O$ = 0.17 mol/m^3 on average, which was slightly smaller than the saturation level of DO under the experimental conditions (C_O^* = 0.21 mol/m^3). With elapsed time, $\widehat{C}_O$ at Z = 0 drastically decreased, achieving $\widehat{C}_O$ = 0.07 mol/m^3 at t = 21 days, which was two-fifth of that at t = 7 days. In addition, $\widehat{C}_O$ at t = 21 days gradually decreased along with gel depth and reached $\widehat{C}_O$ = 0.03 mol/m^3 at Z = 2.0 mm, which was one-sixth of that at t = 7 days. These results suggested that an increase in local cell

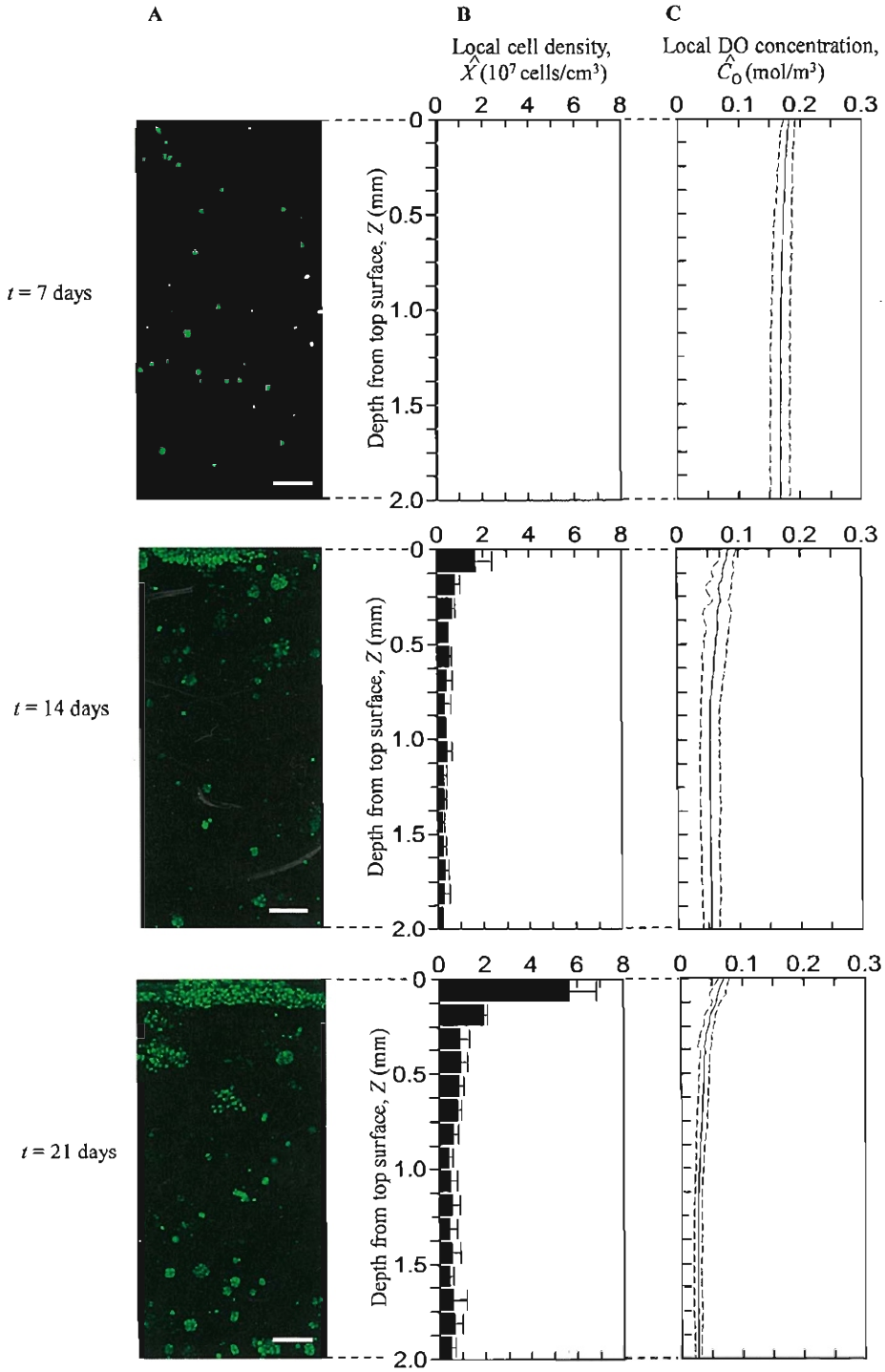

Fig. 3.2 Vertical profiles of cell density and DO concentration in static culture of chondrocytes embedded in gel (Condition 1). Fluorescent images of chondrocytes stained for cytoplasm. The scale bars represent: 200 μm (A). Local cell density estimated by SCDA. The bars show the SDs (B). Local DO concentration measured by optical sensor system. The solid and broken lines show the mean and 95% confidence interval, respectively (C).

density led to further demand of oxygen, and the limitation of oxygen transfer caused the lower level of DO not only inside the gel but also at top surface of the gel.

3.3.2 Profiles of cell density and DO concentration in culture with enhanced oxygen supply

To examine the influence of enhanced oxygen supply from top and bottom surfaces of the gel on the profiles of cell density and DO concentration inside the gel, the shaking cultures were performed for t = 21 days using the conventional dish (Condition 2) and the modified-bottom dish with gas-permeable film (Condition 3). The X values at t = 21 days were 2.1 x 10^7 and 2.9 x 10^7cells/cm^3 under Conditions 2 and 3, respectively, which were 2.1 and 2.9 times that in the static culture using the conventional dish (**Fig. 3.2**). As shown in **Fig. 3.3A**, the thickness of cell aggregates at the top region as well as the aggregate size at the bottom region in the gel increased under Condition 2. A further increase in the thickness of top region was observed under Condition 3 (**Fig. 3.4A**), although the aggregate size at the bottom region was almost equivalent to that under Condition 2. As shown in **Fig. 3.3B and 3.4B**, the packed cells existed in the ranges of $0 < Z \leq 0.25$ mm and $0 < Z \leq 0.5$ mm under Conditions 2 and 3, respectively, and $\widehat{X}$ at the top region ($0 < Z \leq 0.13$ mm) was at the levels of $\widehat{X}$ = 4.3 x 10^7 (Condition 2) and 3.0 x 10^7 cells/cm^3 (Condition 3), being almost the same as that under Condition 1. Although a decrease in $\widehat{X}$ along with Z occurred, $\widehat{X}$ at the bottom surface reached 7.2 x 10^6 and 1.3 x 10^7 cells/cm^3 under Conditions 2 and 3, respectively, being 1.4 and 2.6 times higher than that under Condition 1. In addition, as seen in **Fig. 3.3C**, the $\widehat{C}_O$ levels at the top region were enhanced, compared to that under Condition 1. Especially, $\widehat{C}_O$ at Z = 0 reached 0.18 mol/m^3 which was close to the saturation DO level of C_O^* = 0.21 mol/m^3. The $\widehat{C}_O$ under Condition 2 decreased drastically along with Z, approaching the value

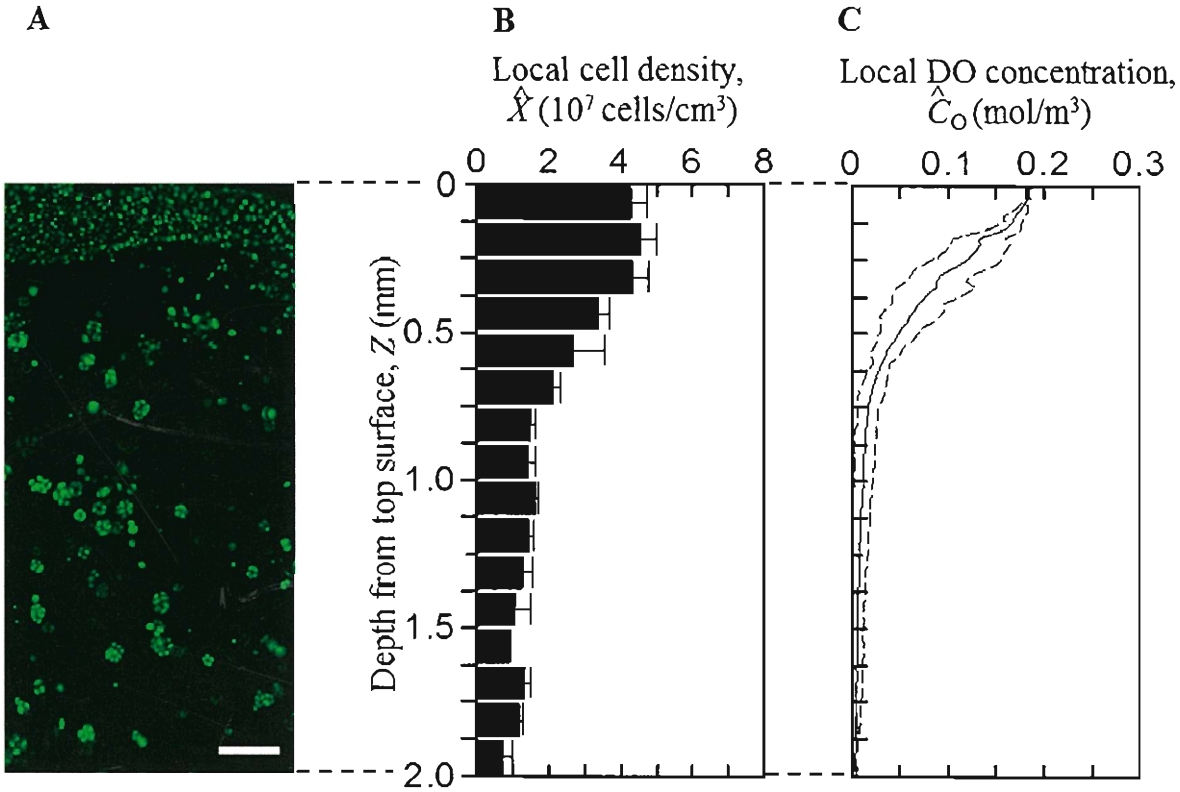

Fig. 3.3 Vertical profiles of cell densities and DO concentrations in shaking culture using conventional dish (Condition 2). Fluorescent images of chondrocytes stained for cytoplasm. The scale bars represent 200 μm (A). Local cell densities estimated by SCDA. The bars show the SDs (B). Local DO concentrations measured by optical sensor system. The solid and broken lines show the mean and 95% confidence interval, respectively (C).

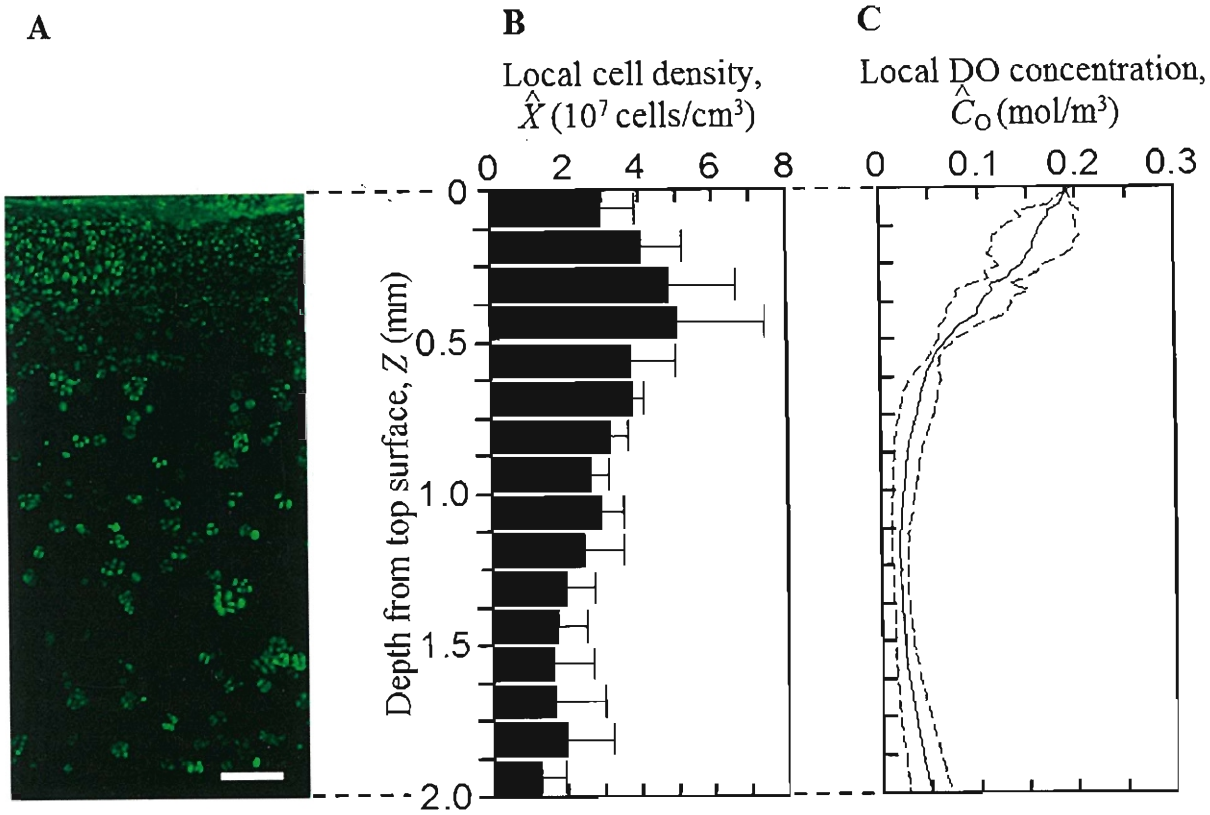

Fig. 3.4 Vertical profiles of cell densities and DO concentrations in shaking culture using modified dish with gas-permeable film at bottom (Condition 3). Fluorescent images of chondrocytes stained for cytoplasm. The scale bars represent 200 μm (A). Local cell densities estimated by SCDA. The bars show the SDs (B). Local DO concentrations measured by optical sensor system. The solid and broken lines show the mean and 95% confidence interval, respectively (C).

of $\hat{C}_O$ = 0.004 mol/m^3 at level Z = 2.0 mm, which was lower than that under Condition 1. The $\hat{C}_O$ profile under Condition 3 showed the different manner, compared to those under Conditions 1 and 2 due to oxygen supplement from the bottom surface, and $\hat{C}_O$ at Z = 2.0 mm was recorded to be 0.05 mol/m^3, which was 12.5 times higher than that under Condition 2.

3.4 Discussion

The heterogeneous distribution of chondrocytes has been reported in the 3-D constructs of cultured cartilage (Kellner *et al.*, 2002; Kino-oka *et al.*, 2008; Park *et al.*, 2007; Kobayashi *et al.*, 2008), suggesting that the uneven nutrient concentration inside the construct occurred through the balance of nutrient consumption and possible components, which become rate-determining substrates for proliferation, are glucose, proteins and/or oxygen.

In the culture of bovine chondrocytes, Malda *et al.* (2003) reported that the cell proliferation on micro-carriers was not affected in the DO range of 4×10^{-2} to 2.1×10^{-1} mol/m^3. In has been reported that the low DO level of 3×10^{-2} mol/m^3 had a suppressive effect on the proliferation of rabbit chondrocytes, giving a saturation constant of $K_o = 6.3 \times 10^{-2}$ mol/m^3 in a Monod-type equation (Yashiki *et al.*, 2004; Kino-oka *et al.*, 2005a). The reduction of growth activity caused by the low DO level can be responsible for allowing a factor to provide the uneven cell distribution in the cultured tissues. Concerning the chondrocyte differentiation, Grimshaw and Mason (2005) demonstrated that the expressions of aggrecan genes remained unchanged in the alginate-embedded culture of bovine chondrocytes in the DO range of 0 to 2.1×10^{-1} mol/m^3, associated with the up-regulation of collagen type II as well as the down-regulations of interleukin-1β, transforming growth factor-β and connective tissue growth factor under a hypoxic condition. On the other hand, Murphy and Polak (2004) performed the alginate-embedded cultures of human chondrocytes at the DO concentrations of 5×10^{-2} and 2.1×10^{-1} mol/m^3, and reported that the gene expressions of collagen type II as well as aggrecan were up-regulated at the DO level of 5×10^{-2} mol/m^3. Malda *et al.* (2003) suggested that these contrary DO effects on the gene expressions in the cultures of chondrocytes may arise from the differences in the cell species and culture conditions employed.

Radisic *et al.* (2006) estimated the DO concentration in a disc-shaped construct of neonatal rat cardiomyocytes cultured in collagen scaffold for 16 days under a static condition, and showed that the DO concentration and cell viability decreased linearly and the living cell density decreased exponentially along the distance from the construct surface. In addition, they mentioned that medium flow significantly increased the DO concentration within the construct, which could be correlated with the improved tissue properties of the constructs cultured in a convectively mixed bioreactor.

Previous work (Kino-oka *et al.*, 2005a) reported the simulation of chondrocyte growth in the Atelocollagen gel by developing the kinetic model with DO as a rate-determining substrate and predicted heterogenous distributions in cell and DO concentrations in the gel. In addition, the predicted cell distribution was confirmed to have good agreement with the profile estimated by SDCA. The current work revealed that the cell distribution was related to that of DO concentration and the heterogeneities of cell density and DO concentration in the construct developed with elapsed time. The above-mentioned evidences suggested that the creation of DO gradient in the construct and active cell proliferation could occur dominantly in top surface of the construct. Once the gradient of cell concentration emerged along with distance from top surface, the cell clustering in the top surface made a barrier to oxygen diffusion into a deeper region of the construct, forming the heterogeneous distribution in DO concentration. Consequently, the heterogeneity of DO concentration makes insufficient supply of oxygen, causing low proliferation in a deeper region of the construct. Thus, the inevitable mechanism leads to developing in the heterogeneity of cell distribution.

In the static culture, the DO concentration at the surface of the gel decreased with elapsed time (**Fig. 3.2C**). The DO concentration in a liquid phase at the vicinity of the gel drastically decreased with approaching to the surface, although the DO concentration in a

bulk phase was almost equal to the saturation level (data not shown). A profile of DO concentration in a liquid phase was calculated by Zhou *et al.* (2008), indicating that the DO concentration at surface depended on the culture conditions including medium depth, volume of construct, cell density and so on, although the resistance of oxygen transfer at interface between liquid and solid was well known to be negligible in perfusion culture. Thus, the shaking culture was conducted in the current study (**Fig. 3.3**). This improvement of oxygen supply led to the increment of cell growth although the DO concentration in the deeper region decreased similarly to that in the static culture.

Further improvement of oxygen supply was carried out in the shaking culture using the dish with gas-permeable bottom (**Fig. 3.4**). In this culture, the DO concentration in deeper region was enhanced, compared to that in shaking culture with the conventional dish (**Fig. 3.3C**), and the growth in middle and deeper regions were slightly promoted, enhancing the cell density in whole construct. However, the cell density at the bottom was much lower than that at top surface, leading to the development of heterogeneous cell distribution similarly to those in static and shaking cultures using the conventional dish. In the previous study (Yashiki *et al.*, 2004), the culture was performed on a porous filter which can permeate the nutrients to supply at both sides of top and bottom of the construct, showing symmetrical cell distribution along with construct depth. These results suggest that macromolecules may be possible rate-determining substrates even under sufficient oxygen supply.

In conclusion, this chapter showed that in the static culture of rabbit chondrocytes, the heterogeneity of cell distribution in the gel notably developed owing to the limitation of oxygen supply into a deeper part of the gel. The shaking operation and use of gas-permeable bottom improved oxygen supply from the top and bottom surfaces of gel, respectively, and the enhancement of $\widehat{C}_O$ at top and bottom regions of the gel. This improvement facilitated the

cell proliferation, causing the thick region with packed cells expanded, compared to those in static and shaking cultures using conventional dishes. The local cell density at bottom surface was enhanced by the operation but the level was still lower than that at top surface, suggesting that limitation of alternative nutrients such as proteins caused insufficient growth under the improved conditions of oxygen supply.

3.5 Summary

In the static culture of rabbit chondrocytes in collagen gel, the direct measurement of DO concentration revealed that the DO level at the top surface of gel decreased due to an increase in overall cell density with elapsed time. The local cell density at the top surface on day 21 was 5.7×10^7 cells/cm^3, being 11 times that at the bottom of gel. This heterogeneity of cell distribution in the gel was considered to occur by limitation of oxygen supply into a deeper part of the gel. In the shaking culture using a dish with gas-permeable film, the DO level was enhanced inside the gel and the overall cell density in the gel was achieved to be 2.9 times that in the static culture.

Chapter 4

Effect of chondrocytes and extracellular matrix on nutrient permeation and diffusivity

4.1 Introduction

The typical paradigm for *in vitro* tissue engineering of articular cartilage involves the isolation and culture of donor chondrocytes within 3-D scaffold biomaterials under conditions that support tissue growth. However, one major constraint in the use of 3-D scaffolds has been tissue ingrowth within the constructs. Because cells located in the interior scaffold receive nutrients only through diffusion from the surrounding media in a static culture, the high cell density on the peripheral of the scaffold could lead to transport limitation and decreased nutrient permeability from the bulk solution into the scaffold (Freed *et al.*, 1994), causing a lower nutrient level and cell density inside the scaffold.

In a study on the supply of nutrients to cells from the nucleus pulposus of intervertebral discs, Horner and Urban (2001) demonstrated that glucose rather than oxygen was the critical nutrient. Similarly, in Chapter 3, even with the improvement in the oxygen supply in the bottom region of the CL gel, the local cell density was still lower than that at the top surface, suggesting that the insufficient growth was caused by limitations of alternative nutrients such as protein.

In the present work, nutrient diffusion and related changes in CL gel permeability to oxygen and the candidate protein bovine serum albumin (BSA) after long-term culture were evaluated using a system mimicking the periphery of the gel construct described in Chapter 3.

4.2 Materials and Methods

4.2.1 Preparation of system mimicking the gel periphery

Freshly isolated chondrocytes were introduced onto the 0.33 cm^2 membranes of Transwell® Permeable Supports (Transwell) and the 1.12 cm^2 membranes of Snapwell™ Inserts (Snapwell) placed in 24 and 12-well culture vessels (all purchased from Corning, Inc.), respectively, at an initial seeding density (X_0) of 1.0×10^5 cells/cm^2. The cells were cultured for the indicated time period at 37°C in a 5% CO_2 atmosphere using medium as described elsewhere (Kino-oka *et al.*, 2008). Medium changes were conducted every 3 days.

4.2.2 Determination of the thickness of the cell/ECM layer and the ratio of ECM to cell cytoplasm

In the current study, collagen type II was selected as the candidate ECM for understanding the relationship between changes in the ECM to the permeability and diffusion of nutrients. The specimens underwent double-staining for living cell cytoplasm (green) and collagen type II (red) as described in a previous study (Khoshfetrat *et al.*, 2009). The thickness of the cell/ECM layer (d_{cell}) on the microporous membranes was estimated using custom-made software programmed by LabVIEW (National Instruments) as described in **Appendix A**. In brief, at least nine random positions of each specimen were scanned at 1.0 μm intervals to yield slice images for vertical direction determination. The 8-bit images (256 × 256 pixels) of both colors in each slice were converted into binary images, allowing for distinction between colored and non-colored pixels. The colored pixels, which were derived from the green fluorescent original images, denoted the green pixels for cell

cytoplasm (N_C). On the other hand, the non-colored pixels derived from the green fluorescent original images together with the colored pixels derived from the red fluorescent original images denoted the red pixels for collagen type II (N_E). The number of N_C and N_E in each slice was counted and normalized using the maximum N_C and N_E values, respectively, found in all of the slice images. Slices with >10% of N_C or N_E were regarded to exist inside the cell/ECM layer, from which the vertical positions at the top and bottom of the cell/ECM layer and d_{cell} were determined. The ratio of N_E to the sum of N_C and N_E was denoted as R_{ECM}.

4.2.3 Permeation and diffusivity of oxygen and BSA

The specimens were rinsed twice with PBS (Sigma) and then incubated for 1 h with sodium azide solution (PBS containing 0.1% sodium azide; Wako Pure Chemical Industries, Ltd., Osaka) at 37°C in a 5% CO_2 atmosphere to stop the metabolism of cells.

Figure 4.1 shows the experimental set-up for understanding the permeation and diffusivity of oxygen. Snapwells containing the cell/ECM layers were placed in a diffusion chamber equipped with an oxygen microsensor (PreSens Co.) described in Section 3.2.3. The oxygen concentration at the bottom chamber was measured in a 5% CO_2 atmosphere at 37°C. Specimens with CL gel (without chondrocytes) on the Snapwell membranes were used as reference. The permeability coefficient of oxygen P_i (i = O2) was determined using the following equation:

$$\left(\frac{dC_b}{dt}\right) = P_{O2}\,(C_{sat} - C_b)A \tag{4.1}$$

where C_{sat} is the concentration of oxygen in the surrounding medium (0.21 mol/m^3), C_b is the nutrient concentration in the bottom chamber, and A is the surface area of the Snapwell membrane. The diffusion coefficient (D_{cell}) of oxygen was calculated as follows:

$$D_{cell} = P \times d \tag{4.2}$$

where d indicates the thickness of the gel (d_{gel}) or cell/ECM layer (d_{cell}).

Immediately prior to performance of the experiment concerning BSA permeability and diffusion, the Transwell chambers containing the cell/ECM layers were washed with BSA solution (PBS containing 0.2% BSA; Wako Pure Chemical Industries, Ltd. and

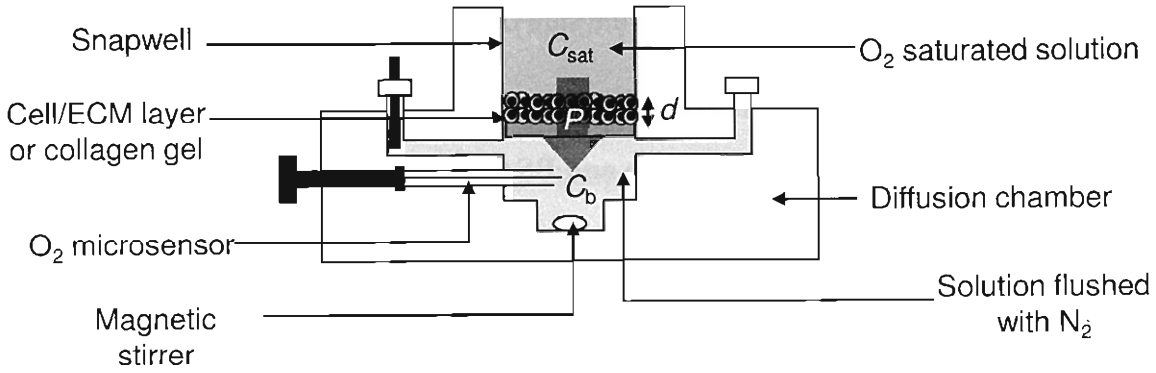

Fig. 4.1 Experimental set-up for understanding the permeation and diffusivity of oxygen.

0.1% sodium azide) and placed in a new 24-well culture vessel containing 0.8 ml of sodium azide solution. BSA solution (0.2 ml) was inserted into the Transwell chamber containing the cell/ECM layer and incubated for 3 days at 37°C in a 5% CO_2 atmosphere. The setup for the BSA diffusion experiment is shown in **Fig. 4.2.** Specimens with CL gel (without chondrocytes) on the Transwell membranes were used as reference. Sampling of solutions in Transwell chamber and 24-well culture vessels was conducted every day. The concentration of BSA was measured at an absorbance of 278 nm (A_{278}) with a spectrophotometer (UV-160; Shimadzu Corp., Kyoto) and applied to the following equation for determination of P_i (i = BSA) for BSA:

$$-\left(\frac{dC_a}{dt}\right) = P_{BSA}\,(C_a - C_b)A \tag{4.3}$$

Here, C_a is the nutrient concentration in the Transwell chamber, C_b is the nutrient concentration in the well, and A is the surface area of the Transwell membrane. The D_{cell} value for BSA was calculated using Equation 4.2.

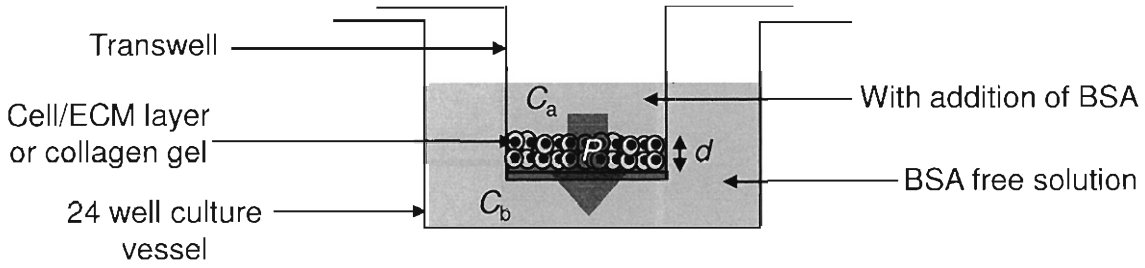

Fig. 4.2 Experimental set-up for understanding the permeability and diffusion of BSA.

4.3 Results

4.3.1 Effect of cell/ECM layer on nutrient permeation

To understand the development of the cell/ECM layer, the fluorescence stained specimens were evaluated at 3, 5, 7, and 10 days of culture. At 3 days, a large part of the membrane surface was not covered by cells or collagen type II (**Fig. 4.3A**). Here, the majority of chondrocytes had round morphology with poor collagen type II production, suggesting that the cells were in a lag phase without division. However, at 5 days, a significantly large part of the membrane surface was covered by either cells or collagen type II (**Fig. 4.3B**), yielding d_{cell} = 25.9. Active cell growth and collagen type II production was observed at 7 days of culture as evident from the d_{cell} value, which was twice that at 5 days of culture (**Fig. 4.3C**). In addition, some of the chondrocytes were surrounded by collagen type II, creating spaces between neighboring cells. At 10 days, high production of collagen type II by chondrocytes resulted in each cell being separated by a significant amount of collagen type II-filled space (**Fig. 4.3D**). Here, a thick cell/ECM layer of

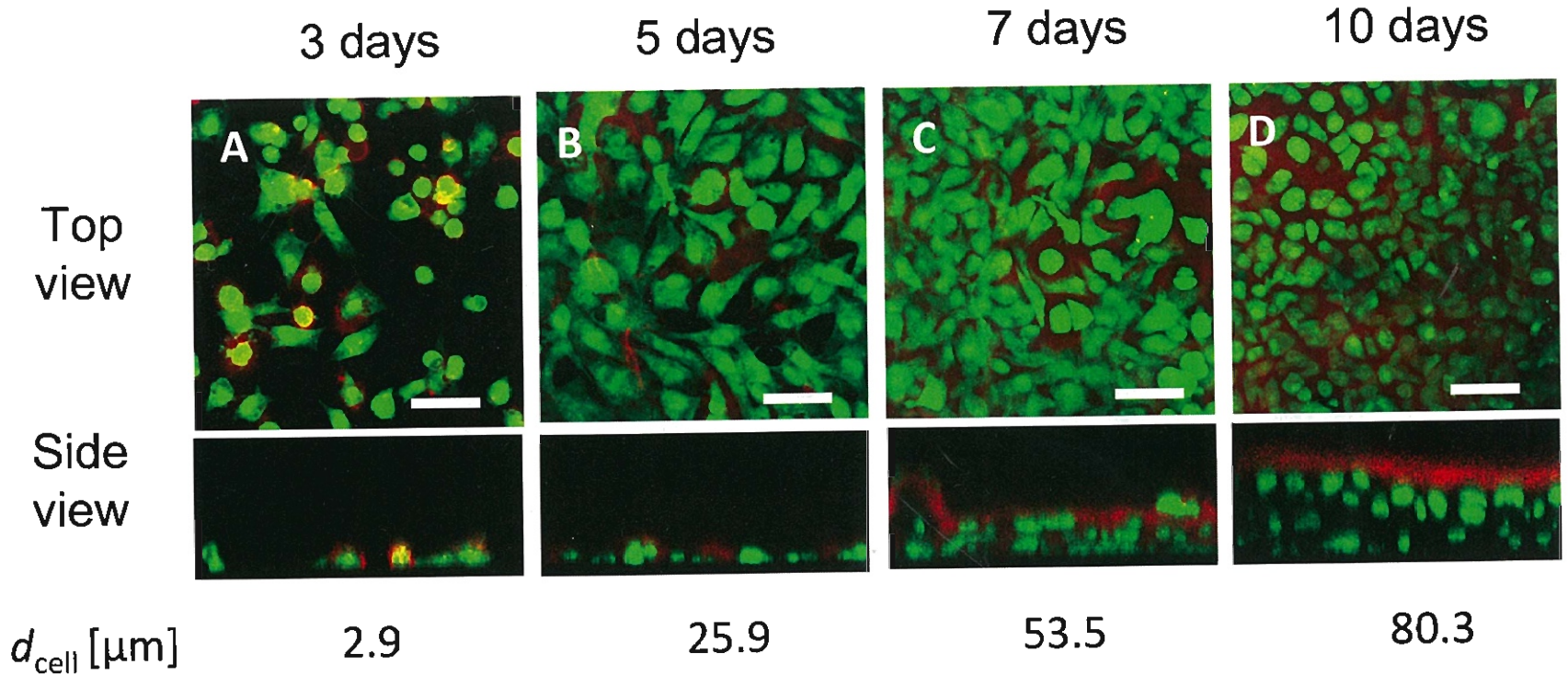

Fig. 4.3 Representative images showing the cell/ECM layer on the Transwell and Snapwell membranes seeded with freshly isolated chondrocytes at $X_0 = 1.0 \times 10^5$ cells/cm^2. The chondrocytes (green) and collagen type II (red) were labeled with fluorescent dyes, and the fluorescent images were taken at various culture times until 10 days. Scale bar: 50 μm.

d_{cell} = 80.3 was achieved, which was 3 times higher than that at 5 days' culture. Furthermore, based on the quantitative estimation of cell cytoplasm and collagen type II, it was revealed that the cell/ECM layer was constructed primarily from collagen type II (**Fig. 4.4**).

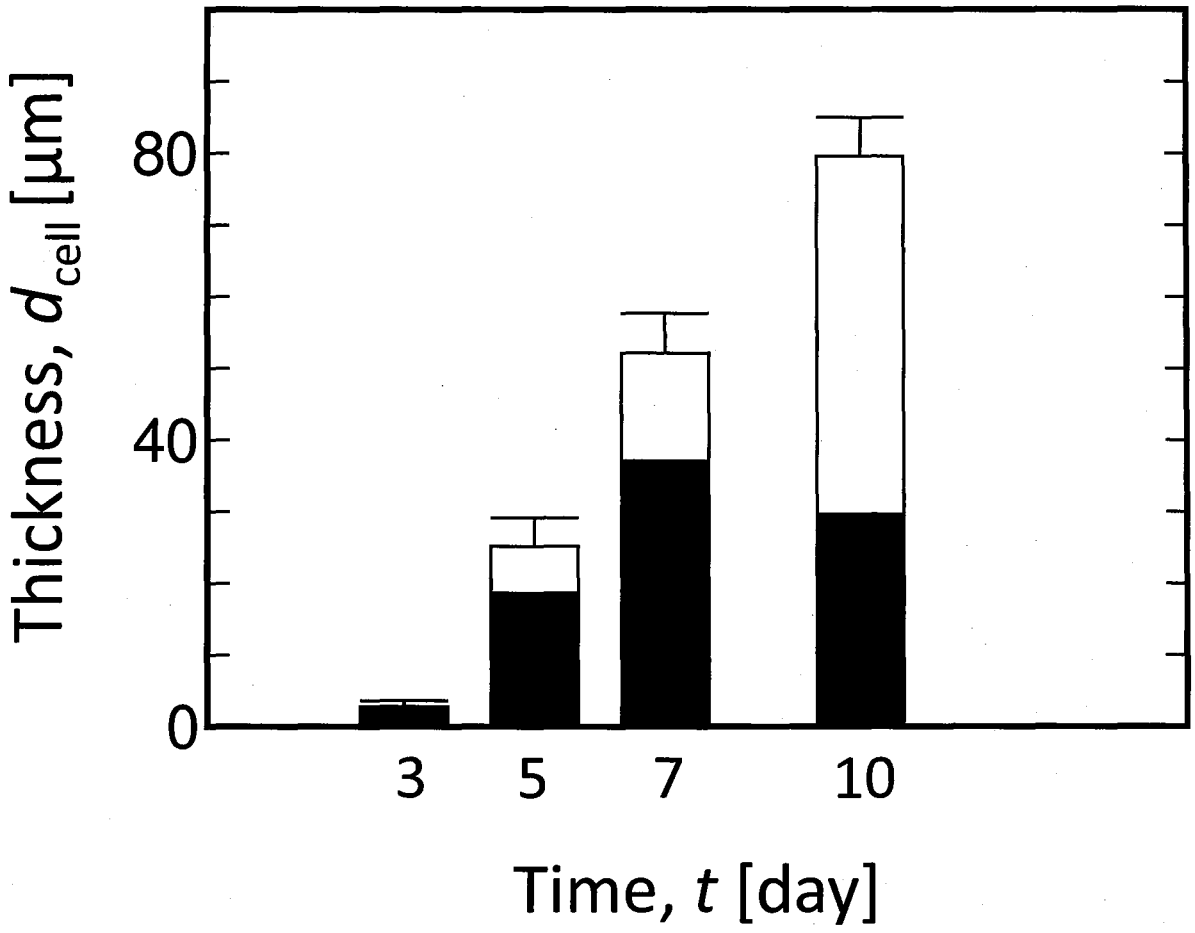

Fig. 4.4 The changes in the ratio of collagen type II and cell cytoplasm in the cell/ECM layer. Symbols: Open bar, collagen type II and closed bar, cell cytoplasm. The vertical bars show the SDs.

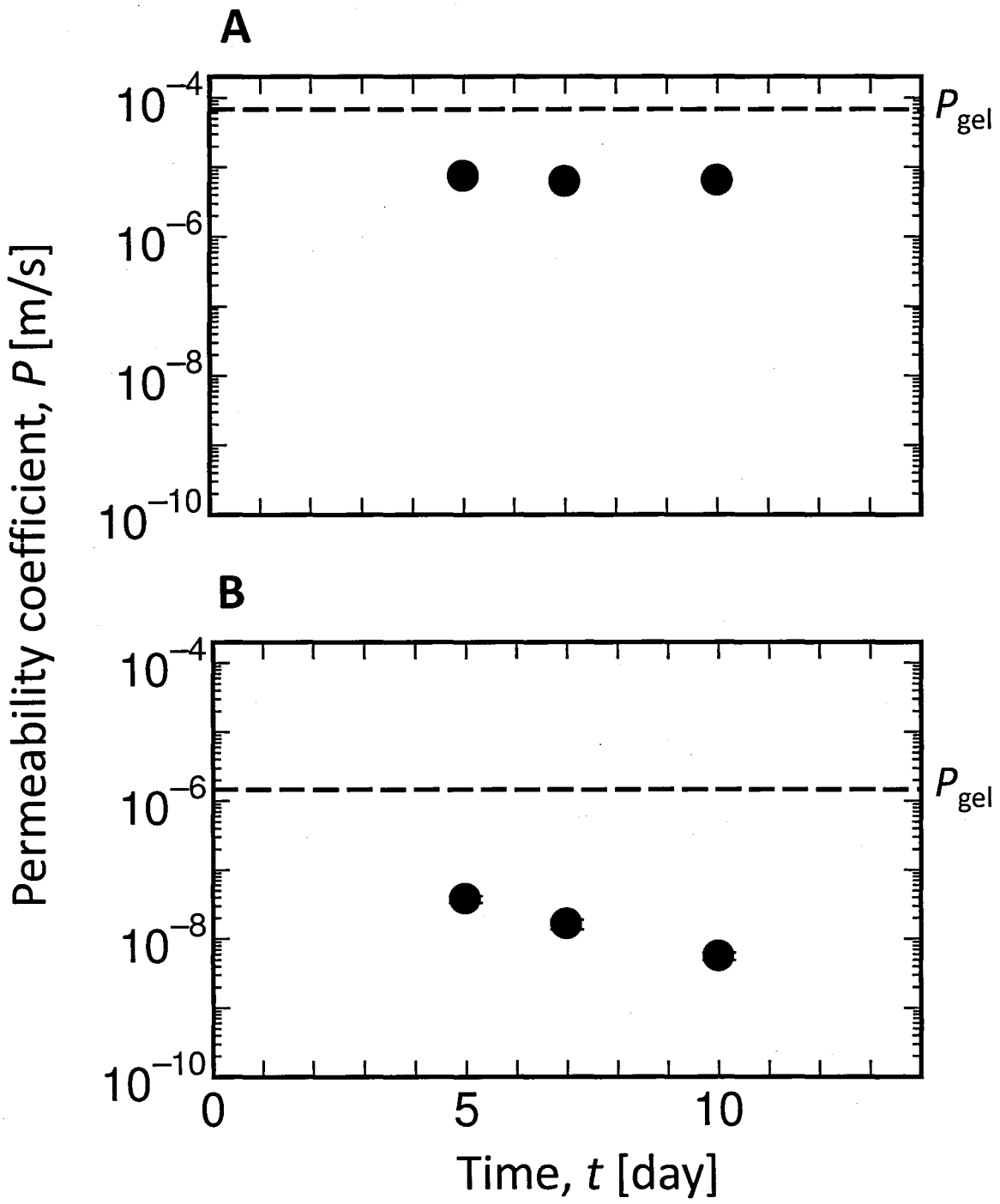

Fig. 4.5 The permeation of oxygen, P_{O2} (A) and BSA, P_{BSA} (B) across the cell/ECM layers at various culture times. In this study, P_{gel} represents the permeability coefficient of nutrients through the collagen gel on the membranes of culture inserts.

As shown in **Fig. 4.4 and 4.5A**, the increase in cells and collagen type II in the cell/ECM layer did not affect the permeability to oxygen; the mean P_{O2} was 6.6×10^{-6} m/s, which was about 10 times lower than the P_{gel}. On the other hand, the increase in cells and collagen type II reduced the permeability of the cell/ECM layer to BSA as shown by the decreasing trend of P_{BSA} (**Fig. 4.4 and 4.5B**), which was about 40 times lower than P_{gel} at 5 days and nearly 300 times lower at 10 days.

4.3.2 Influence of ECM and types of nutrients on diffusivity

Collagen type II increased with culture time (**Fig. 4.4**) and became the major component of the cell/ECM layer at 10 days. To understand the influence of

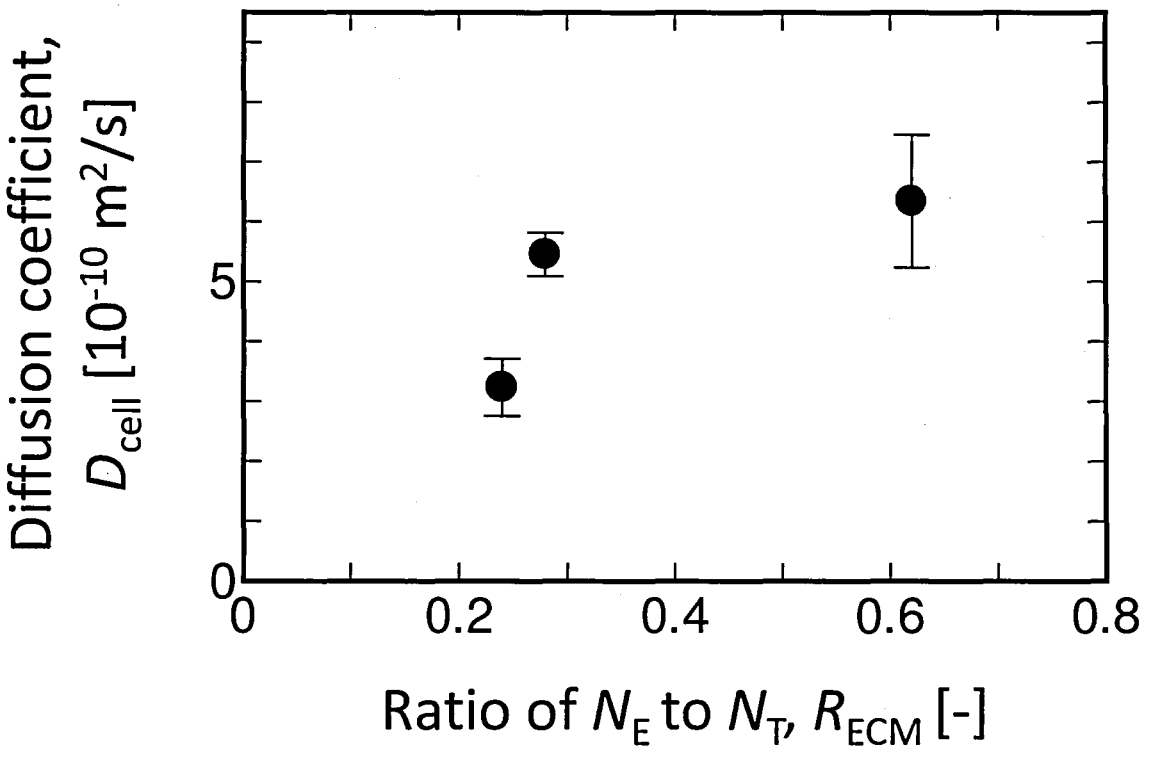

Fig. 4.6 Influence of various R_{ECM} on the diffusion of oxygen. The vertical bars show the SDs.

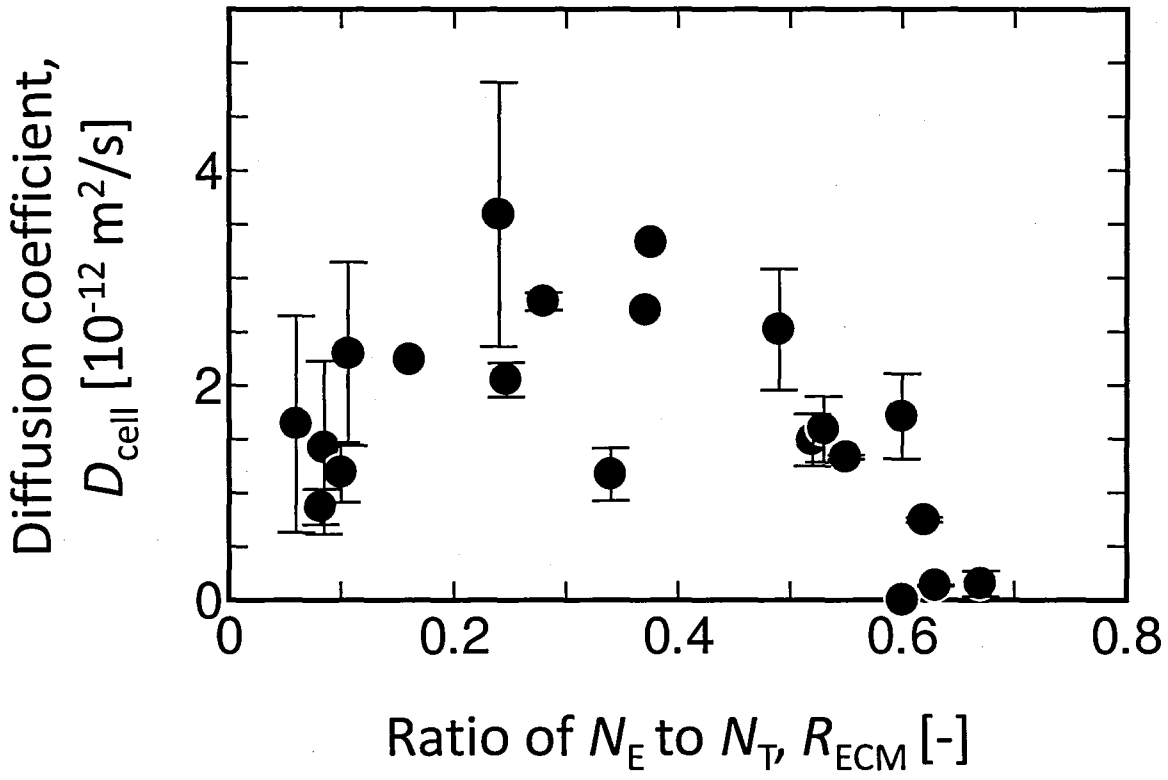

Fig. 4.7 Influence of various R_{ECM} on the diffusion of BSA. The vertical bars show the SDs.

collagen type II in the cell/ECM layer on nutrient transport, the diffusion of oxygen and BSA was evaluated with the changing ratio of collagen type II to cell cytoplasm. As shown in **Fig. 4.6**, the diffusion of oxygen through the cell/ECM layer was faster with the increase in R_{ECM}, with a significant increase in D_{cell} occurring in the range of R_{ECM} = 0.2 to 0.3. The diffusion of BSA (**Fig. 4.7**) was relatively low in the specimen with little collagen type II (R_{ECM} = 0.1). The D_{cell} of BSA gradually increased with increasing R_{ECM}, reaching a maximum in the range of R_{ECM} = 0.2 to 0.4. However, an opposite trend occurred at higher R_{ECM}, with diffusion of BSA completely inhibited in the vicinity of R_{ECM} = 0.6.

4.4 Discussion

In long-term culture of CL gel with $X_0 = 2.0 \times 10^6$ cells/cm^3, the periphery of the gel typically comprises dense chondrocyte aggregate and ECM. The aim of the present study was to determine the influence of the components of the gel periphery on permeability and nutrient diffusion. Thus, a system using a cell/ECM layer on a permeable membrane was utilized. Oxygen (with molecular weight of 32) and BSA (with molecular weight of 66,500), the main nutrients during cell culture were used as candidates in the experiment. The cell/ECM layer had a varied ratio of cells to the main ECM component, collagen type II, at 5, 7, and 10 days of culture, with the cells being the main component at 5 and 7 days and, collagen type II being the primary component at 10 days (**Fig. 4.4**). Subczynski *et al.* (1992) reported a permeability coefficient of oxygen across the Chinese hamster ovary plasma membrane of 4.2×10^{-1} m/s, which was 2 times lower than the permeability coefficient across a water layer of the same thickness. The P_{O2} was 6.1 to 7.3×10^{-6} m/s, with the lowest value at 7 days (**Fig. 4.5A**), indicating that the cell membrane was the dominant factor in the slightly low permeability of oxygen. As **Fig. 4.4 and 4.5B** show, the P_{BSA} exhibited a good inverse correlation with time and the amount of collagen type II in the cell/ECM layer, with a minimum P_{BSA} value of 5.6×10^{-9} m/s. Even with the large amount of collagen type II at 10 days, this value was higher than the permeability coefficient to cultured endothelial cell monolayers, which was 8.5×10^{-10} m/s, because of the presence of tight intercellular junctions between endothelial cells (Smith *et al.*, 1989).

In the current study, the diffusion of oxygen and BSA occurred passively as evident from the inverse relationship of the permeability coefficients (P_{O2} and P_{BSA}) with the molecular weight of the nutrients. **Figure 4.6** shows that the diffusion of oxygen was faster in the cell/ECM layer with high collagen type II content, which was within the vicinity of

R_{ECM} = 0.6. On the other hand, the diffusion of BSA (**Fig. 4.7**) showed an opposite trend, being completely inhibited at a high R_{ECM}. Interestingly, the diffusion of BSA, which was low around the vicinity of R_{ECM} = 0.1, increased with an increasing content of collagen type II before attaining a decreasing trend within an R_{ECM} of 0.5. This changing resistance to BSA transport and the increase in oxygen transport at a high R_{ECM} may have been caused by the structure and orientation of the collagen network as well as varying matrix porosity (Maroudas, 1968; Leddy and Guilak, 2003; Leddy *et al.*, 2006). Rather widely spaced collagen fibrils (Hall and Newman, 1991) have been suggested to obstruct diffusion of large molecules (40 to 500 kDa). Large molecules also reportedly result in a higher diffusion coefficient along the primary orientation of collagen fibers, compared with being perpendicular to the fibers (Leddy *et al.*, 2006). The formation of space between cells secondary to increased production of collagen type II may have initially caused an increase in BSA diffusion, but the subsequent increase in collagen type II formed a dense wall around each cell and resulted in the inhibition of BSA diffusion. However, it seems that the dense collagen type II wall only formed a barrier to the diffusion of large molecules, not to small molecules, as evident from the rapid diffusion of oxygen.

In conclusion, this chapter shows that the permeability of oxygen was not significantly affected by the changes in the composition of the cell/ECM layer mimicking the periphery of CL gel. On the other hand, permeability of BSA showed an inverse relationship to the content of collagen type II. The low collagen type II content was found to hinder the diffusion of oxygen and BSA, probably owing to the barrier formed by cell membranes situated close to one another. Increased collagen type II production led to the formation of space between cells, allowing rapid diffusion of oxygen and BSA across the cell/ECM layer. However, the subsequent increase in collagen type II content caused the development of dense wall surrounding each cell and inhibited the diffusion of BSA without affecting the

diffusion of oxygen. These findings indicate that the cell-cell distances, matrix structures, and nutrient size are important factors influencing the transport of nutrients at the periphery of the CL gel.

4.5 Appendix A

Figure 4.8 presents a flowchart of the image analyzing process for determining the thickness of the cell/ECM layer and the pixel density of the cell cytoplasm and collagen type II.

4.6 Summary

A system mimicking the periphery of the CL gel seeded at $X_0 = 2.0 \times 10^6$ cells/cm^3 was used to evaluate the nutrient diffusion and related changes in gel permeability to oxygen and BSA after long-term culture. The permeability of oxygen was not significantly affected by the changes in the composition of the cell/ECM layer used as the mimic. On the other hand, permeability of BSA showed an inverse relationship to the content of collagen type II. In the vicinity of $R_{ECM} = 0.1$, the diffusion of oxygen and BSA were slow, probably owing to the barrier formed by cell membranes situated close to one another. However, the diffusion of oxygen and BSA became faster with an increasing content of collagen type II. The development of a dense wall surrounding each cell within the vicinity of $R_{ECM} = 0.6$ inhibited the diffusion of BSA without affecting the diffusion of oxygen. These findings indicate that the cell-cell distances, matrix structures, and nutrient size are important factors influencing the transport of nutrients at the periphery of the CL gel.

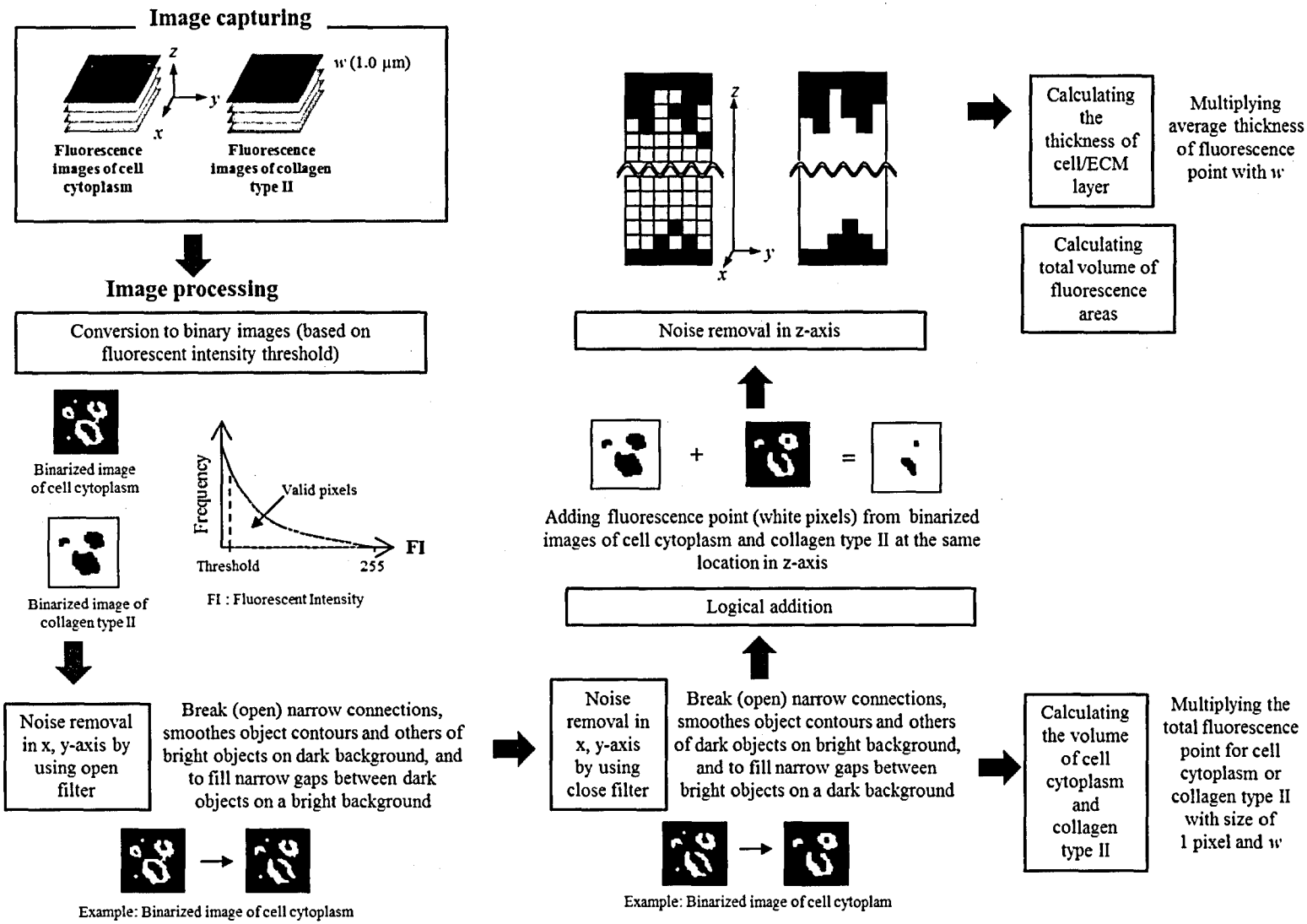

Fig. 4.8 Image processing to determine thickness of the cell/ECM layer and pixel density of the cell cytoplasm and collagen type II.

Chapter 5

Potential of low seeding density culture with supplementation of insulin-like growth factor-1 in modulation of chondrocyte behavior at initial culture phase

5.1 Introduction

In Chapter 3, it was shown that chondrocytes seeded at a high density of 2.0×10^6 cells/cm^3 in CL gel grew predominantly at the periphery of the gel, which formed a barrier to the diffusion of oxygen, subsequently causing a DO concentration gradient. Furthermore, as demonstrated in Chapter 4, the cell/ECM layer at the periphery of the construct may interfere with the transport of protein. The insufficient supply of nutrients resulted in a lack of cell growth in the deeper region of the construct, leading to a heterogeneous cell distribution.

In clinical practice, a cultured cartilage should ideally contain the appropriate amount of primary ECM components with a spatially uniform cell distribution within the construct. One strategy to obtain these desired traits in tissue-engineered constructs is to prepare the CL gel at a low cell density to reduce the cell growth at the periphery of the gel. Kino-oka *et al.* (2008) reported that in a CL gel with a low cell seeding density of 2.0×10^5 cells/cm^3, chondrocytes had an active growth rate throughout 21 days of culture, ultimately reaching the same level of cell density as that in a culture with a higher initial cell seeding density. Furthermore, cells were found to have a relatively homogenous spatial distribution in the top and middle regions of the CL gel after long-term culture. The low seeding density culture, however, resulted in the formation of loose aggregates of spindle-shaped cells, none of which produced collagen type II. This architecture of cell aggregates

was caused by the migration and gathering of individual chondrocytes, particularly at an early stage of the culture (Khosfetrat *et al.*, 2009). Therefore, regulating the cell behaviors in an initial culture phase will enable the manufacturing of cultured cartilage with a desired quality for practical use.

It is well-known that insulin-like growth factor-1 (IGF-1) is the main anabolic growth factor for articular cartilage. *In vitro* studies have demonstrated that IGF-1 increases the synthesis of proteoglycan by chondrocytes while retarding the degradation of proteoglycans (Luyten *et al.*, 1988). Furthermore, IGF-1 was found to maintain chondrocyte morphology and enhance the phenotypic expression of collagen type II (Fortier *et al.*, 1999). In this chapter, the effect of IGF-1 on the behavior of individual chondrocytes and cell aggregates in CL gel seeded at a low cell density was evaluated.

5.2 Materials and Methods

5.2.1 Chondrocyte preparation and incubation of cells embedded in collagen gel

Chondrocyte isolation was conducted as described in Section 1.2.3. CL gel with freshly isolated chondrocytes of $X_0 = 2.0 \times 10^5$ cells/cm^3 was prepared as indicated in Section 2.2.3. The CL gel culture was conducted at 37°C for the prescribed number of days in a 5% CO_2 atmosphere using medium as described elsewhere (Kino-oka *et al.*, 2008). The CL gel culture was also conducted using medium supplemented with 100 ng/ml IGF-1 (Human Recombinant; PeproTech, Rocky Hill, NJ, USA). Medium changes were conducted every 3 days.

5.2.2 Stereoscopic observation and analysis of chondrocyte morphology

The specimens were subjected to double-staining for living cell cytoplasm and collagen type II as described in a previous study (Khoshfetrat *et al.*, 2009). The CL gel specimen was mounted on a glass-bottomed dish (Asahi Glass Co., Ltd.) for 3-D observation of cell morphology and collagen type II using a CLSM (model FV-300; Olympus). Low magnifying-power views through an objective lens (10×) were taken to observe the spatial distribution of cell aggregates and formation of collagen type II. To acquire highlighted images, observation was conducted at higher magnification with an objective lens (20× or 40×).

Cells stained with CellTracker™ Green CMFDA (Invitrogen) as indicated previously (Khoshfetrat *et al.*, 2009) were subjected to time-lapse observation at 5 days of culture. Cells were observed at higher magnification with an objective lens (60×) using a CLSM (model: Fluoview FV10i; Olympus) for 8 h.

Analysis of individual cell morphology at 5 days was conducted by capturing images with a resolution of 256 pixels on both the horizontal and vertical lines at a step size of 0.9 μm with an objective lens (60×). The 3-D geometry of cytoplasm representing cell morphology was reconstructed from the image data with a threshold value for fluorescent intensity to evaluate the sphericity of each cell, S_C, defined by the following equation:

$$S_C = \frac{6V}{D.S} \tag{5.1}$$

where V, D, and S denote the volume, equivalent diameter, and surface area of a single cell, respectively. The S_C value was determined by examining > 50 cells in each gel. As described in a previous study (Khoshfetrat *et al.*, 2009), the cytoplasmic images offered a sphericity of $0 < S_C \leq 1$ for single cells. Here, the spindle-shaped cells were regarded as being capable of migrating, and by setting a threshold value of S_C = 0.95, the cell morphology

was categorized into three types of cell populations: dividing cells (DC), non-migrating cells (NMC) ($0.95 \leq S_C \leq 1.0$), and migrating cells (MC) ($S_C < 0.95$). The frequency, f_i (i=DC, NMC, and MC), was defined as follows.

$$f_i = \frac{\text{number of cells categorized to each population}}{\text{number of all cells examined}} \tag{5.2}$$

5.2.3 Total RNA extraction and real-time RT-PCR analysis

Gene expression was examined by means of quantitative real-time PCR with a Chromo4™ detector and furnished program (Bio-Rad Laboratories) according to procedures explained in Section 2.2.4. Specific primers for GAPDH and collagen types I and II were designed as indicated in **Table 2.1** in Section 2.2.4. The primers for membrane type 1-matrix metalloproteinase (MT1-MMP) was designed as follows: 5'-TCT CTT CTG GAT GCC CAA TG-3' and 5'-GAT GCC TTC CCA CAC TTT GA-3'.

5.3 Results

5.3.1 Effect of IGF-1 on behavior of chondrocytes in initial culture phase

Initially, the behavior of individual chondrocytes in CL gel with $X_0 = 2.0 \times 10^5$ cells/cm^3 was studied quantitatively in the early culture phase (5 days) in the presence and absence of IGF-1. Based on the stereoscopic shapes of cells examined by cytoplasm staining, the paired or dividing cells were apparently distinguished from the singly occurring cells. As shown in **Fig. 5.1**, the frequency of MC (f_{MC}) significantly decreased in the culture with IGF-1, giving $f_{MC} = 0.04$, which was more than 2 times lower than that in the IGF-1 free culture. On the other hand, the frequency of DC (f_{DC}) increased in the presence of IGF-1, being 1.5 times higher than that in the IGF-1 free culture. The frequency of NMC (f_{NMC}) exhibited no change with the addition of IGF-1, depicting a value of $f_{NMC} = 0.83$.

These results suggest that IGF-1 suppressed the migration of chondrocytes in the CL gel while stimulating chondrocyte propagation at 5 days.

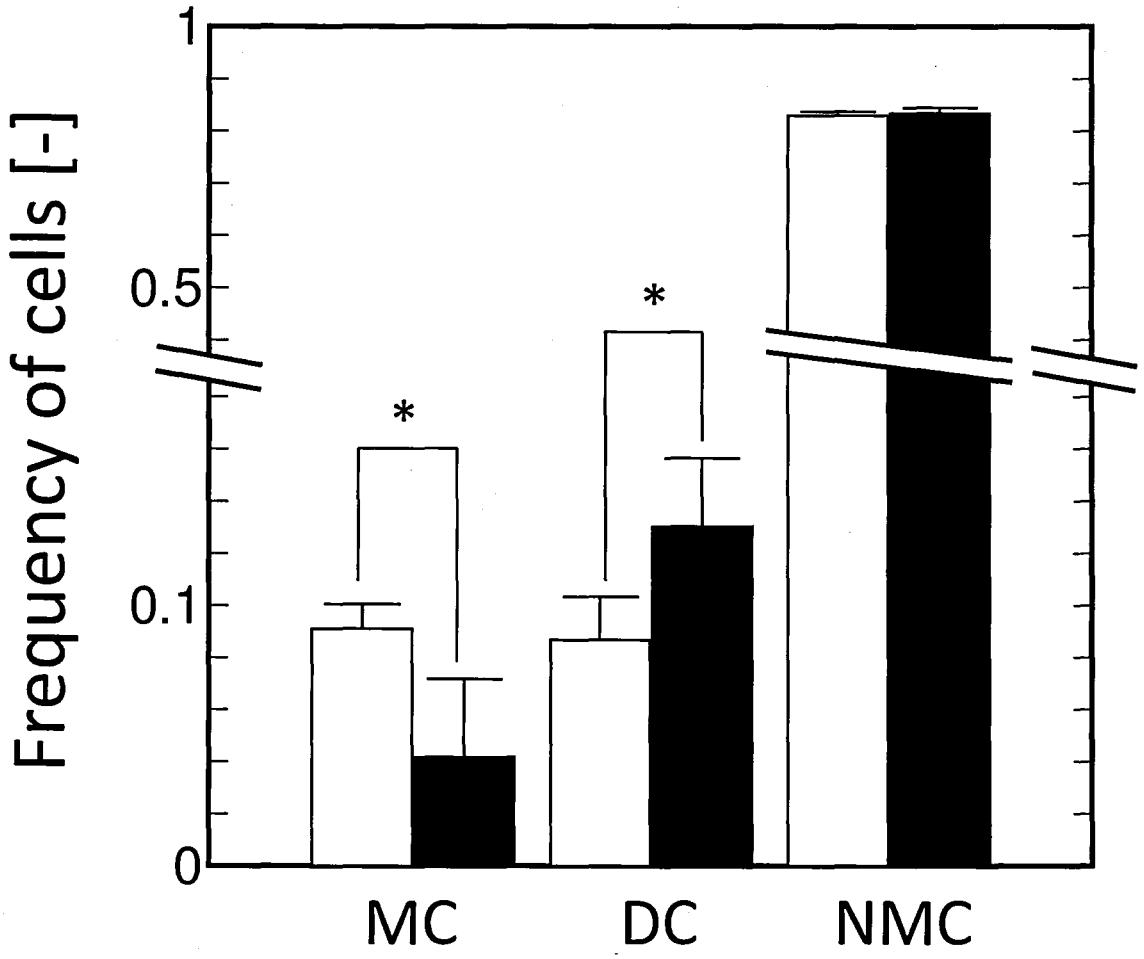

Fig. 5.1 Frequencies of dividing cells (DC), non-migrating cells (NMC), and migrating cells (MC) in CL gel cultures. The cultures were performed for 5 days. Symbols: Open bar, without IGF-1; closed bar, with 100 ng/ml of IGF-1. The vertical bars show the SDs. The statistical significance among the data sets was accessed by Student's *t*-test ($^*p < 0.05$).

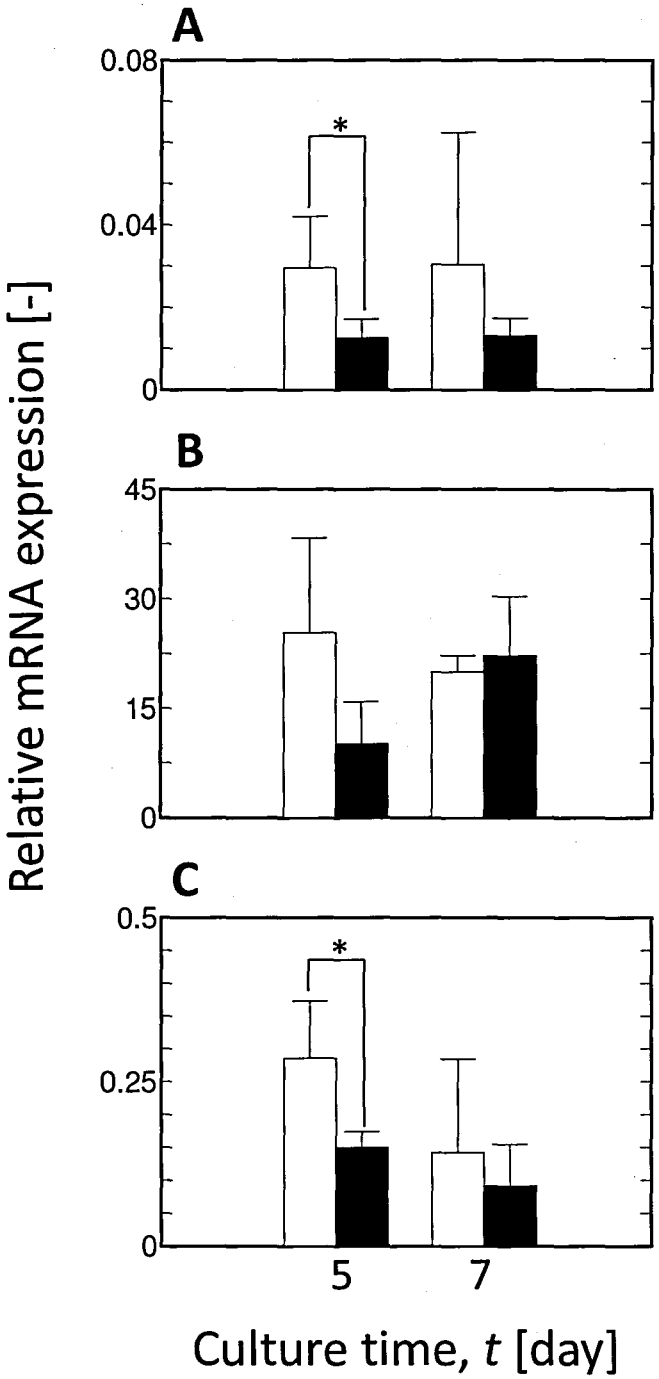

Fig. 5.2 Gene expressions of collagen types I (A) and II (B), and MT1-MMP (C) in chondrocytes in CL gel cultures. Symbols: Open bar, without IGF-1; closed bar, with 100 ng/ml of IGF-1. The mRNA expression levels were standardized by GAPDH expression. The vertical bars show the SDs. The statistical significance among the data sets was accessed by Student's *t*-test ($*p \leq 0.05$).

5.3.2 Gene expression relating to differentiation and migration

The gels were picked up from the cultures with and without IGF-1 at 5 and 7 days and subjected to quantitative analysis for mRNA expression of collagen type I and II genes, relating to differentiation, and of MT1-MMP, relating to cellular remodeling of the surrounding matrix. As shown in **Fig. 5.2**, the mRNA level of collagen type I at 5 days in the culture with IGF-1 was down-regulated to more than 2 times lower than that in the IGF-1 free culture, and this trend was maintained at 7 days of culture. The mRNA levels of collagen type II showed a similar trend at 5 days. However, when cultured for 7 days, the expression level in the culture with IGF-1 was up-regulated to a level about similar to that in the IGF-1 free culture. The expression level of MT1-MMP was significantly down-regulated at 5 days in the culture with IGF-1, being about 2 times lower than that in the IGF-1 free culture. At 7 days, the mRNA levels of MT1-MMP showed a slight down-regulation compared with those at 5 days whether IGF-1 existed or not.

5.3.3 Morphology of aggregates and ECM formation

To understand the fate of cell behavior when exposed to IGF-1 in the initial culture phase, histological observation of aggregate shapes in the CL gels was performed at 7 days in the cultures with and without this growth factor. The fate of chondrocytes was also studied in the late culture phase; observation of aggregate shapes and collagen type II formation in the CL gel was conducted at 14 days. As seen in **Fig. 5.3**, at 7 days, aggregates with spindle-shaped cells emerged in the gel when cultured in the absence of IGF-1 (**Fig. 5.3A and A-1**). However, this type of aggregate was not observed in the culture with IGF-1 (**Fig. 5.3B**). A magnified image (**Fig. 5.3B-1**) elucidated that the aggregate in the culture with IGF-1 comprised chondrocytes with an ellipsoid morphology.

At 14 days of culture, the loose aggregates of spindle and spherical-shaped cells were observed at the rims of the gels cultured without IGF-1 (**Fig. 5.4A**). Immunodetection of collagen type II revealed that the loose aggregates of spindle-shaped cells were accompanied

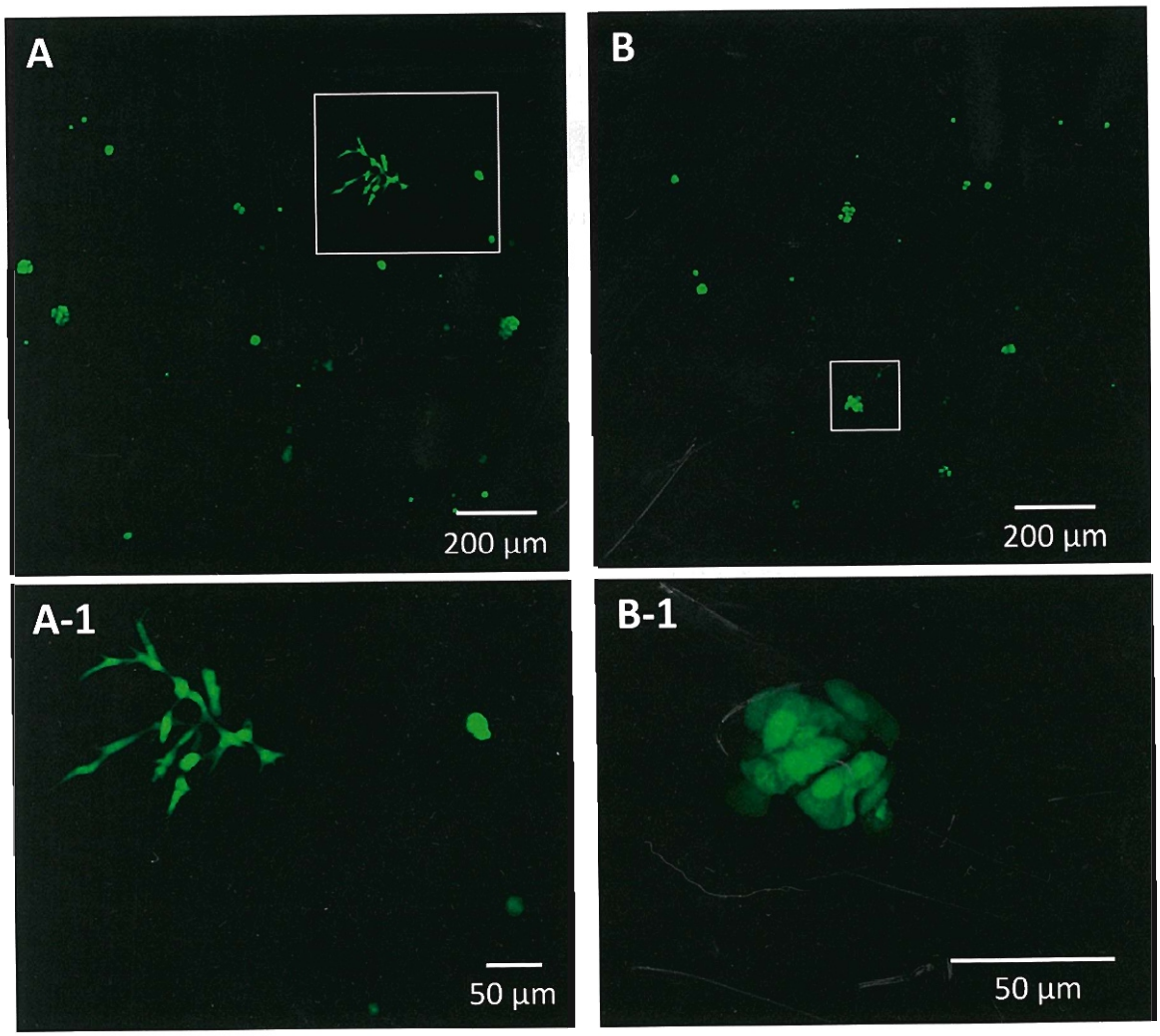

Fig. 5.3 Fluorescent images showing spatial distribution and morphology of chondrocytes in collagen gels. The cultures were performed for 7 days without IGF-1 (A) and with 100 ng/ml of IGF-1 (B). The boxed regions on the images, A and B, are highlighted by the magnifications, A-1 and B-1, respectively.

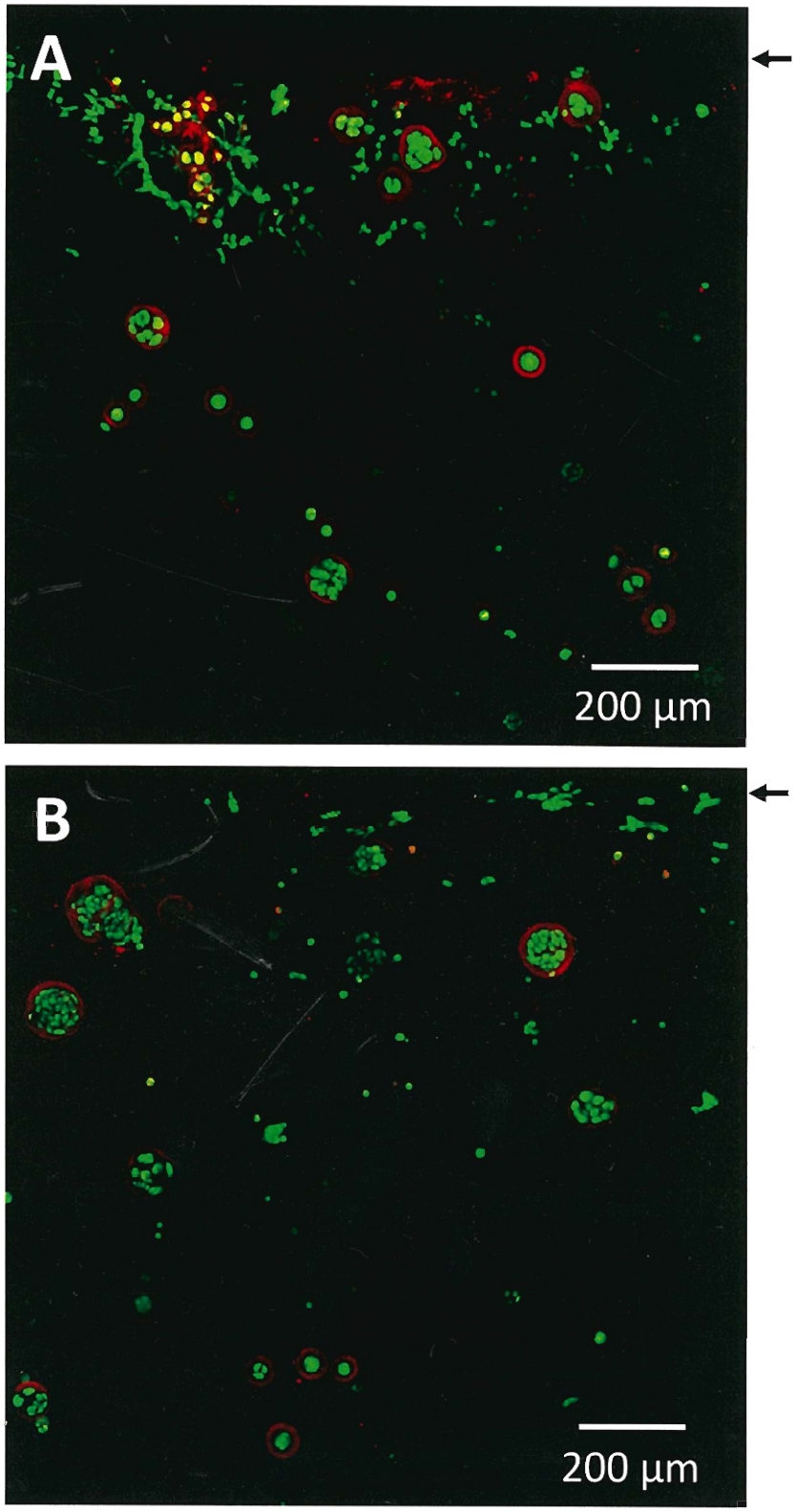

Fig. 5.4 Fluorescent images showing spatial distribution of chondrocytes (green) and collagen type II (red) in collagen gels. The cultures were performed for 14 days without IGF-1 (A) and with 100 ng/ml of IGF-1 (B). The arrows show the top surfaces of the gels.

by poor production of collagen type II, whereas the spherical-shaped cells localized in the loose aggregates exhibited territorial production of collagen type II. In the culture with IGF-1, few cells were located at the rims of gels (**Fig. 5.4B**). Furthermore, a majority of the aggregates comprised tightly packed spherical-shaped cells that were abundant in collagen type II and were larger in size compared with those in the culture without IGF-1.

5.4 Discussion

In Chapter 3, rabbit chondrocytes were shown to be predominant in the top region of CL gel with $X_0 = 2.0 \times 10^6$ cells/cm^3, subsequently causing a DO concentration gradient. In addition, it was revealed in Chapter 4 that the presence of a large number of chondrocytes coupled with a high amount of collagen type II at the periphery of gel formed a barrier to the diffusion of proteins such as BSA. This cell/ECM barrier at the periphery of the gel resulted in a lack of nutrients in the inner region of the CL gel and low cell propagation. To prevent the formation of a dense cell/ECM layer at the periphery of the gel, CL gel was seeded at a low density of $X_0 = 2.0 \times 10^5$ cells/cm^3. However, chondrocytes migrated in the low seeding density CL gel, resulting in the formation of loose aggregates of spindle-shaped cells without the production of collagen type II (Khosfetrat *et al.*, 2009).

In the present study, IGF-1 was administered in the CL gel culture seeded at low cell density. Based on the evaluation of cell sphericity at 5 days in the CL gels, it was found that IGF-1 suppressed cell migration. The inhibition of chondrocyte migration was accompanied by active cell division in the early culture phase. Cell migration involves coordinated adhesion as well as proteolytic interaction with the surrounding matrix, resulting in degradation and remodeling of the matrix barrier (Friedl and Wolf, 2009). Upon cell progression, multiple classes of ECM-degrading enzymes are up-regulated and activated,

including matrix metalloproteinase (MMPs). It is well known that MT1-MMP plays a pivotal role in ECM remodeling, cell migration and invasion. MT1-MMP could cleave directly ECM proteins such as gelatin, collagen type I and fibronectin (Ohuchi *et al.*, 1997). In addition, Kim *et al.* (2005) reported the expression of MT1-MMP in migrating chondrocytes from the cartilage endplate into the nucleus pulposus in rat intervertebral discs. The results shown in **Fig. 5.3A-1 and 5.2C** indicated the dedifferentiation of chondrocytes with the acquisition of spindle morphology and the expression of MT1-MMP, which suggests that the chondrocytes in the CL gels adopted protease-dependent migration strategy (Friedl and Wolf, 2003). Considering the down-regulation of collagen type I and MT1-MMP expression, and the lack of spindle-shaped cells (**Fig. 5.2A, C and 5.3B**) in the culture with IGF-1, it seems that the protease-dependent migration was suppressed by IGF-1.

To our knowledge, there is no report describing the suppression of this mode of chondrocyte migration by the down-regulations of collagen type I and MT1-MMP by IGF-1. The expressions of MT1-MMP in Lewis lung carcinoma subline H-59 cells have been reported to be up-regulated in response to 10 ng/ml of IGF-1 (Zhang and Brodt, 2003). Furthermore, this induction of MT1-MMP by IGF-1 has been demonstrated to be related to PI 3-kinase/Akt/mTOR signaling mechanism. At a high dose of 100 ng/ml of IGF-1, however, activation of ERK pathway appears to dominate, exhibiting an inhibitory effect on the PI 3-kinase/Akt/mTOR signaling (Zhang *et al.*, 2004). Considering these reports, it is thought that 100 ng/ml IGF-1 has a negative regulatory effect on the synthesis of MT1-MMP. In addition, it has been reported that MCF-7 human breast carcinoma cell migration was depressed at 100 ng/ml of IGF-1 (Mira *et al.*, 1999), which is consistent with our results in the current study.

In 3-D, cell could migrate collectively, as described previously for primary melanoma explants (Friedl *et al.*, 1995; Hegerfeldt *et al.*, 2002). In the current study, some cells in the

culture without IGF-1 migrated in clusters in the initial culture phase, where cell at the leading edge generated the migration path whereas cells at the trailing edge remained largely non-motile (**Fig. 5.5**), being compatible with the down-regulation of MT1-MMP expression at day 7 (**Fig. 5.2C**).

In HT-1080 fibrosarcoma cells, the blocking of MMPs, serine proteases, and cathepsins has resulted in a transition of the cell mobility mode from a proteolytic mode to protease-independent one (Wolf *et al.*, 2003). This protease-independent mobility mode has been widely reported in leukocytes and tumor cells (Condeelis *et al.*, 1992; Devreotes and Zigmond, 1988; Friedl *et al.*, 2001; Wolf *et al.*, 2003). The typical characteristics of cells in this mode include a round or ellipsoid shape and the frequent protrusion and retraction of the plasma membrane (Friedl and Wolf, 2003; Fackler and Grosse, 2008). In the current study, the chondrocytes maintained an ellipsoid shape at 5 days with recurring protrusion and

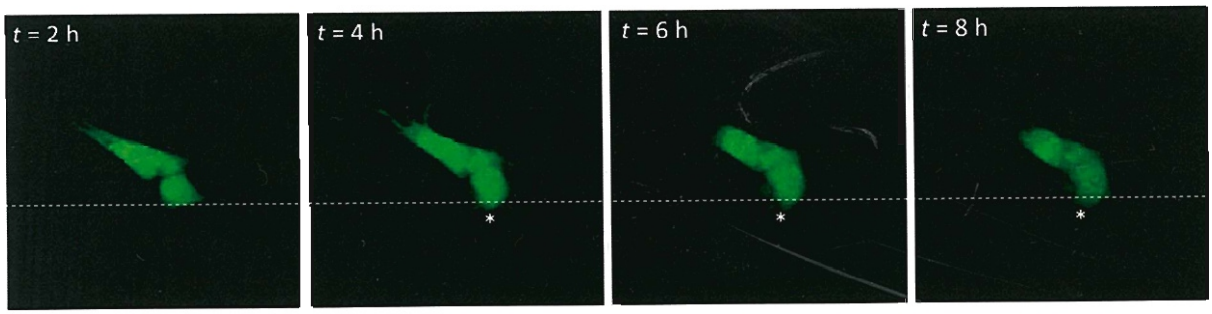

Fig. 5.5 Time lapse of chondrocytes at 5 days in culture without IGF-1. Representative images show cells that adopted a collective migration strategy. The migration path was determined by the lead cell. The leading edge of the lead cell is indicated by the asterisk.

retraction of the plasma membrane (**Fig. 5.6**). These findings suggest that the down-regulation of MT1-MMP by IGF-1 does not thoroughly suppress cell migration, but rather lead the chondrocytes to the adoption of a protease-independent migration strategy.

The inability to actively degrade the dense matrix surrounding the cells seems to prevent them from migrating from their original positions, resulting in formation of large aggregates with spherical-shaped cells owing to cell division, and a paucity of cells existing at the gel periphery at 14 days.

In conclusion, based on the morphological evaluation of individual cells and the gene expression analysis, it was found that in the CL gel culture with the low seeding density, the presence of IGF-1 caused the suppression of chondrocyte dedifferentiation and protease-dependent migration in the early culture phase. This administration of IGF-1 contributed to the creation of large aggregates containing spherical-shaped cells with collagen type II production in the prolonged culture.

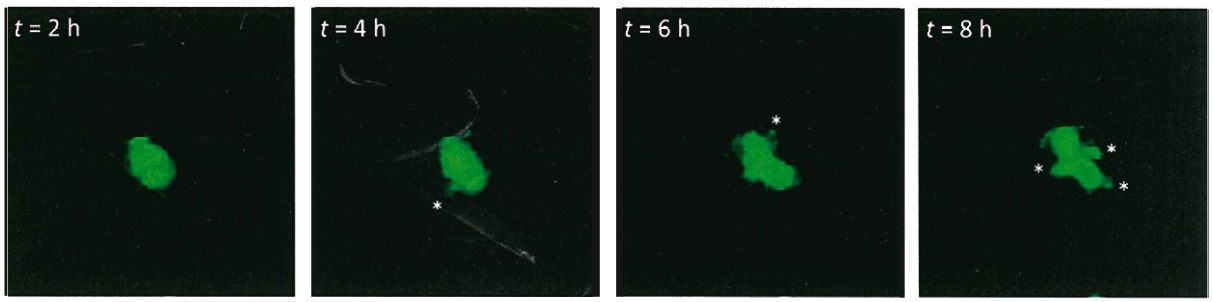

Fig. 5.6 Time lapse of chondrocyte at 5 days in culture with IGF-1. The cell exhibited ellipsoid shape. The protrusion of the cell plasma membrane is indicated by the asterisk.

5.5 Summary

The effect of IGF-1 on cell behavior in the CL gel culture with $X_0 = 2.0 \times 10^5$ cells/cm^3 was examined. At day 5, the f_{MC} significantly decreased in the culture with IGF-1, giving a value of 0.04, which was more than 2 times lower than that in the IGF-1 free culture. On the other hand, the f_{DC} increased in the presence of IGF-1, being 1.5 times higher than that in the IGF-1 free culture. These results suggest that IGF-1

suppressed the migration of chondrocytes in the CL gel while stimulating the cell division in the initial culture phase. The proteolytic migration of cells was thought to be suppressed owing to the down-regulation of MT1-MMP by IGF-1. This contributed to the formation of aggregates with spherical-shaped cells that produced collagen type II.

General Conclusion

Overall, the present study highlights the significance of chondrocyte fate and the nutrition property in acquiring clinically applicable cultured cartilage. The chondrocyte fate at young, middle and old ages led to various qualities of cultured cartilage. In addition, an example of cultured construct with young chondrocytes at seeding density of $X_0 = 2.0 \times 10^6$ cells/cm^3 demonstrated the importance of nutrition availability in obtaining high quality cultured cartilage. The administrations of IGF-1 to the chondrocytes in CL gels seeded at low density of $X_0 = 2.0 \times 10^5$ cells/cm^3 revealed the possibility of regulating the chondrocyte fate for obtaining the desired structural and functional properties of cultured construct. The major findings obtained throughout this thesis are concluded as follows.

In the first part, including Chapter 1 and 2, the chondrocyte fate at various cell ages was characterized by evaluation of cell morphology on CL substrate. In Chapter 1, to clarify the relationship between the morphology of young chondrocytes ($PD = 0$) to the structure of CL substrate, the morphological evaluation of cells was conducted after 1 day incubation on substrates preserved under atmosphere of nitrogen gas or air. The varying preservation conditions altered the degree of collagen fibril formation. It was found that the decay of collagen fibril formation caused the spreading of cells, indicating that the non-preserved CL substrate is most suitable for a cell evaluation purpose.

Chapter 2 emphasizes on the comprehension of the influence of PD levels to the chondrocyte fate with age in the cultured cartilage. The cell phenotype was distinguished by utilizing the non-preserved CL substrate as an evaluation tool. Morphological assessment and ALP staining were conducted and correlated with the cell population in CL gel. With increasing age of cell population ($PD = 0$ to 14.5), the frequency of non-dividing spindle-shaped cells without ALP activity increased, accompanied with an increase in gene

expression of collagen type I, meaning the senescence of dedifferentiated cells. At the middle age of cell population (PD = 5.1 and 6.6), the high frequency of polygonal shaped cells with ALP activity existed on the CL substrate together with up-regulated expressions of collagen types II and X , indicating the terminal differentiation of chondrocytes. When the chondrocytes passaged up to the middle age were embedded in CL gel at the high seeding density of $X_0 = 2.0 \times 10^6$ cells/cm^3, the high frequency of single hypertrophic cells with collagen type II formation was recognized, which supports the consideration that the high gene expression of collagen type II was attributed to terminal differentiation rather than redifferentiation.

In Part 2, which includes Chapters 3, 4 and 5, characterization of the nutrition property in CL gel with young chondrocytes at $X_0 = 2.0 \times 10^6$ cells/cm^3 was conducted. Furthermore, regulation of chondrocytes fate in the cultured construct was carried out by seeding the CL gel at a low density of $X_0 = 2.0 \times 10^5$ cells/cm^3 and administration of IGF-1. In Chapter 3, a direct measurement system was constructed to estimate the DO level in a cultured cartilage of conventional static culture, in culture subjected to shaking operation and with a gas-permeable bottom. It was revealed that in the static culture, the DO level at the top surface of gel decreased due to an increase in overall cell density with elapsed time. The local cell density at the top surface on day 21 was 5.7 x 10^7 cells/cm^3, being 11 times that at the bottom of gel. This heterogeneity of cell distribution in the gel was considered to occur by limitation of oxygen supply into the deeper part of the gel. In the shaking culture using a dish with gas-permeable film, the DO level was enhanced inside the gel and the overall cell density in the gel was achieved to be 2.9 times that in the static culture. The local cell density at the bottom surface was enhanced by the operation but the level was still lower than that at the top surface, suggesting that limitation of alternative nutrients such as proteins caused insufficient growth under the improved conditions of oxygen supply.

Chapter 4 deals with the nutrient diffusion and the related changes in gel permeability to oxygen and BSA at the periphery of CL gel seeded at $X_0 = 2.0 \times 10^6$ cells/cm^3 after long-term culture. The changes in the composition of the cell/ECM layer used to mimic the periphery of the gel construct did not significantly affect the permeability of oxygen. On the other hand, permeability of BSA showed an inverse relationship to the content of collagen type II. In the vicinity of $R_{ECM} = 0.1$, the diffusion of oxygen and BSA was slow, probably owing to the barrier formed by cell membranes situated close to one another. However, the diffusion of oxygen and BSA became faster with increasing content of collagen type II. The development of dense wall surrounding each cell within the vicinity of $R_{ECM} = 0.6$ inhibited the diffusion of BSA without affecting the diffusion of oxygen. These indicate that the cell-cell distances, matrix structures and nutrient size are important factors influencing the transport of nutrient at the periphery of the CL gel.

Taking the finding obtained in Chapters 3 and 4 into consideration, in Chapter 5, a low seeding density culture of $X_0 = 2.0 \times 10^5$ cells/cm^3 was used to limit the cell growth and ECM production at the periphery of the cultured cartilage. In addition, the effect of IGF-1 to the cell behavior at initial culture phase was examined. It was found that the f_{MC} significantly decreased in the culture with IGF-1, giving a value of 0.04, which was more than 2 times lower than that in the IGF-1 free culture. On the other hand, the f_{DC} increased in the presence of IGF-1, being 1.5 times higher than that in the IGF-1 free culture. These results suggest that IGF-1 suppressed the migration of chondrocytes in the CL gel while stimulating the cell division in the initial culture phase. The proteolytic migration of cells was thought to be suppressed owing to the down-regulation of MT1-MMP by IGF-1. This contributed to the formation of aggregates with spherical-shaped cells that produced collagen type II.

In summary, the present research demonstrates the importance of characterizing the chondrocyte fate with relation to cells age and behavior, and also the nutrition property in

cultured cartilage. In addition, IGF-1 was found to be feasible in regulating chondrocytes behavior in CL gel while maintaining the chondrogenic phenotype. It is considered that the knowledge in this study could be applied for designing and generating high quality cultured cartilage for clinical uses.

Proposals for Future Work

To extend the findings obtained in this study, the following researches are recommended with respect to the application of tissue engineering.

1) Application of CL substrate for screening of anti-rheumatic drugs

For drug design, it is mandatory to test candidate substances before applying in the clinic. To meet this challenge, several established animal models are available. However, animal experiments often cause high costs and hardly offer possibility of automation. *In vitro* assay offers the possibility of reducing cost and of automation, e.g., anti-rheumatic drug screening. In addition, due to lower complexity, this assay would provide more reproducible data. As shown in Part 1, CL substrate enabled evaluation of chondrocytes differentiated and terminal differentiated phenotypes, which are native to the articular cartilage. In addition, the collagen structure of CL substrate could easily be modified by preservation. Therefore, the CL substrate could be subjected to treatment to mimic the ECM of an arthritic cartilage and used in the osteoarthritis research.

2) Application of direct measurement system to estimate DO level of cultured bone

The transplantation of cultured bone cells is expected to be applicable to patients who have lost large segments of bone due to tumors, etc. The amount of bone formation *in vitro* may be influenced by factors such as hormones, sufficient oxygen and nutrient supplies, and appropriate mechanical stress on cells. Using the direct measurement system described in Chapter 3, the influence of the DO concentration on the quality of engineered bone and osteogenesis *in vitro* could be comprehended.

Nomenclature

$\hat{C}_o$	dissolved oxygen concentration	[mol/m^3]
$\hat{V}_g$	volume at the local region	[cm^3]
A_C	projected area of a single cell	[μm^2]
f_R	frequency of round-shaped cells	[-]
l_C	peripheral length of a single cell	[μm]
n_C	number of viable cells	[cells]
R_C	cell roundness	[-]
S_C	sphericity of single cell	[-]
X_0	initial seeding density	[cells/cm^2] or [cells/cm^3]
C_a	nutrient concentration in the chamber of Transwell	[mol/m^3]
C_b	nutrient concentration at the bottom chamber or well	[mol/m^3]
C_o^*	saturation level of dissolved oxygen concentration	[mol/m^3]
C_{sat}	concentration of oxygen in the surrounding	[mol/m^3]
D_{cell}	diffusion coefficient of oxygen or bovine serum albumin	[m^2/s]
K_o	saturation constant	[mol/m^3]
N_C	pixels for cell cytoplasm	[pixels]
N_E	pixels for collagen type II	[pixels]
P_{BSA}	permeability coefficient of bovine serum albumin	[m/s]
P_C	probability of cell existence	[-]
P_{gel}	permeability coefficient of collagen gel	[m/s]
P_{O2}	permeability coefficient of oxygen	[m/s]
R_{ECM}	ratio of pixels for collagen type II to the total pixels	[pixels]

V_g	total volume	[cm^3]
$\hat{X}$	local cell density	[cells/cm^3]
d_{cell}	thickness of cell/ECM layer	[m]
d_{gell}	thickness of gel	[m]
f_{DC}	frequency of dividing cells	[-]
f_{MC}	frequency of migrating cells	[-]
f_{NMC}	frequency of non-migrating cells	[-]
A	surface area of membrane	[m^2]
Ct	cycle threshold value	[-]
D	equivalent diameter of single cell	[µm]
P	permeability coefficient	[m/s]
PD	population doubling	[-]
S	surface area of single cell	[μm^2]
t	culture time	[h] or [days]
V	volume of single cell	[μm^3]
X	overall cell density	[cells/cm^3]
Z	depth	[mm]
Δn_C	differential in the number of viable cells	[cells]
ΔCt	differential in cycle threshold value	[-]
ΔPD	differential value of population doubling	[-]

Abbreviation

2-D	:	two-dimensional
3-D	:	three-dimensional
ACT	:	autologous chondrocytes transplantation
ALP	:	alkaline phosphatase
BSA	:	bovine serum albumin
CL gel	:	collagen gel
CL substrate	:	high density collagen type I coated substrate
CLSM	:	confocal laser scanning microscope
DC	:	dividing cells
DO	:	dissolved oxygen
ECM	:	extracellular matrix
EDC	:	1-ethyl-3-(3-dimethylaminopropyl)-carbodiimide
FI	:	fluorescent intensity
GAG	:	glycosaminoglycan
IGF-1	:	insulin-like growth factor-1
MC	:	migrating cells
MMP	:	matrix metalloproteinase
MT1-MMP	:	membrane type 1-matrix metalloproteinase
n	:	sample size
NMC	:	non-migrating cells
PBS	:	phosphate buffered saline

PS surface	:	tissue culture polystyrene surface
SCDA	:	spatial cell distribution analyzer
SEM	:	scanning electron microscope

Literature Cited

Adams, C. S. and Horton, W. E.: Chondrocyte apoptosis increases with age in the articular cartilage of adult animals. *Anat. Rec.*, **250**, 418-425 (1998).

Adams, C. S. and Shapiro, I. M.: The fate of the terminally differentiated chondrocyte: Evidence for microenvironmental regulation of chondrocyte apoptosis. *Crit. Rev. Oral Biol. Med.*, **13**, 465-473 (2002).

Ballock, R. T. and Reddi, A. H.: Thyroxine is the serum factor that regulates morphogenesis of columnar cartilage from isolated chondrocytes in chemically defined medium. *J. Cell Biol.*, **126**, 1311-1318 (1994).

Benya, P. D. and Shaffer, J. D.: Dedifferentiated chondrocytes reexpress the differentiated collagen phenotype when cultured in agarose gels. *Cell,* **30**, 215- 224 (1982).

Bhosale, A. M. and Richardson, J. B.: Articular cartilage: Structure, injuries and review of management. *Brit. Med. Bull.*, **87**, 77-95 (2008).

Blunk, T., Sieminski, A. L., Gooch, K. J., Courter, D. L., Hollander, A. P., Nahir, A. M., Langer, R., Vunjak-Novakovic, G., and Freed, L. E.: Differential effects of growth factors on tissue-engineered cartilage. *Tissue Eng.*, **8**, 73-84 (2002).

Brittberg, M., Lindahl, A., Nilsson, A., Ohlsson, C., Isaksson, O., and Peterson, L.: Treatment of deep cartilage defects in the knee with autologous chondrocyte transplantation. *N. Engl. J. Med.*, **331**, 889- 895 (1994).

Buckwalter, J. A. and Mankin, H. J.: Articular cartilage: Part I: Tissue design and chondrocytes matrix interactions. *J. Bone Joint Surg.*, **79-A**, 600-611 (1997a).

Buckwalter, J. A. and Mankin, H. J.: Articular cartilage: Part II: Degeneration and osteoarthritis, repair, regeneration and transplantation. *J. Bone Joint Surg.*, **79-A**, 612-632 (1997b).

Buschmann, M. D., Gluzband, Y. A., Grodzinsky, A. J., and Hunziker, E. B.: Mechanical compression modulates matrix biosynthesis in chondrocyte/agarose culture. *J. Cell Sci.*, **108**, 1497-1508 (1995).

Buttitta, L. A. and Edgar, B. A.: Mechanisms controlling cell cycle exit upon terminal differentiation. *Curr. Opin. Cell Biol.*, **19**, 697-704 (2007).

Chacko, S., Abbott, J., Holtzer, S., and Holtzer, H.: The loss of phenotypic traits by differentiated cells: VI. Behavior of the progeny of a single chondrocyte. *J. Exp. Med.*, **130**, 417-442 (1969).

Condeelis, J., Jones, J., and Segall, J. E.: Chemotaxis of metastatic tumor cells: Clues to mechanisms from the *Dictyostelium* paradigm. *Cancer Metast. Rev.*, **11**, 55–68 (1992).

Cristofalo, V. J. and Kritchevsky, D.: Cell size and nucleic acid content in the human diploid cell line WI-38 during aging. *Med. Exp.*, **19**, 313-320 (1969).

Cristofalo, V. J. and Sharf, B. B.: Cellular senescence and DNA synthesis: Thymidine incorporation as a measure of population age in human diploid cells. *Exp. Cell Res.*, **76**, 419-427 (1973).

Darling, E. M. and Athanasiou, K. A.: Rapid phenotypic changes in passaged articular chondrocyte subpopulations. *J. Orthopaed. Res.*, **23**, 425-432 (2005).

Démarteau, O., Wendt, D., Braccini, A., Jakob, M., Schäfer, D., Heberer, M., and Martin, I.: Dynamic compression of cartilage constructs engineered from expanded human articular chondrocytes. *Biochem. Biophys. Res. Commun.*, **310**, 580-588 (2003).

Devreotes, P. N. and Zigmond, S. H.: Chemotaxis in eukaryotic cells: A focus on leukocytes and *Dictyostelium*. *Annu. Rev. Cell Biol.*, **4**, 649–686 (1988).

Dominice, J., Levasseur, C., Larno, S., Ronot, X., and Adolphe, M.: Age-related changes in rabbit articular chondrocytes. *Mech. Ageing Dev.*, **37**, 231-240 (1986).

Dupont-Gillain, C. C., Pamula, E., Denis, F. A., and Rouxhet, P. G.: Nanostructured layers of adsorbed collagen: Conditions, mechanisms and applications. *Progr. Colloid Polym. Sci.*, **128**, 98-104 (2004).

Engler, A., Bacakova, L., Newman, C., Hategan, A., Griffin, M., and Discher, D.: Substrate compliance versus ligand density in cell on gel responses. *Biophys. J.*, **86**, 617-628 (2004).

Enomoto, H., Furuichi, T., Zanma, A., Yamana, K., Yoshida, C., Sumitani, S., Yamamoto, H., Enomoto-Iwamoto, M., Iwamoto, M., and Komori, T.: *Runx2* deficiency in chondrocytes causes adipogenic changes in vitro. *J. Cell Sci.*, **117**, 417-425 (2004).

Fackler, O. T. and Grosse, R.: Cell motility through plasma membrane blebbing. *J. Cell Biol.*, **181**, 879-884 (2008).

Fortier, L. A., Lust, G., Mohammed, H. O., and Nixon, A. J.: Coordinate upregulation of cartilage matrix synthesis in fibrin cultures supplemented with exogenous insulin-like growth factor-I. *J. Orthopaed. Res.*, **17**, 467-474 (1999).

Freed, L. E., Vunjak-Novakovic, G., Marquis, J. C., and Langer, R.: Kinetics of chondrocyte growth in cell-polymer implants. *Biotechnol. Bioeng.*, **43**, 597-604 (1994).

Friedl, P. and Wolf, K.: Proteolytic interstitial cell migration: A five-step process. *Cancer Metast. Rev.*, **28**, 129-135 (2009).

Friedl, P. and Wolf, K.: Tumour-cell invasion and migration: Diversity and escape mechanisms. *Nat. Rev. Cancer*, **3**, 362-374 (2003).

Friedl, P., Borgmann, S., and Brocker, E. B.: Leukocyte crawling through extracellular matrix and the *Dictyostelium* paradigm of movement: Lessons from a social amoeba. *J. Leukoc. Biol.* **70**, 491–509 (2001).

Friedl, P., Noble, P. B., Walton, P. A., Laird, D. W., Chauvin, P. J., Tabah, R. J., Black, M., and Zänker, K. S.: Migration of coordinated cell clusters in mesenchymal and epithelial cancer explants in vitro. *Cancer Res.*, **55**, 4557-4560 (1995).

Fujimura, T., Moriwaki, S., Imokawa, G., and Takema, Y.: Crucial role of fibroblast integrins α2 and ß1 in maintaining the structure and mechanical properties of skin. *J. Dermatol. Sci.*, **45**, 45-53 (2007).

Gaudet, C., Marganski, W. A., Kim, S., Brown, C. T., Gunderia, V., Dembo, M., and Wong, J. Y.: Influence of type I collagen surface density on fibroblast spreading, motility, and contractility. *Biophys. J.*, **85**, 3329-3335 (2003).

Gavénis, K., Klee, D., Pereira-Paz, R. M., von Walter, M., Mollenhauer, J., Schneider, U., and Schmidt-Rohlfing, B.: BMP-7 loaded microspheres as a new delivery system for the cultivation of human chondrocytes in a collagen type-I gel. *J. Biomed. Mater. Res. Part B Appl. Biomater.*, **82B**, 275-283 (2007).

Gilles, C., Polette, M., Seiki, M., Birembaut, P., and Thompson, E. W.: Implication of collagen type I-induced membrane-type 1-matrix metalloproteinase expression and matrix metalloproteinase-2 activation in the metastatic progression of breast carcinoma. *Lab. Invest.*, **76**, 651-660 (1997).

Gooch, K. J., Kwon, J. H., Blunk, T., Langer, R., Freed, L. E., and Vunjak-Novakovic, G.: Effects of mixing intensity on tissue-engineered cartilage. *Biotechnol. Bioeng.*, **72**, 402-407 (2001).

Grande, D. A., Pitman, M. I., Peterson, L., Menche, D., and Klein, M.: The repair of experimentally produced defects in rabbit articular cartilage by autologous chondrocyte transplantation. *J. Orthop. Res.*, **7**, 208- 218 (1989).

Greenwood, S. K., Hill, R. B., Sun, J. T., Armstrong, M. J., Johnson, T. E., Gara, J. P., and Galloway, S. M.: Population doubling: A simple and more accurate estimation of cell growth suppression in the in vitro assay for chromosomal aberrations that reduces irrelevant positive results. *Environ. Mol. Mutagen.*, **43**, 36-44 (2004).

Grimshaw, M. J. and Mason R. M.: Modulation of bovine articular chondrocyte gene expression in vitro by oxygen tension. *Osteoarthr. Cartilage*, **9**, 357-364 (2001).

Guerne, P. A., Blanco, F., Kaelin, A., Desgeorges, A., and Lotz, M.: Growth factor responsiveness of human articular chondrocytes in aging and development. *Arthritis Rheum.*, **38**, 960-968 (1995).

Haas, T. L., Davis, S. J., and Madri, J. A.: Three-dimensional type I collagen lattices induce coordinate expression of matrix metalloproteinases MT1-MMP and MMP-2 in microvascular endothelial cells. *J. Biol. Chem.*, **273**, 3604-3610 (1998).

Habuchi, H., Conrad, H. E., and Glaser, J. H.: Coordinate regulation of collagen and alkaline phosphatise levels in chick embryo chondrocytes. *J. Biol. Chem.*, **260**, 13029-13034 (1985).

Hall, B. K. and Newman, S.: p. 61. *Cartilage: Molecular aspects*, CRC press, Boca Raton, FL/London, (1991).

Hegerfeldt, Y., Tusch, M., Bröcker, E-B., and Friedl, P.: Collective cell movement in primary melanoma explants: Plasticity of cell-cell interaction, β1-integrin function, and migration strategies. *Cancer Res.*, **62**, 2125-2130 (2002).

Heywood, H. K., Sembi, P. K., Lee, D. A., and Bader, D. L.: Cellular utilization determines viability and matrix distribution profiles in chondrocyte-seeded alginate constructs. *Tissue Eng.*, **10**, 1467-1479 (2004).

Hirsch, M. S., Lunsford, L. E., Trinkaus-Randall, V., and Svoboda, K. K. H.: Chondrocyte survival and differentiation in situ are integrin mediated. *Dev. Dyn.*, **210**, 249-263 (1997).

Horner, H. A. and Urban, J. P.: 2001 Volvo award winner in basic science studies: Effect of nutrient supply on the viability of cells from the nucleus pulposus of the intervertebral disc. *Spine*, **26**, 2543-2549 (2001).

Horton, W. and Hassel, J. R.: Independence of cell shape and loss of cartilage matrix production during retinoic acid treatment of cultured chondrocytes. *Dev. Biol.*, **115**, 392-397 (1986).

Hunziker, E. B., Schenk, R. K., and Cruz-Orive, L. M.: Quantification of chondrocyte performance in growth-plate cartilage during longitudinal bone growth. *J. Bone Joint Surg. Am.*, **69**, 162-173 (1987).

Ishaug-Riley, S.: Bone formation by three-dimensional stromal osteoblast culture in biodegradable polymer scaffolds. *J. Biomed. Mater. Res.*, **36**, 17-28 (1997).

Jacquemart, I., Pamula, E., De Cupere, V. M., Rouxhet, P. G., and Dupont-Gillain, C. C.: Nanostructured collagen layers obtained by adsorption and drying. *J. Colloid Interface Sci.*, **278**, 63-70 (2004).

Kadler, K. E., Hojima, Y., and Prockop, D. J.: Assembly of collagen fibrils *de novo* by cleavage of the type I pC-collagen with procollagen C-proteinase. Assay of critical concentration demonstrates that collagen self-assembly is a classic example of an entropy-driven process. *J. Biol. Chem.*, **260**, 15696-15701 (1987).

Kadler, K. E., Holmes, D. F., Trotter, J. A., and Chapman, J. A.: Collagen fibril formation. *Biochem. J.*, **316**, 1-11 (1996).

Kato, Y., Iwamoto, M., Koike, T., Suzuki, F., and Takano, Y.: Terminal differentiation and calcification in rabbit chondrocyte cultures grown in centrifuge tubes: Regulation by transforming growth factor β and serum factors. *Proc. Natl. Acad. Sci. U.S.A.*, **85**, 9552-9556 (1988).

Kellner, K., Liebsch, G., Klimant, I., Wolfbeis, O. S., Blunk, T., Schulz, M. B., and Göpferich, A.: Determination of oxygen gradients in engineered tissue using a fluorescent sensor. *Biotechnol. Bioeng.*, **80**, 73-83 (2002).

Khoshfetrat, A. B., Kino-oka, M., Takezawa, Y., Yamamoto, T., Sugawara, K., and Taya, M.: Seeding density modulates migration and morphology of rabbit chondrocytes cultured in collagen gels. *Biotechnol. Bioeng.*, **102**, 294-302 (2009).

Kim, K-W., Ha, K-Y, Park, J-B, Woo, Y-K, Chung, H-N., and An, H. S.: Expression of membrane-type I matrix metalloproteinase, Ki-67 protein, and type II collagen by chondrocytes migrating from cartilage endplate into nucleus pulposus in rat intervertebral discs: A cartilage endplate-fracture model using an intervertebral disc organ culture. *Spine*, **30**, 1373-1378 (2005).

Kinner, B., Capito, R. M., and Spector, M.: Regeneration of articular cartilage. *Adv. Biochem. Eng. Biotechnol.*, **94**, 91-123 (2005).

Kino-oka, M., Agatahama, Y., Hata, N., and Taya, M.: Evaluation of growth potential of human epithelial cells by motion analysis of pairwise rotation under glucose-limited condition. *Biochem. Eng. J.*, **19**, 109-117 (2004).

Kino-oka, M., Maeda, Y., Sato, Y., Khoshfetrat, A. B., Yamamoto, T., Sugawara, K., and Taya, M.: Characterization of spatial growth and distribution of chondrocyte cells embedded in collagen gels through a stereoscopic cell imaging system. *Biotechnol. Bioeng.*, **99**, 1230-1240 (2008).

Kino-oka, M., Maeda, Y., Sato, Y., Maruyama, N., Takezawa, Y., Khoshfetrat, A. B., Sugawara, K., and Taya, M.: Morphological evaluation of chondrogenic potency in passaged cell populations. *J. Biosci. Bioeng.*, **107**, 544-551 (2009).

Kino-oka, M., Maeda, Y., Yamamoto, T., Sugawara, K., and Taya, M.: A kinetic modeling of chondrocyte culture for manufacture of tissue-engineered cartilage. *J. Biosci. Bioeng.*, **99**, 197-207 (2005a).

Kino-oka, M., Morinaga, Y., Kim, M-H., Takezawa, Y., Kawase, M., Yagi, K., and Taya, M.: Morphological regulation of rabbit chondrocytes on glucose-displayed surface. *Biomaterials*, **28**, 1680-1688 (2007).

Kino-oka, M., Yashiki, S., Ota, Y., Mushiaki, Y., Sugawara, K., Yamamoto, T., Takezawa, T., and Taya, M.: Subculture of chondrocytes on a collagen type I-coated substrate with suppressed cellular dedifferentiation. *Tissue Eng.*, **11**, 597-608 (2005b).

Kobayashi, S., Meir, A., and Urban, J.: Effect of cell density on the rate of glycosaminoglycan accumulation by dics and cartilage cells in vitro. *J. Orthop. Res.*, **26**, 493-503 (2008).

Kobayashi, T. and Sokabe, M.: Sensing substrate rigidity by mechanosensitive ion channels with stress fibers and focal adhesions. *Curr. Opin. Cell Biol.*, **22**, 669-676 (2010).

Krishna, O. D. and Kiick, K. L.: Supramolecular assembly of electrostatically stabilized, hydroxyproline-lacking collagen-mimetic peptides. *Biomacromolecules*, **10**, 2626-2631 (2009).

Kronenberg, H. M.: Developmental regulation of the growth plate. *Nature,* **423**, 332-336 (2003).

Kusaka, O., Ochi, M., Ishida, O., Oseto, M., and Ikuta, Y.: Experimental study on nerve repair by using collagen tubes. *J. Jpn. Soc. Surg. Hand*, **4**, 69-73 (1987).

Leddy, H. A. and Guilak, F.: Site-specific molecular diffusion in articular cartilage measured using fluorescence recovery after photobleaching. *Ann. Biomed. Eng.*, **31**, 753-760 (2003).

Leddy, H. A., Haider, M. A., and Guilak, F.: Diffusional anisotropy in collagenous tissues: Fluorescence imaging of continuous point photobleaching. *Biophys. J.*, **91**, 311-316 (2006).

Lin, T-H., Lin, C-H., and Chung, C. A.: Comutational study of oxygen and glucose transport in engineered cartilage constructs. *J. Mech.*, **27**, 337-346 (2011).

Luyten, F. P., Hascall, V. C., Nissley, S. P., Morales, T. I., and Reddi, A. H.: Insulin-like growth factors maintain steady-state metabolism of proteoglycans in bovine articular cartilage explants. *Arch. Biochem. Biophys.*, **267**, 416-425 (1988).

Malda, J., Martens, D. E., Tramper, J., van Blitterswijk, C. A., and Riesle, J.: Cartilage tissue engineering: Controversy in the effect of oxygen. *Crit. Rev Biotechnol.* **23**, 175-194 (2003).

Malda, J., Rouwkema, J., Martens, D. E., le Comte, E. P., Kooy, F. K., Tramper, J., van Blitterswijk, C. A., and Riesle, J.: Oxygen gradients in tissue-engineered PEGT/PBT cartilaginous constructs: Measurement and modeling. *Biotechnol. Bioeng.*, **86**, 9-18 (2004a).

Malda, J., Van Den Brink, P., Meeuwse, P., Grojec, M., Martens, D. E., Tramper, J., Riesle, J., and Van Blitterswijk, C. A.: Effect of oxygen tension on adult articular chondrocytes in microcarrier bioreactor culture. *Tissue Eng.*, **10**, 987-994 (2004b).

Maroudas, A.: Physicochemical properties of cartilage in the light of ion exchange theory. *Biophys. J.*, **8**, 575-595 (1968).

Martin, J. A. and Buckwalter, J. A.: Telomere erosion and senescence in human articular cartilage chondrocytes. *J. Gerontol. A Biol. Sci. Med. Sci.*, **56**, B172-179 (2001).

Mcpherson, J. M. and Tubo, R.: Articular cartilage injury, p. 697-709. In Lanza, R. P. and Langer, R. (ed.), *Principles of tissue engineering*, Academic Press, California, (2000).

Mira, E., Mañes, S., Lacalle, R. A., Márquez, G., and Martínez-A, C.: Insulin-like growth factor I-triggered cell migration and invasion are mediated by matrix metalloproteinase-9. *Endocrinology*, **140**, 1657-1664 (1999).

Mukaida, T., Urabe, K., Naruse, K., Aikawa, J., Katano, M., Hyon, S. H., and Itoman, M.: Influence of three-dimenional culture in a type II collagen sponge on primary cultured and dedifferentiated chondrocytes. *J. Orthop. Sci.*, **10**, 521-528 (2005)

Munirah, S., Ruszymah, B. H., Samsudin, O. C., Badrul, A. H., Azmi, B., and Aminuddin, B. S.: Autologous versus pooled human serum for articular chondrocyte growth. *J. Orthop. Surg. (Hong Kong)*, **16**, 220-229 (2008).

Murphy, C. L. and Polak J. M.: Control of human articular chondrocyte differentiation by reduced oxygen tension. *J. Cell. Physiol.*, **199**,451-459 (2004).

Ochi, M., Adachi, N., Nobuto, H., Yanada, S., Ito, Y., and Agung, M.: Articular cartilage repair using tissue engineering technique-novel approach with minimally invasive procedure. *Artif. Organs*, **28**, 28-32 (2004).

Ochi, M., Uchio, Y., Kawasaki, K., Wakitani, S., and Iwasa, J.: Transplantation of cartilage-like tissue made by tissue engineering in the treatment of cartilage defects of the knee. *J. Bone Joint Surg. Br.*, **84-B**, 571- 578 (2002).

Ochi, M., Uchio, Y., Tobita, M., and Kuriwaka, M.: Current concepts in tissue engineering technique for repair of cartilage defect. *Artif. Organs,* **25**, 172- 179 (2001).

Ohuchi, E., Imai, K., Fujii, Y., Sato, H., Seiki, M., and Okada, Y.: Membrane type 1 matrix metalloproteinase digests interstitial collagens and other extracellular matrix macromolecules. *J. Biol. Chem.*, **272**, 2446-2451 (1997).

Park, K., Min, B-H., Han, D. K., and Hasty, K.: Quantitative analysis of temporal and spatial variations of chondrocyte behavior in engineered cartilage during long-term culture. *Ann. Biomed. Eng.*, **35**, 419-428 (2007).

Pazzano, D., Mercier, K. A., Moran, J. M., Fong, S. S., DiBiasio, D. D., Rulfs, J. X., Kohles, S. S., and Bonassar, L. J.: Comparison of chondrogensis in static and perfused bioreactor culture. *Biotechnol. Prog.*, **16**, 893-896 (2000).

Rada, J. A., Cornuet, P. K., and Hassel, J. R.: Regulation of corneal collagen fibrillogenesis in vitro by corneal proteoglycan (lumican and decorin) core proteins. *Exp. Eye Res.*, **56**, 635-648 (1993).

Radisic, M., Malda, J., Epping, E., Geng, W., Langer, R., and Vunjak-Novakovic, G.: Oxygen gradients correlate with cell density and cell viability in engineered cardiac tissue. *Biotechnol. Bioeng.*, **93**, 332-343 (2006).

Shakibaei, M., De Souza, P., and Merker, H. J.: Integrin expression and collagen type II implicated in maintenance of chondrocytes shape in monolayer culture: An immunomorphological study. *Cell Biol. Int.*, **21**, 115-125 (1997).

Smith, K. R. and Borchardt, R. T.: Permeability and mechanism of albumin, cationized albumin, and glycosylated albumin transcellular transport across monolayers of cultured bovine brain capillary endothelial cells. *Pharmaceut. Res.*, **6**, 466-473 (1989).

Solon, J., Levental, I., Sengupta, K., Georges, P. C., and Janmey, P. A.: Fibroblast adaptation and stiffness matching to soft elastic substrates. *Biophys. J.*, **93**, 4453-4461 (2007).

Solursh, M., Jensen, K. L., Reiter, R. S., Schmid, T. M., and Linsenmayer, T. F.: Environmental regulation of type X collagen production by cultures of limb mesenchyme, mesectoderm, and sternal chondrocytes. *Dev. Biol.*, **117**, 90-101 (1986).

Stephens, M., Kwan, A. P. L., Bayliss, M. T., and Archer, C. W.: Human articular surface chondrocytes initiate alkaline phosphatase and type X collagen synthesis in suspension culture. *J. Cell Sci.*, **103**, 1111-1116 (1992).

Subczynski, W. K., Hopwood, L. E., and Hyde, J. S.: Is the mammalian cell plasma membrane a barrier to oxygen transport? *J. Gen. Physiol.* **100**, 69-87 (1992).

Temenoff, J. S. and Mikos, A. G.: Review: Tissue engineering for regeneration of articular cartilage. *Biomaterials*, **21**, 431-440 (2000).

Uchio, Y., Ochi, M., Matsusaki, M., Kurioka, H., and Katsube, K.: Human chondrocyte proliferation and matrix synthesis cultured in Atelocollagen® gel. *J. Biomed. Mater. Res.*, **50**, 138-143 (2000).

von der Mark, K., Gauss, V., von der Mark, H., and Muller, P.: Relationship between cell shape and type of collagen synthesized as chondrocytes lose their cartilage phenotype in culture. *Nature*, **267**, 531-532 (1977).

Wolf, K., Mazo, I., Leung, H., Engelke, K., von Adrian, U. H., Deryugina, E. I., Strongin, A. Y., Bröcker, E-B., and Friedl, P.: Compensation mechanism in tumor cell migration: Mesenchymal-amoeboid transition after blocking of pericellular proteolysis. *J. Cell Biol.*, **160**, 267-277 (2003).

Wood, G. C.: The formation of fibrils from collagen solutions. 2. A mechanism of collagen fibril formation. *Biochem. J.*, **75**, 598-605 (1960).

Yamamoto, T., Katoh, M., Fukushima, R., Kurushima, T., and Ochi, M.: Effect of glycosaminoglycan production on hardness of cultured cartilage fabricated by the collagen-gel embedding method. *Tissue Eng.*, **8**, 119-129 (2002).

Yashiki, S., Hara, T., Kino-oka, M., and Taya, M.: A three-dimensional growth model for chondrocytes embedded in collagen gel. *Kagaku Kogaku Ronbunshu*, **30**, 515-521 (2004) (in Japanese).

Yunoki, S. and Matsuda, T.: Simultaneous processing of fibril formation and cross-linking improves mechanical properties of collagen. *Biomacromolecules*, **9**, 879-885 (2008).

Yunoki, S., Nagai, N., Suzuki, T., and Munekata, M.: Novel biomaterial from reinforced salmon collagen gel prepared by fibril formation and cross-linking. *J. Biosci. Bioeng.*, **98**, 40-47 (2004).

Zhang, D. and Brodt, P.: Type 1 insulin-like growth factor regulates MT1-MMP synthesis and tumor invasion via PI 3-kinase/Akt signaling. *Oncogene*, **22**, 974-982 (2003).

Zhang, D., Bar-Eli, M., Meloche, S., and Brodt, P.: Dual regulation of MMP-2 expression by the type 1 insulin-like growth factor receptor: The phosphatidylinositol 3-kinase/Akt and Raf/ERK pathways transmit opposing signals. *J. Biol. Chem.*, **279**, 19683-19690 (2004).

Zhou, S., Cui, Z., and Urban, J. P. G.: Nutrient gradients in engineered cartilage: Metabolic kinetics measurement and mass transfer modelling. *Biotechnol. Bioeng.*, **101**, 408-421 (2008).

List of Publications

Original Papers

1. Kino-oka, M., Kagita, S., Nadzir, M. M., Inoue, H., Sugawara, K., and Taya, M.: Direct measurement of oxygen concentration inside cultured cartilage for relating to spatial growth of rabbit chondrocytes. *J. Biosci. Bioeng.*, **110**, 363-366 (2010).

2. Nadzir, M. M., Kino-oka, M., Maruyama, N., Sato, Y., Kim, M-H., Sugawara, K., and Taya, M.: Comprehension of terminal differentiation and dedifferentiation of chondrocytes during passage cultures. *J. Biosci. Bioeng.*, **112**, 395-401 (2011).

3. Nadzir, M. M., Kino-oka, M., Sugawara, K., and Taya, M.: Effect of preservation conditions of collagen substrate on its fibril formation and rabbit chondrocyte morphology. *J. Biosci. Bioeng.*, **114**, 360-363 (2012).

4. Nadzir, M. M., Kino-oka, M., Sugawara, K., and Taya, M.: Insulin-like growth factor-1 for modulating chondrocyte migration and aggregation in cultured cartilage. (Submitted).

Original Papers (not included in dissertation)

1. Jamal, P., Alam, M. Z., Salleh, M. R. M., and Nadzir, M. M.: Screening of *Aspergillus* for citric acid production from palm oil mill effluent. *Biotechnology*, **4**, 275-278 (2005).

2. Alam, M. Z., Jamal, P., and Nadzir, M. M.: Bioconversion of palm oil mill effluent for citric acid production: Statistical optimization of fermentation media and time by central composite design. *World J. Microbiol. Biotechnol.*, **24**, 1177-1185 (2008).

International Conference Proceedings

1. Nadzir, M. M., Maruyama, N., Kino-oka, M., and Taya, M.: Quality assessment of collagen substrate by morphological response of chondrocytes. Asia Pacific Biochemical Engineering Conference, S34 (2009).

2. Nadzir, M. M., Kino-oka, M., Kim, M-H., and Taya, M.: Influence of extracellular matrix produced by chondrocytes on nutrient diffusion in cultured cartilage. The 23rd Annual and International Meeting of the Japanese Association for Animal Cell Technology, 128 (2010).

3. Nadzir, M. M., Taya, M., and Kino-oka, M.: Architecture of chondrocytes aggregates embedded in collagen gel. International Conference on Biofabrication, Japan, 64 (2011).

Award

1. Best student poster award

   "Quality assessment of collagen substrate by morphological response of chondrocytes" Asia Pacific Biochemical Engineering Conference, S34 (2009)

Acknowledgements

I would like to express my gratitude to all the people who make it possible for me to complete this thesis. First and foremost, I would like to give my deepest appreciation to my supervisor Professor Masahito Taya (Division of Chemical Engineering, Graduate School of Engineering Science, Osaka University) who gave me the opportunity to conduct my doctoral studies at the Laboratory of Bioreaction Engineering, Osaka University, and guide me throughout the research work with useful suggestions and constructive criticism. I am also greatly thankful to my research advisor Professor Masahiro Kino-oka (Department of Biotechnology, Graduate School of Engineering, Osaka University) for his guidance throughout the years in various aspects of the research works and daily life in Japan. I am truly grateful for their support and patience from the starting of my study until the day I obtained my doctoral degree.

I would also like to thank Dr. Shinji Sakai, Dr. Yoshihiro Ojima and Dr. Mee-Hae Kim for their advices and comments to my research work.

Special thanks to Dr. Ali Baradar Khoshfetrat, Dr. Shiplu Roy Chowdhury, Ms. Nao Maruyama, Mr. Naoki Tsubakino, Mr. Shogo Kagita, Mr. Yasuaki Sato, Dr. Katsura Sugawara, Mr. Trung Xuan Ngo, Ms. Nguyen Hong Minh, Mr. Shingo Uratochi, Mr. Shota Ohno, Mr. Tomoaki Ashida, Ms. Liu Yang, Mr. Prayoga Suryadarma and Ms. Retno Nurhayati for their supports and helps during these years. I also owe my warm thanks to Mr. Kawashima (GHAS lab, Division of Chemical Engineering, Graduate School of Engineering Science, Osaka University) and all other students of the Laboratory of Bioreaction Engineering for their assistance.

My heartfelt gratitude to Ms. Emiko Tasaka (International student center, Graduate School of Engineering Science, Osaka University) and Ms. Masako Karita (Laboratory of

Bioreaction Engineering, Graduate School of Engineering Science, Osaka University) for their supports and help in my daily life in Japan, and in understanding the Japanese culture.

My appreciation goes to my friends in the Faculty of Engineering Science, Osaka University and all the other friends for making my stay in Japan such an interesting and enjoyable experience.

My very special appreciation goes to my parents and sisters for their understanding, patients and hearty encouragements.